

ABSTRACT

Title of Document: EFFECT OF BOROHYDRIDE REDUCTION
AND PH ON THE OPTICAL PROPERTIES OF
HUMIC SUBSTANCES

Tara Marie Schendorf, Masters of Science, 2014

Directed By: Professor Neil V. Blough, Department of
Chemistry and Biochemistry

Despite decades of research, the structural basis for the optical properties of chromophoric dissolved organic matter (CDOM) and humic substances (HS) are still not clear. Through several analytical techniques, it is known that CDOM contains carbonyls (aromatic ketones, aldehydes, and quinones), carboxylic acids, and phenols. The charge-transfer model proposed to explain the optical properties of these materials assigns the short-wavelength absorption (<350 nm) and fluorescence emission to electron donors (phenols) and acceptors (carbonyls), while the long-wavelength absorption is attributed to charge-transfer interactions among these species. Because carbonyls are reducible species a method was developed to eliminate them and to investigate its effects on the optical properties of HS in relation to their structure. In addition, the effect of pH on the optical absorption spectra for both untreated and borohydride reduced HS was examined and related to the deprotonation of carboxylic acids and phenolic moieties.

EFFECT OF BOROHYDRIDE REDUCTION AND PH ON THE OPTICAL
PROPERTIES OF HUMIC SUBSTANCES

By

Tara Marie Schendorf

Thesis submitted to the Faculty of the Graduate School of the
University of Maryland, College Park, in partial fulfillment
of the requirements for the degree of
Masters of Science
2014

Advisory Committee:
Professor Neil Blough, Chair
Professor George Helz
Professor Alice Mignerey

© Copyright by
Tara Marie Schendorf
2014

Acknowledgements

I would like to express my gratitude to my supervisors, Dr. Neil Blough and Dr. Rossana Del Vecchio, for the many hours spent in collaboration, deliberation and engagement throughout this process. Their insights and support were instrumental in the completion of this master thesis. Additionally, I would like to thank my lab group, particularly Andrea Andrew, Dan Baluha, Kevin Koech, Carmen Cartisano, and Marla Bianca, for their stimulating discussion and assistance with experiments. Furthermore, I would like to thank my husband and family, who have supported and encouraged me throughout this endeavor. Finally, I would like to express my sincerest thanks and appreciation to the United States Coast Guard for the opportunity to pursue this research and thesis.

Table of Contents

Acknowledgements.....	ii
Table of Contents.....	iii
List of Tables.....	iv
List of Figures.....	v
Chapter 1: Introduction.....	1
Chapter 2: Standardization of the Borohydride Reduction Method.....	7
Chapter 3: Dependence of the Optical Properties of Humic Substances on pH and Borohydride Reduction.....	34
Chapter 4: Conclusion.....	59
Appendices.....	62
Bibliography.....	125

List of Tables

Table 1. Chemical Properties of IHSS Samples ⁸	6
Table 2. Fractional loss in Absorbance Due to Reduction at pH 10.....	14
Table 3. Fractional loss in Absorbance Due to Reduction.....	23
Table 4. NaBH ₄ to Carbon Mole Ratios	24
Table 5. Loss in absorbance due to pH for untreated HS	43
Table 6. Loss in absorbance due to pH for reduced HS.....	48

List of Figures

- Figure 1. Logarithmic dependence of the fractional absorbance loss (300 nm left and 450 nm right) based on the NaBH_4 reduction amount for each HS at pH 10. Top: x-axis displayed on a linear scale. Bottom: x-axis displayed on a logarithmic scale. ... 13
- Figure 2. Kinetics of NaBH_4 reduction at 450 nm at pH 10. 14
- Figure 3. Changes in the absorbance of SRFA (100 mg/L, pH 10) following NaBH_4 reduction (5x, 10x, 25x, 50x, 75x, and 100x) from 1 hour after reduction till the reduction was complete at 96 hours. The sharp peaks at 1 hour for the 50-fold and 100-fold mass excess reductions are due to scattering from the hydrogen gas bubbles formed during the reduction process. 16
- Figure 4. Effect of initial pH on the extent of reduction after 96 hours for SRFA (100 mg/L); initial pH 7 (blue) versus initial pH 10 (red). 17
- Figure 5. Effect of NaBH_4 phase on the reduction extent for LAC. NaBH_4 solid phase (blue) versus aqueous phase (red). 18
- Figure 6. Logarithmic dependence of the fractional absorbance loss (300 nm left and 450 nm right) based on the NaBH_4 reduction amount for each HS at pH 7. Top: x-axis displayed on a linear scale. Bottom: x-axis displayed on a logarithmic scale. 21
- Figure 7. Optical changes upon reduction for SRFA adjusted to pH 7. Left panel, from top to bottom: Absorbance (A); Fluorescence emission spectra (D, excitation 300 nm; G, excitation 440 nm). Middle panel, from top to bottom, ΔA (B), where $\Delta A > 0$ indicates a loss in absorbance; ΔF (E, excitation 300 nm; H, excitation 440 nm), where $\Delta F > 0$ represents a gain in fluorescence signal while $\Delta F < 0$ represents a loss in fluorescence signal. Right panel, from top to bottom, $A(t)/A(0)$ (C), < 1 indicates a loss in absorbance; $F(t)/F(0)$ (F, excitation 300 nm; I, excitation 440 nm), where > 1 represents a gain in fluorescence signal while < 1 represents a loss in fluorescence signal. 25
- Figure 8. Optical changes upon reduction for SRHA adjusted to pH 7. Left panel, from top to bottom: Absorbance (A); Fluorescence emission spectra (D, excitation 300 nm; G, excitation 440 nm). Middle panel, from top to bottom, ΔA (B), where $\Delta A > 0$ indicates a loss in absorbance; ΔF (E, excitation 300 nm; H, excitation 440 nm), where $\Delta F > 0$ represents a gain in fluorescence signal while $\Delta F < 0$ represents a loss in fluorescence signal. Right panel, from top to bottom, $A(t)/A(0)$ (C), < 1 indicates a loss in absorbance; $F(t)/F(0)$ (F, excitation 300 nm; I, excitation 440 nm), where > 1 represents a gain in fluorescence signal while < 1 represents a loss in fluorescence signal. 26
- Figure 9. Optical changes upon reduction for LAC adjusted to pH 7. Left panel, from top to bottom: Absorbance (A); Fluorescence emission spectra (D, excitation 300 nm; G, excitation 440 nm). Middle panel, from top to bottom, ΔA (B), where $\Delta A > 0$ indicates a loss in absorbance; ΔF (E, excitation 300 nm; H, excitation 440 nm), where $\Delta F > 0$ represents a gain in fluorescence signal while $\Delta F < 0$ represents a loss in fluorescence signal. Right panel, from top to bottom, $A(t)/A(0)$ (C), < 1 indicates a

loss in absorbance; $F(t)/F(0)$ (F, excitation 300 nm; I, excitation 440 nm), where > 1 represents a gain in fluorescence signal while < 1 represents a loss in fluorescence signal. 27

Figure 10. Optical changes upon reduction for PLFA adjusted to pH 7. Left panel, from top to bottom: Absorbance (A); Fluorescence emission spectra (D, excitation 300 nm; G, excitation 440 nm). Middle panel, from top to bottom, ΔA (B), where $\Delta A > 0$ indicates a loss in absorbance; ΔF (E, excitation 300 nm; H, excitation 440 nm), where $\Delta F > 0$ represents a gain in fluorescence signal while $\Delta F < 0$ represents a loss in fluorescence signal. Right panel, from top to bottom, $A(t)/A(0)$ (C), < 1 indicates a loss in absorbance; $F(t)/F(0)$ (F, excitation 300 nm; I, excitation 440 nm), where > 1 represents a gain in fluorescence signal while < 1 represents a loss in fluorescence signal. 28

Figure 11. Optical changes upon reduction for LHA adjusted to pH 7. Left panel, from top to bottom: Absorbance (A); Fluorescence emission spectra (D, excitation 300 nm; G, excitation 440 nm). Middle panel, from top to bottom, ΔA (B), where $\Delta A > 0$ indicates a loss in absorbance; ΔF (E, excitation 300 nm; H, excitation 440 nm), where $\Delta F > 0$ represents a gain in fluorescence signal while $\Delta F < 0$ represents a loss in fluorescence signal. Right panel, from top to bottom, $A(t)/A(0)$ (C), < 1 indicates a loss in absorbance; $F(t)/F(0)$ (F, excitation 300 nm; I, excitation 440 nm), where > 1 represents a gain in fluorescence signal while < 1 represents a loss in fluorescence signal. 29

Figure 12. Optical changes upon reduction for EHA adjusted to pH 7. Left panel, from top to bottom: Absorbance (A); Fluorescence emission spectra (D, excitation 300 nm; G, excitation 440 nm). Middle panel, from top to bottom, ΔA (B), where $\Delta A > 0$ indicates a loss in absorbance; ΔF (E, excitation 300 nm; H, excitation 440 nm), where $\Delta F > 0$ represents a gain in fluorescence signal while $\Delta F < 0$ represents a loss in fluorescence signal. Right panel, from top to bottom, $A(t)/A(0)$ (C), < 1 indicates a loss in absorbance; $F(t)/F(0)$ (F, excitation 300 nm; I, excitation 440 nm), where > 1 represents a gain in fluorescence signal while < 1 represents a loss in fluorescence signal. 30

Figure 13. Logarithmic dependence of the fluorescence emission gain (excitation 300 nm, integrated over the 300-700 nm range) based on NaBH_4 reduction amount for humic substance at pH 7. Left: x-axis displayed on a linear scale. Right: x-axis displayed on a logarithmic scale. 31

Figure 14. Fluorescence emission spectra at pH 7 for excitation 300-440 nm (black) and 400-600 nm (gray), exciting every 20 nm at the concentrations reported below and the corresponding absorbance for each HS at 100 mg/L pH 7 inset. SRFA was 25 mg/L, SRHA was 16 mg/L, PLFA and LAC were 40 mg/L and EHA and LHA were 10 mg/L for the visible region. SRFA, PLFA and LAC were 10 mg/L, SRHA was 5 mg/L, and EHA and LHA were 3 mg/L for the UV region. 39

Figure 15. Fluorescence emission spectra at pH 7 for a 25-fold mass of borohydride for excitation 300-440 nm (black) and 400-600 nm (gray), exciting every 20 nm with concentrations reported below and the corresponding absorbance for each reduced HS pH 7 inset. SRFA was 25 mg/L, SRHA was 16 mg/L, PLFA and LAC were 40 mg/L

and EHA and LHA were 10 mg/L for the visible region. SRFA, PLFA and LAC were 10 mg/L, SRHA was 5 mg/L, and EHA and LHA were 3 mg/L for the UV region. . 40

Figure 16. Dependence of the absorption spectra on pH following corrections for dilution. SRFA and SRHA were 50 mg/L, LAC was 43 mg/L, PLFA was 44 mg/L, and LHA and EHA were 25 mg/L. 41

Figure 17. Fractional loss of absorbance due to change in pH, relative to pH 12. 43

Figure 18. Mass normalized total difference spectra for each untreated HS. The pH 2 spectra serve as the reference spectra for each sample. SRFA and SRHA were 50 mg/L, LAC was 43 mg/L, PLFA was 44 mg/L, and LHA and EHA were 25 mg/L.. 45

Figure 19. Mass normalized carboxylic acids difference spectra for each untreated HS over the carboxylic acids pK_a range. The pH 3 spectra serve as the reference spectra for each sample. SRFA and SRHA were 50 mg/L, LAC was 43 mg/L, PLFA was 44 mg/L, and LHA and EHA were 25 mg/L. 46

Figure 20. Mass normalized phenolic groups difference spectra for each untreated HS over the phenolic groups pK_a range. The pH 8 spectra serve as the reference spectra for each sample. SRFA and SRHA were 50 mg/L, LAC was 43 mg/L, PLFA was 44 mg/L, and LHA and EHA were 25 mg/L. 47

Figure 21. Dependence of the absorption spectra on pH following corrections for dilution for the reduced HS sample. SRFA and SRHA were 50 mg/L, LAC was 43 mg/L, PLFA was 44 mg/L, and LHA and EHA were 25 mg/L..... 48

Figure 22. Mass normalized total difference spectra for 25-fold mass excess borohydride reduced HS. The pH 2 spectra serve as the reference spectra for each sample. SRFA and SRHA were 50 mg/L, LAC was 43 mg/L, PLFA was 44 mg/L, and LHA and EHA were 25 mg/L. 50

Figure 23. Mass normalized carboxylic acids difference spectra for 25-fold mass excess borohydride reduced HS over the carboxylic acids pK_a range. The pH 3 spectra serve as the reference spectra for each sample. SRFA and SRHA were 50 mg/L, LAC was 43 mg/L, PLFA was 44 mg/L, and LHA and EHA were 25 mg/L.. 51

Figure 24. Mass normalized phenolic groups difference spectra for 25-fold mass excess borohydride reduced HS over the phenolic groups pK_a range. The pH 8 spectra serve as the reference spectra for each sample. SRFA and SRHA were 50 mg/L, LAC was 43 mg/L, PLFA was 44 mg/L, and LHA and EHA were 25 mg/L..... 52

Figure 25. Comparison of the unreduced versus 25-fold mass excess reduced SRFA, SRHA, and LAC at 300 and 400 nm. 53

Figure 26. Comparison of the unreduced versus 25-fold mass excess reduced EHA, LHA, and PLFA at 300 and 400 nm. 54

Figure 27. Difference absorbance spectra for the untreated versus reduced samples over the carboxylic acids pK_a range. 55

Figure 28. Difference absorbance spectra for the untreated versus reduced samples over the phenolic groups pK_a range. 56

Chapter 1: Introduction

Approximately 70% of the earth's surface is covered by oceans, playing a major role in everything from the climate of the earth to the lifecycle of marine fauna. The ocean is an integral part of the global carbon cycle, which is vital to regulating life on earth. A portion of organic carbon found in the ocean consists of dissolved organic matter (DOM).¹ Chromophoric dissolved organic matter (CDOM) represents the portion of DOM that absorbs light in the UV and visible region.^{2,3}

The study of CDOM is currently focused on characterizing its structural basis, with a subset of CDOM originating from materials known as humic substances (HS).^{4,5,6} HS are “complex organic materials found ubiquitously in nature where they play an essential role in numerous environmentally important processes.”⁷ HS found in natural waters can be from two different fractions, either humic acids (HA), which are insoluble at $\text{pH} < 2$, or fulvic acids (FA), which are soluble at all pH values.⁸ CDOM and HS both are vital to the biogeochemical processes in natural waters. Because CDOM absorbs light, it controls the depth at which light penetrates through the water. This means that CDOM can protect organisms from harmful radiation, can alter the light available for photosynthesis, and can produce photochemically reactive oxygen species (H_2O_2 , $\text{O}_2^{\cdot -}$, $^1\text{O}_2$, OH^{\cdot}), among other interactions.^{2,4,7,9}

Despite years of research geared towards determining the structural basis of HS and CDOM optical and photochemical properties, and given the extreme complexity and multiple potential sources of CDOM, making a precise structural determination has been nearly impossible. What is known about their structure is based on a variety of analytical techniques that have provided evidence for the presence of carboxylic acids, phenols,

ketones, aldehydes, and quinones among other structures within CDOM.⁵ Understanding the structural basis of CDOM and HS is vital to being able to understand how reactions occur in the ocean, how changes in the ocean chemistry will affect these reactions, and the importance of these chemicals to the marine ecosystem.

The optical properties of CDOM and HS from natural waters have been studied for decades. CDOM and HS standards show an approximately exponential decrease in absorbance with increasing wavelength giving rise to a broad, featureless spectrum, and a broad, unstructured emission spectrum that continuously red-shifts with increasing excitation wavelength.^{5,7,10,11} These observations, along with others, suggest a large number of absorbing and emitting species or states.¹⁰

Two models have been developed to try to explain the optical properties of CDOM and HS: the superposition model and the electronic interaction or charge-transfer model. The superposition model assumes that the absorption and emission results from a simple sum of the absorption and emission of the individual chromophores within CDOM.¹¹ Some of the structures known to be in CDOM and HS, for example quinones, aromatic ketones, and phenols, absorb light in the UV region, but only quinones show minor absorption past 450 nm. Previous studies have shown that the molar absorptivity of the quinones are extremely small, making it unlikely that any of the long wavelength absorbance seen in CDOM and HS could come from these compounds.¹¹ In addition, this model ignores the potential for interactions between the individual chromophores and assumes they independently absorb and emit light. Thus, this model can only account for the optical properties in the UV region.⁵

A more accurate and encompassing description is provided by the electronic interaction model. This model stipulates that the long wavelength optical properties arise in part through electronic interactions between the donors and acceptors within CDOM.^{5, 7,9,10,11} This interaction leads to a spectrum that is not the simple sum of the isolated chromophores.^{5, 7,9,10,11} The principle proposition of the charge-transfer model is that the long wavelength absorbance seen in HS and CDOM develop from intramolecular charge-transfer interactions, while the absorbance in the UV arises from the individual chromophores. According to this theory, phenols could represent the principle electron donors in HS, while ketones, aldehydes, and quinones could account for the principle electron acceptors.^{5, 7} Not only would these interactions account for the long wavelength absorbance, but the interactions also account for the emission of HS and CDOM in the visible.

Because CDOM and HS contains carboxylic acids, phenols, ketones, aldehydes, and quinones⁵ and because ketones, aldehydes, and quinones are reducible species, borohydride can be employed to selectively reduce such functional groups and observe the impact on the optical properties in an effort to further understand the nature and structure of HS.¹¹ Borohydride reduces ketones, aldehydes, and quinones to alcohols and hydroquinones, which in turn means that the electron acceptors in the charge transfer model are removed from the system.¹¹ With no acceptors available to interact with the phenolic donors, the long wavelength absorbance would be expected to be eliminated or decreased. In addition, the reduction would cause a decrease in emission in the visible due to the loss of charge-transfer interactions and an increase in emission in the UV (blue-shifted) due to the loss of quenching of the donors caused by the acceptors.¹¹ These

results should be amplified with increasing borohydride concentrations until all the acceptors are reduced.

Sodium borohydride has been used as a reduction method in many different forms previously, with some of the research geared towards highlighting HS optical properties.⁹¹¹ The first goal of this study was to determine a standard method of sodium borohydride reduction to create a consistent technique that could be easily implemented and further to determine the effects of reduction on the optical properties of HS. The end result was a simple, straightforward method for both the reduction and the purification of HS samples. In addition, the results provided further insight into the potential role of charge-transfer interactions.

In addition to using the sodium borohydride reduction as a method of exploring the chemical composition of CDOM and HS, altering the pH of the samples is another method that can be used to probe the structural basis of HS. Previous research has shown that by increasing the pH of the samples, the UV-visible absorption of HS also increases.^{12,13} This effect was further evaluated by determining the difference spectra across the pH range, using the lowest pH measured as the reference.¹³ The resulting spectra showed two distinct groups that are thought to be partially responsible for the optical properties of HS, carboxylic acids and phenolic groups.¹³ Previous work has determine that the pK_a range for carboxylic acids is between 3 and 6 while the phenolic groups pK_a range is greater than 8.¹² As discussed previously, because phenols account for the electron donors in the charge-transfer model, these pH observations could have further implications for this model.

The second goal of this study was to analyze the optical properties of HS from pH 2 to pH 12 for both the untreated and reduced samples. The optical properties of the unreduced samples showed a greater dependence on pH than the reduced samples, which could be due to the elimination of the donors and thus of the charge-transfer interactions after reduction. The effect of pH on the untreated versus reduced samples created many other interesting characteristics that need to be further investigate.

To test these theories, six different samples were analyzed to observe their varying optical properties. Five of these samples were standards received from the International Humic Substances Society (IHSS). To ensure that a wide range of HS was studied, both HAs and FAs from sources considered aquatic, terrestrial, and microbial were used. For the aquatic sources, Suwanee River Fulvic Acid (SRFA) and Suwanee River Humic Acid (SRHA) were used. These samples were collected from the Suwanee River in Georgia. The terrestrial sources were Leonardite Humic Acid (LHA) and Elliott Soil Humic Acid (EHA), which were collected from the Mid-West region of the United States. Finally, the microbial sample was Pony Lake Fulvic Acid (PLFA), which came from Pony Lake, Antarctica. In addition to the five standards studied from the IHSS and since terrestrial HS is thought to derive from the breakdown of plant materials to lignins, alkali-extracted and carboxylated lignin (LAC) was used as the sixth reference material. These substances have been extensively researched and their basic properties are well known (Table 1).⁸ As noted previously, while information such as the elemental composition of HS is known, the structural basis of HS is still relatively unknown.

Table 1. Chemical Properties of IHSS Samples⁸

		SRFA	SRHA	PLFA	EHA	LHA
Elemental Composition¹⁴	% (w/w)					
	Carbon	52.34	52.63	52.47	58.13	63.81
	Hydrogen	4.36	4.28	5.39	3.68	3.70
	Oxygen	42.98	42.04	31.38	34.08	31.27
	Nitrogen	0.67	1.17	6.51	4.14	1.23
	Sulfur	0.46	0.54	3.03	0.44	0.76
	Phosphorus	0.004	0.013	0.55	0.24	<0.01
Acidic Functional Groups¹²	Charge Density (meq/g C)					
	Carboxylic	11.17	9.13	NA	8.28	7.46
	Phenolic	2.84	3.72	NA	1.87	2.31
¹³C NMR Estimates of Carbon Distribution¹⁵	Integrated Peak Area (%)					
	Carbonyl (220-190 ppm)	5	6	1.2	6	8
	Carboxyl (190-165 ppm)	17	15	17	18	15
	Aromatic (165-110 ppm)	22	31	12	50	58

Chapter 2: Standardization of the Borohydride Reduction Method

Introduction

Sodium borohydride (NaBH_4) has been used for years to selectively reduce carbonyl moieties within humic substances (HS) and chromophoric dissolved organic matter (CDOM) in an effort to gain insight into their contributions to the structure of this material. NaBH_4 selectively reduces ketones and aldehydes to alcohols and quinones to hydroquinones in competition with its reduction with the hydronium ion (H_3O^+) to form borate and hydrogen gas. Currently, there is no standard method to follow when reducing substances in the laboratory, despite the various laboratories using NaBH_4 in some manner as a reductant. In one example, NaBH_4 was used in a one to one mass ratio with a sample of HS, allowed to reduce for four hours, excess NaBH_4 was then decomposed by the addition of hydrochloric acid before subsequent isolation by solid phase extraction.¹⁶ Another method used NaBH_4 to reduce HS in a 33 to 1 mass ratio (10 to 1 for concentrations greater than 500 mg/L) for 24 hours and then ran the reduced samples through a small Sephadex G-10 column.¹¹ Both methods showed a decrease in absorbance due to reduction, but neither fully reduced the samples and both used different methods of processing the samples after reduction.

In an effort to create a standard reduction method and to further clarify the effects of this reduction on the optical properties of HS, a systematic set of experiments was conducted to determine the best methods currently available for maximizing reduction to determine the ultimate effects on HS optical properties. Several variables were tested to ensure their efficacy including initial pH, NaBH_4 phase, pH prior to G-10 column

purification, and G-10 column length. The optical properties of the untreated and reduced samples were analyzed and compared with previous research.

Material and Methods

Materials. Suwannee River fulvic and humic acid (SRFA; Lot 2S101F and SRHA; Lot 2S101H), Pony Lake fulvic acid (PLFA; Lot 1R109F), Leonardite humic acid (LHA; Lot 1S104H-5), and Elliot Soil humic acid (EHA; Lot 1S102H) were obtained from the International Humic Substances Society (IHSS). Alkali-extracted and carboxylated lignin (LAC; Lot 19714 DS) was obtained from Sigma-Aldrich. Sodium borohydride (NaBH_4 ; Lot 083480B) was obtained from Fisher Scientific. Sephadex G-10 (Lot SLBF7082V) was obtained from Sigma-Aldrich. Quinine sulfate (QS) was obtained from MC/B. Water was obtained from a Milli-Q Plus purification system (Millipore). Tumeric Analytical Test Strips were obtained from Scientific Equipment of Houston (Lot 4012).

Apparatus. A Shimadzu UVPC 2401 spectrophotometer was employed to acquire UV-visible absorption spectra. An Aminco-Bowman AB-2 luminescence spectrometer was employed for the fluorescence measurements (monochromator excitation and emission band-passes set to 4 nm). A Thermoscientific micro pH electrode coupled to an Orion 4 Star pH ISE bench top meter was employed for the pH measurements.

Optical Measurements. Absorption spectra were recorded using 1-cm quartz cuvettes over the range from 190 to 820 nm against air and were MQ subtracted afterward. Fluorescence emission spectra were collected over the 280-600 nm excitation range, while the absorbance was kept at < 0.05 - 0.1 OD at the excitation wavelength.⁷

Emission spectra were MQ subtracted and corrected for the instrument response by applying the correction factors provided by the manufacturer.

Borohydride (NaBH₄) reductions. Three milliliters of 100 mg/L of SRFA, SRHA, LAC, PLFA, LHA, and EHA in MQ adjusted to pH 7 were transferred to 1-cm cuvettes. Solid NaBH₄ was added at a 5-fold, 10-fold, 25-fold, 50-fold, 75-fold, and 100-fold mass excess of NaBH₄ to HS. Samples were treated in the dark and the optical properties were measured prior to and during the reduction at 24 hour intervals until the reduction was complete (approximately 96 hours). As the goal of these experiments was to determine a standard amount of NaBH₄ required to drive reductions to completion as monitored through their optical properties, reductions were performed under aerobic conditions.

The following optical changes upon treatment were defined as described for the duration of the chapter unless otherwise noted. The absorbance loss (ΔA) and the fractional absorbance (FA) are defined as

$$\Delta A = A(0) - A(t) \quad (1)$$

$$FA = A(t)/A(0) \quad (2)$$

where $A(t)$ is the absorbance of the treated samples and $A(0)$ is that of the original sample. The fluorescence gain or loss (ΔF) and the fractional fluorescence intensity (FI) are defined as

$$\Delta F = F(t) - F(0) \quad (3)$$

$$FI = F(t)/F(0) \quad (4)$$

where $F(t)$ is the fluorescence emission of the treated samples and $F(0)$ is that of the original sample.

The pH of the unbuffered samples increased to 10 during the reduction due to the reaction of NaBH_4 with H_3O^+ and the formation of borate. Because of the pH dependence of the HS optical properties (see also Chapter 3)^{12,13}, to look at the changes in optical properties during reduction, an aliquot of each untreated HS was brought to pH 10 with sodium hydroxide (0.25 M) and employed as a reference. This allowed for a straightforward comparison of the absorbance data prior to running the sample through the column to remove the borate (see below).

To test whether the reduction proceeds to the same extent independently of the initial pH (7 versus 10), a selected HS, SRFA, was reduced in duplicate with an initial pH of 7 and 10.

Because these reductions can be performed with both the solid and alkaline solutions of NaBH_4 , it was necessary to verify that both reduction methods produce equivalent results. Thus, a selected sample, LAC, was reduced as above with solid NaBH_4 and with a stock solution of NaBH_4 . This stock solution of NaBH_4 was prepared by dissolving ~300 mg of solid NaBH_4 in 3 mL of MQ adjusted to pH 12 with approximately 120 μL NaOH (1.0M). The NaBH_4 was slowly added to the MQ and was stirred continuously for approximately 1 hour to fully dissolve. Three milliliters of 100 mg/L of LAC in MQ adjusted to pH 7 were transferred to 1-cm cuvettes. 15 μL , 75 μL , 150 μL , and 300 μL of the NaBH_4 stock were transferred to the cuvettes containing LAC to achieve a 5-fold, 25-fold, 50-fold, and 100-fold mass excess of NaBH_4 relative to the HS. As above, absorbance measurements were recorded every 24 hours until the reaction was complete and compared to those collected during the reduction experiment obtained with solid NaBH_4 .

Due to the large amounts of borate remaining after reduction, a G-10 column was employed to remove the excess borate salt and adjust the pH back to ~ 7 .¹¹ Sephadex G-10 is a method of desalting samples since, as a size exclusion chromatography method, it allows the larger molecules, like HS, to move through the column just after the void volume, while the salts with a smaller molecular size, like borate, pass through at the total volume of the column. Twenty g of G-10 powder was hydrated in MQ overnight (approximately 12 hours) as per the GE Healthcare Gel Filtration Principles and Methods guide.¹⁷ Given that G-10 has a bed volume of 2-3 mL/g, the 20 g of dry powder equates to a height of approximately 10 cm in a column with a diameter of 2.5 cm. The saturated G-10 was then employed to pack the column by creating a slurry in approximately 100 mL of MQ and poured into the column. Gravity was used to pack the column prior to opening the stopcock.

The 2.5 x 10 cm G-10 column was equilibrated with MQ and the absorbance of the eluent MQ was recorded prior to loading the sample into the column to ensure a clean column for every run. Untreated (control) and reduced samples (3 mL each) were run through the column. For each HS series, the untreated sample was run first followed by the reduced samples. Between runs, the column was flushed with approximately 1500 mL of MQ to remove any remaining borate from the column. After completing each HS series, the packing was removed from the column, cleaned with MQ at least 3 times, repacked, and flushed with approximately 500 mL of MQ.

Tumeric test strips and pH measurements were used to determine if borate was completely eliminated from the post column samples. Because of the large amounts of NaBH_4 added to the pre-column solutions, the 10 cm column was only efficient in

removing all borate at the 5-fold, 10-fold, and 25-fold mass excess. Thus, a 15 cm column was tested to determine if it would be more effective in removing borate from all solutions. In addition, a set of reduced SRFA samples were adjusted to pH 7 using concentrated hydrochloric acid prior to running through the column to determine if there was any effect on the column if the pH was adjusted prior to the sample addition into the column.

All post-column samples were filtered using a 0.2 μm nylon filter to ensure there were no remaining impurities, brought to pH 7 using perchloric acid (0.25 M) and the absorption and fluorescence recorded. Due to the similarities in absorption loss for samples treated with 5- and 10-fold mass excess of borohydride and 50- and 75-fold mass excess of borohydride, the 10-fold and 75-fold reductions were omitted from the fluorescence analysis.

Results and Discussion

Pre-column (pH 10). Previous work has shown that HS exhibit a substantial and mostly irreversible decrease in absorbance ($\sim 40\%$ at 450 nm) and an irreversible increase and blue-shift in fluorescence emission after reduction with NaBH_4 (33-fold mass excess), with the reduction complete after approximately 24 hours.¹¹ These results are fully consistent with prior findings and further show that the extent of absorption loss increases logarithmically with increasing amount of NaBH_4 added, plateauing at around a 25-fold mass excess reduction (Fig. 1; Appendix 1). In particular, in the UV region (300 nm) the absorption loss increased from $\sim 15\text{-}25\%$ (5-fold mass excess) to $\sim 20\text{-}35\%$ (≥ 25 -fold mass excess), while in the visible region (450 nm) it increased from $\sim 30\text{-}50\%$ (5-fold

mass excess) to ~40-70 % (≥ 25 -fold mass excess) (Fig. 1; Table 2). In addition, and not surprisingly, the overall reduction ended at longer times with increasing NaBH_4 mass excess (i.e. the 100-fold mass excess sample took 96 hours to completely reduce) (Fig. 2; Appendix 2). These observations suggest the occurrence of a large pool of reducible carbonyl-containing compounds that required large NaBH_4 mass excess (~ 25 -fold) and several hours (≥ 48 hr) to be fully reduced.

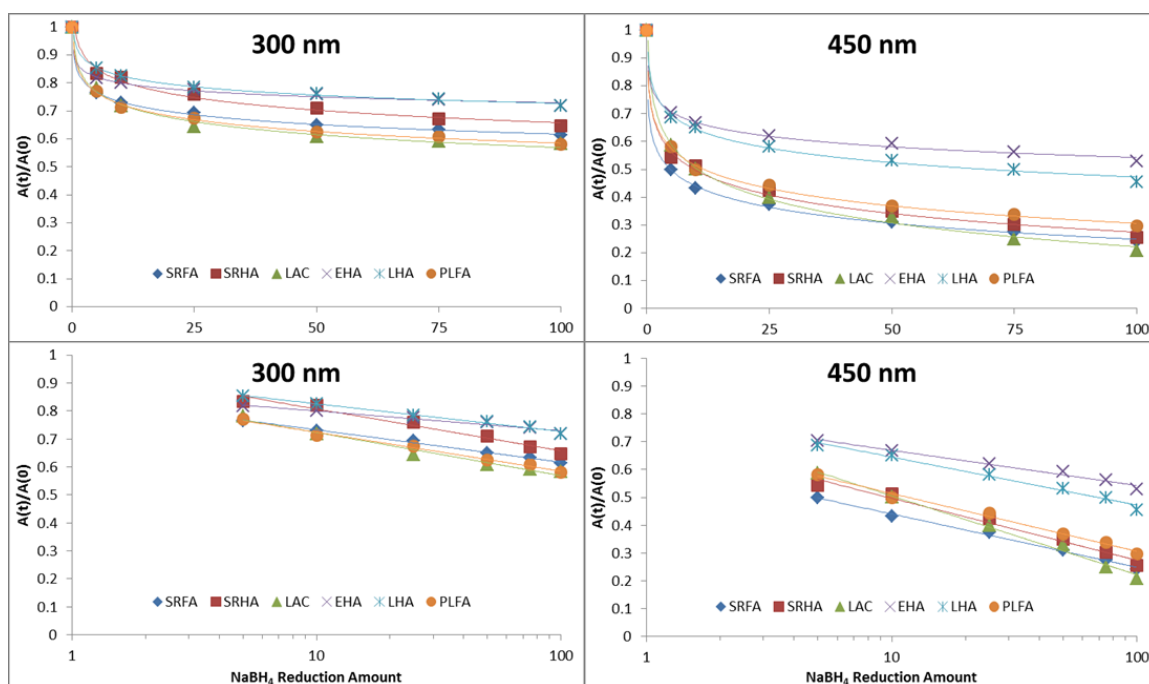


Figure 1. Logarithmic dependence of the fractional absorbance loss (300 nm left and 450 nm right) based on the NaBH_4 reduction amount for each HS at pH 10. Top: x-axis displayed on a linear scale. Bottom: x-axis displayed on a logarithmic scale.

Table 2. Fractional loss in Absorbance Due to Reduction at pH 10

	SRFA	SRHA	LAC	PLFA	EHA	LHA
Wavelength	450 300	450 300	450 300	450 300	450 300	450 300
5x	50% 23%	46% 17%	41% 22%	42% 23%	30% 18%	31% 15%
10x	57% 27%	49% 18%	50% 28%	50% 29%	33% 20%	35% 17%
25x	63% 31%	58% 24%	60% 36%	56% 33%	38% 23%	42% 21%
50x	69% 35%	65% 29%	67% 39%	63% 38%	41% 24%	47% 24%
75x	73% 37%	70% 33%	75% 41%	66% 39%	44% 26%	50% 26%
100x	76% 39%	74% 35%	79% 42%	70% 42%	47% 28%	54% 28%

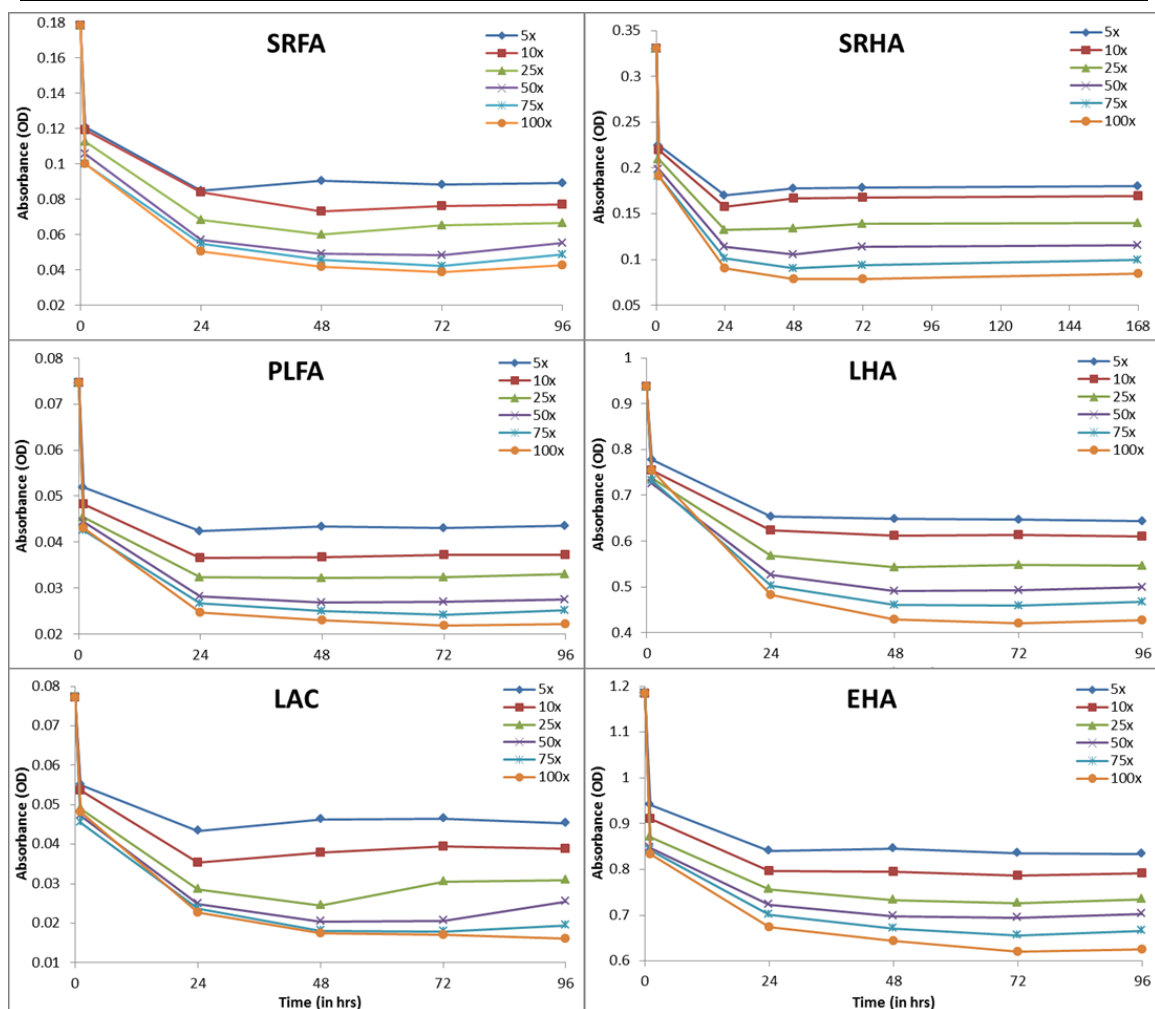


Figure 2. Kinetics of NaBH_4 reduction at 450 nm at pH 10.

Despite the major and irreversible decrease in absorption, minor recoveries (< 20 %) were observed over the visible region (> 450 nm) after at least 48 hours of reduction (Fig. 3). This reversibility was noted for all reduction amounts at increasing time with increasing NaBH₄ mass excess. The increase in time was possibly due to a decrease in O₂ availability with increasing amounts of NaBH₄. Interestingly, while the irreversible absorption loss increased logarithmically with the amount of NaBH₄ added up to the 25-fold excess (Figs. 1-3; Appendix 3), the reversible loss was essentially constant for each given HS despite the increase in NaBH₄ added (Fig. 3, Appendix 2). This finding suggests the occurrence of two subsets of carbonyl-containing compounds, one that is reversibly reduced by NaBH₄ and that minimally contributes to the HS optical properties and the other that is irreversibly reduced by NaBH₄ and significantly contributes to the HS optical properties. Since the reversible component remained constant no matter how much NaBH₄ was added, it could be concluded that the reversible component was completely reduced at the 5-fold and greater mass excess reductions. The reversible and irreversible component findings are consistent with previous work and while the reversible carbonyl-containing compounds have been attributed to quinones,⁷ the irreversible ones have been attributed to aromatic ketones/aldehydes.¹¹ Alcohols formed by reduction of ketones/aldehydes cannot be air oxidized while hydroquinones are easily oxidized by air.

A review of model quinones and aromatic ketones showed that in their untreated form, these compounds absorb mainly in the UV region, with only minor absorption past 450 nm for quinones (see chap 1). Upon reduction, these model quinones and aromatic ketones show a shift in absorbance to the shorter wavelengths and still show very little if

any absorbance in the visible. This shift in absorbance could account for the loss in absorbance in the UV upon reduction of the HS studied.

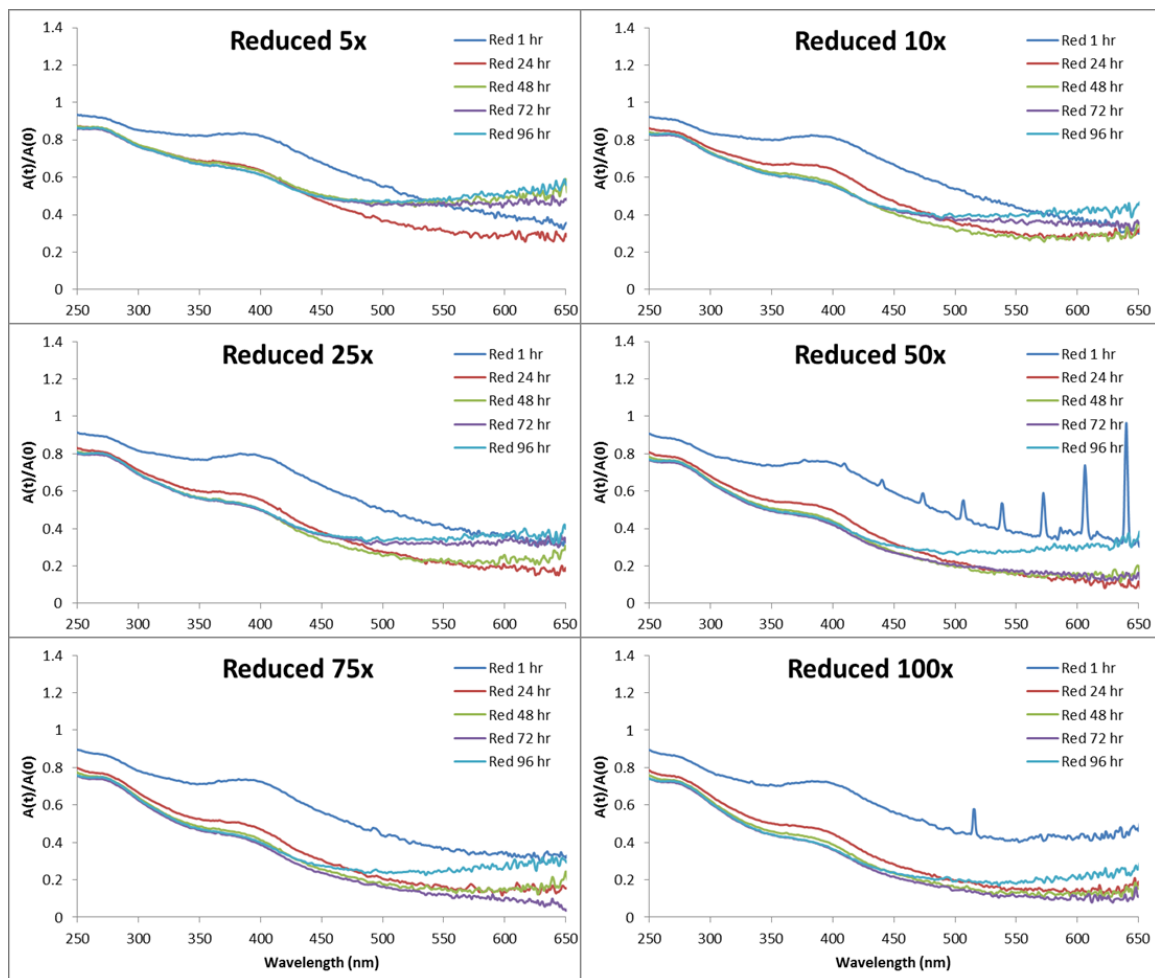


Figure 3. Changes in the absorbance of SRFA (100 mg/L, pH 10) following NaBH_4 reduction (5x, 10x, 25x, 50x, 75x, and 100x) from 1 hour after reduction till the reduction was complete at 96 hours. The sharp peaks at 1 hour for the 50-fold and 100-fold mass excess reductions are due to scattering from the hydrogen gas bubbles formed during the reduction process.

Due to the changes in pH during reduction, the effect of initial pH on the extent of reduction was investigated. The initial pH (7 vs 10) had no effect on the overall extent of reduction despite some minor differences ($< 5\%$) that were possibly due to human error associated with the reduction using solid NaBH_4 (Fig. 4; Appendix 4). Since the starting

pH had no effect on the extent of reduction, pH 7 was chosen as the starting pH to align more closely with naturally occurring waters.

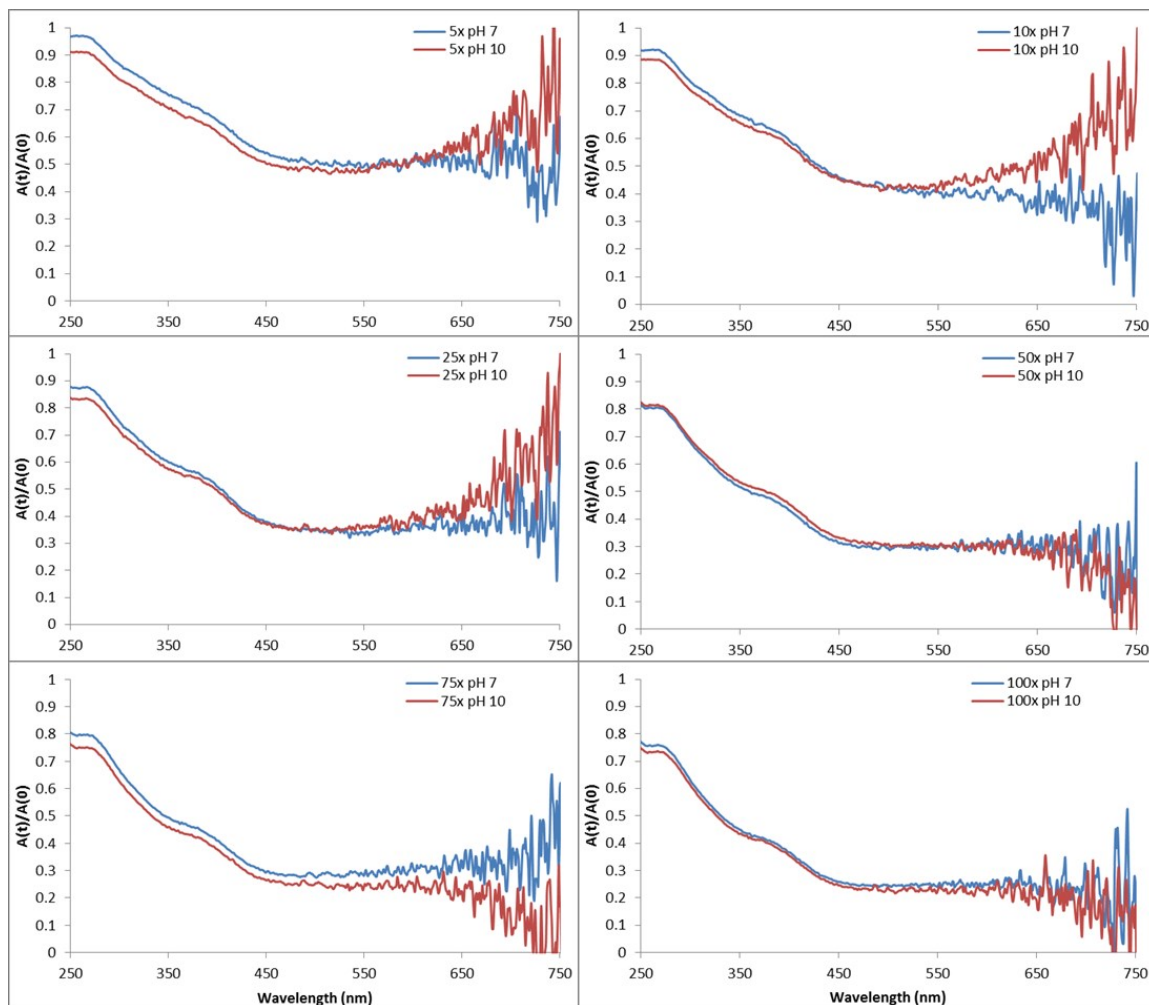


Figure 4. Effect of initial pH on the extent of reduction after 96 hours for SRFA (100 mg/L); initial pH 7 (blue) versus initial pH 10 (red).

The extent of optical changes observed upon reduction with NaBH_4 in either solid or solution form were also investigated. Overall, the form of NaBH_4 had little effect on the extent of optical changes upon reduction with the 5- and 25-fold mass excesses (Fig. 5; Appendix 5). Slight differences were observed between the solid and solution forms for the 50- and 100-fold mass excesses, which may be related to the differences in the

rates of reduction between the solid and solution forms. Reductions with NaBH_4 stocks in solution were easier to conduct and had less contaminants in the sample preparation. The stock solution had a shelf lifetime of approximately 4 days when the MQ was at pH 12,¹⁸ and when added to the HS solutions, caused less hydrogen gas to be produced, making the stock solution reduced method the preferred method for most reductions.

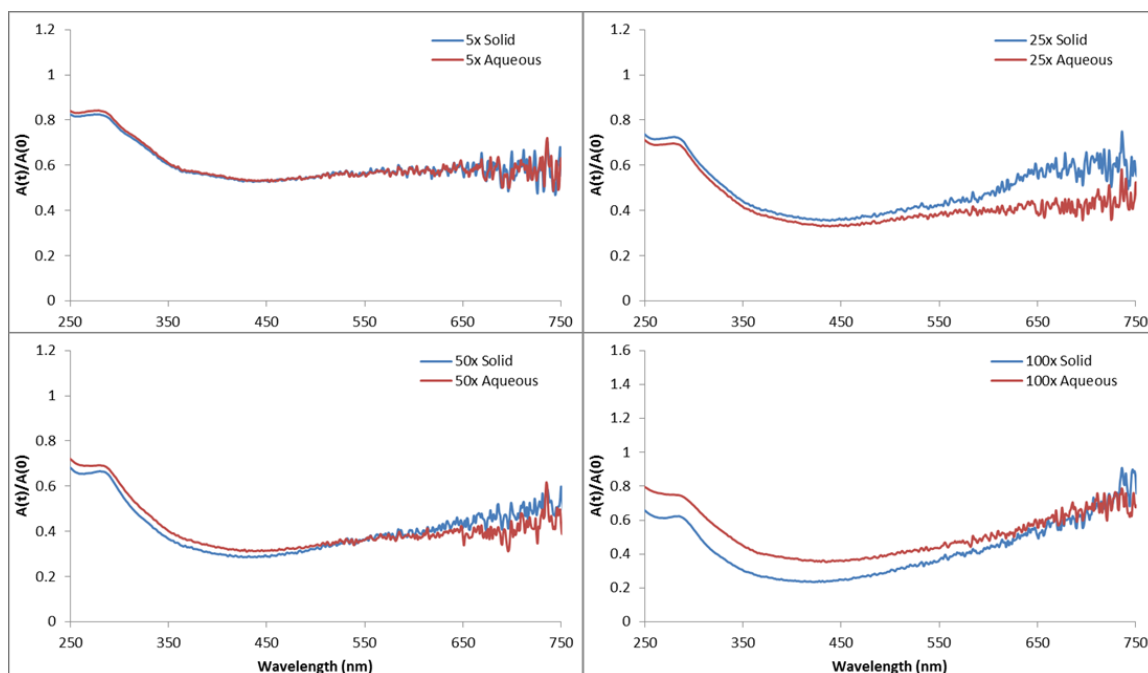


Figure 5. Effect of NaBH_4 phase on the reduction extent for LAC. NaBH_4 solid phase (blue) versus aqueous phase (red).

Because the absorbance was not completely eliminated in the visible with a 100-fold mass excess, the mass excess was further increased to 200- and 300-fold. The 200-fold reduction revealed a further decrease in absorbance, but still not a complete loss of absorbance in the visible (Appendix 6). The 300-fold reduction lead to precipitation and was thus not farther examined. While the 200-fold reduction did further decrease the

absorbance, the increase in borate after reduction lead to increased difficulties with removing the borate and, thus, is not recommended.

Post-column (pH 7). Following reduction (96 hr), the solutions contained substantial amounts of borate causing the pH to remain at approximately 10. In order to remove the excess borate and to bring each sample's pH to a uniform neutral value (pH ~7), the samples were passed over a G-10 column (10 cm) and the pH and borate concentration then measured. Each HS had a different dilution factor for the 10 cm column (Appendix 7). As seen here and in previous experiments¹¹, the post column dilution-factor-corrected absorbance of the samples remained relatively unchanged versus the pre-column absorbances, however not all the samples were borate free. The 50-fold, 75-fold, and 100-fold mass excess samples still exhibited some borate concentration.

Higher mass excesses of borohydride also lead to high hydrogen generation upon introduction to the column due to the change in pH, which in some cases lead to column cracking. If using large amounts of NaBH_4 to reduce the samples, a viable option to help avoid this pH difference is to use concentrated hydrochloric acid to bring the pH of the sample down to 7 prior to running the sample through the column. This would eliminate the pH difference on the column surface and allow removal of the excess hydrogen gas before introduction onto the column. A test conducted to verify the efficacy of decreasing the samples down to pH 7 prior to running the column showed that there was no difference in the resulting dilution factor corrected absorbance with the pre-column pH of either 7 or 10 (the pH when the final absorbance was taken was 7 for all samples) (Appendix 9).

In an effort to remove all of the borate from the 50- to 100-fold mass excess reduced samples, two separate experiments were conducted. In the first experiment, the EHA and LHA samples that still contained borate (50- and 100-fold mass excess) along with the unreduced reference sample were re-run through the 10 cm column a second time. There appeared to be no borate remaining in the samples after the second run and only minor changes were noted in the dilution factor corrected absorbance (Appendix 9). In the second experiment, SRFA reduced under the same conditions as above (5-fold, 25-fold, and 100-fold mass excess) were run through a longer G-10 column (15 cm instead of 10 cm) after reduction (Appendix 10). The post-column samples had no borate and no changes in the dilution-factor- corrected absorbance. However, because the 15 cm column has an additional 5 cm of length to it, the time involved in running each column and cleaning the column between uses increased. In addition, the increase in column length equates to an increase in dilution factor. So if the final concentration of HS needs to be a higher value, the initial concentration prior to reduction needs to be greater, which means that more NaBH_4 would be required to reduce the sample to the same extent, decreasing the effectiveness of the increase in column length. While the 15 cm column did indeed remove all of the borate at high NaBH_4 additions, there were enough negatives to using the 15 cm column that it was viewed as less desirable. Thus, the standard method would be to use lower concentrations of HS and use the 10 cm column to remove excess borate.

All the post-column (10 cm) samples were mostly borate-free and were uniformly adjusted to pH 7 with HClO_4 (0.25N). As reported above for the pH 10 data, the extent of absorption loss increased with the amount of NaBH_4 used to reduce the sample

plateauing around the 25-fold mass excess (Fig. 6). Overall, the fractional loss of absorption (%) was comparable at pH 7 and 10 (compare Figs. 1 and 6, Table 2 and 3). Similarly to the pre-column data (pH 10), most of the absorbance at > 450 nm (~70%) was eliminated with the 100-fold NaBH₄ mass excess for SRFA, SRHA, PLFA and LAC (Figs. 7-10, A-B-C) while much less (~54%) was eliminated for LHA and even less (~42%) for EHA (Figs. 11-12, A-B-C). This argues that while the long-wavelength optical properties of aquatic and microbial HS can be largely explained by charge-transfer interactions involving aromatic ketones/aldehydes, those of terrestrial HS have to invoke a more complex scenario. Alternatively, there may be a fraction of these moieties that are inaccessible to borohydride reduction in these higher molecular weight materials.

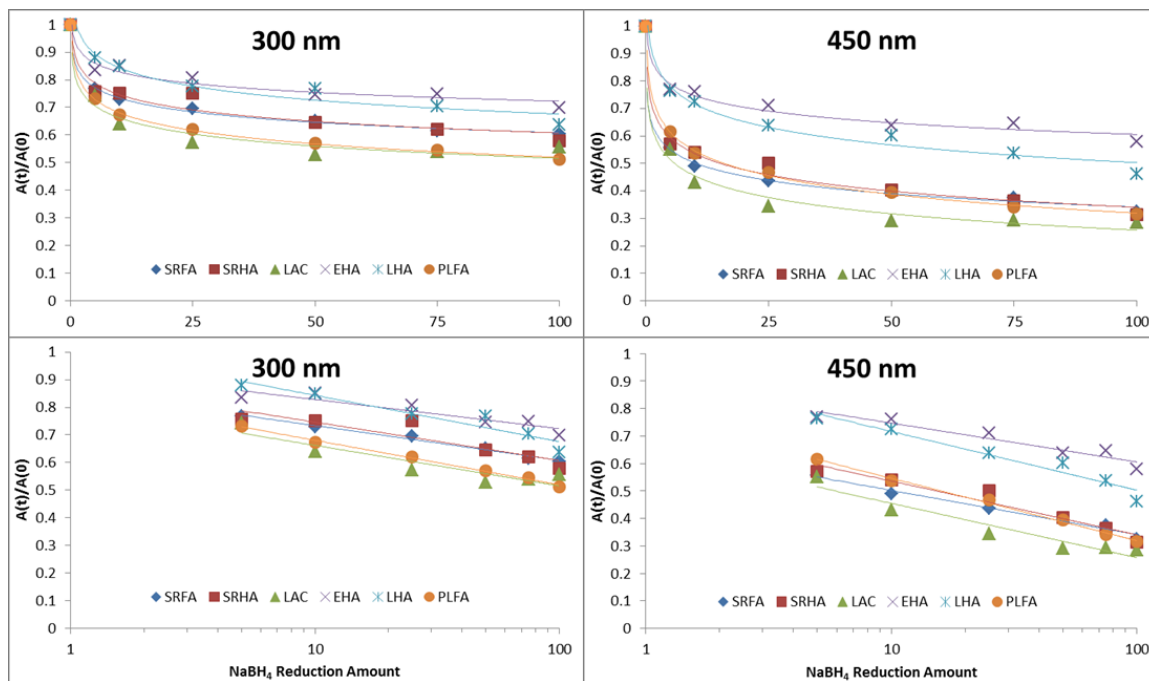


Figure 6. Logarithmic dependence of the fractional absorbance loss (300 nm left and 450 nm right) based on the NaBH₄ reduction amount for each HS at pH 7. Top: x-axis displayed on a linear scale. Bottom: x-axis displayed on a logarithmic scale.

Between the pH 10 pre-column samples and the pH 7 post column samples for each HS, there is an approximately 10 % difference in the fractional loss of absorbance at 450 nm (Tables 2 and 3). For both sets of data, the untreated sample was at the same pH as the reduced samples, meaning there should be no effect of pH on the fractional loss observed. Also, while there was a slight loss in absorbance through the column (<10 %), the untreated sample was passed through the column as well, so all samples were treated in the same fashion. This means that any error associated with the column should have a minimal effect on the fractional loss observed. The most likely cause for this difference is due to the effect of the pH on the optical properties of HS (see also Chap. 3). The absorbance at pH 10 is greater than the absorbance at pH 7 throughout the entire range. This effect has been interpreted as due to an enhancement of charge-transfer interactions from phenolate anions, which are better electron donors than the original phenols. Upon reduction, greater losses are anticipated due to the elimination of a greater number of charge-transfer interactions at pH 10 than at pH 7. This means that upon reduction, the pH 10 samples should have a greater loss in absorbance versus the pH 7 samples.

Table 3. Fractional loss in Absorbance Due to Reduction

	SRFA	SRHA	LAC	PLFA	EHA	LHA
Wavelength	450 300	450 300	450 300	450 300	450 300	450 300
5x	44% 23%	43% 24%	45% 26%	38% 27%	23% 17%	24% 12%
10x	51% 27%	46% 25%	57% 36%	46% 33%	24% 15%	27% 15%
25x	56% 30%	50% 25%	65% 43%	53% 38%	29% 19%	36% 22%
50x	60% 35%	60% 35%	71% 47%	60% 43%	36% 25%	40% 23%
75x	62% 38%	64% 38%	71% 46%	66% 45%	35% 25%	46% 30%
100x	67% 40%	69% 42%	71% 44%	68% 49%	42% 30%	54% 36%

Consistent with previous work, the fluorescence emission is blue shifted at the edge of the visible and significantly enhanced (by 2- to 4-fold) with increasing concentrations of NaBH₄ (Figs. 7-12, D-F; Appendices 11 and 12). Interestingly, the gain in emission (reported as ΔF) exhibited a constant emission maximum with increasing concentrations of NaBH₄ (Figs. 7-12 E) possibly indicating that it originated from a discrete species that is no longer quenched by the acceptors. In contrast, the fluorescence emission in the visible region decreased (by ~ 20%) over the red edge of the spectrum with increasing concentrations of NaBH₄ (Figs. 7-12, G-I), particularly for SRFA and PLFA causing the ΔF to be < 0 (Figs. 7 and 10, H). Such a decrease was not as obvious for the rest of the HS due to the greater gain in fluorescence on the blue edge of the spectrum. This emission loss is consistent with the loss of emission from charge-transfer interactions that are eliminated upon reduction.

While this reduction was completed using the mass of NaBH₄ to the mass of HS for the calculations, it would be possible to extend this work into a mole ratio of NaBH₄ to carbon. Using the concentration of carbon for each HS (see chap 1), the results would be as follows in Table 4.⁸ With the exception of LAC, the average mole ratio for the 25-fold mass excess reduction for each HS is approximately 15, which could be used in place of the mass-to-mass ratio.

Table 4. NaBH₄ to Carbon Mole Ratios

	SRFA	SRHA	LAC*	PLFA	EHA	LHA
5x	3.05	3.01	7.22	3.03	2.74	2.50
10x	6.10	6.01	14.42	6.05	5.47	4.99
25x	15.23	15.00	36.00	15.11	13.66	12.45
50x	30.54	30.10	72.18	30.31	27.38	24.97
75x	45.77	45.08	108.18	45.42	41.03	37.42
100x	61.00	60.08	144.18	60.53	54.69	49.87

Note: IHSS data provided %C (*LAC determined by TOC); mass of carbon was determined by multiplying %C by the mass of HS per sample.⁸ The resulting masses were converted to moles of carbon; the molar ratios were determined by dividing moles of NaBH₄ added by moles of carbon.

Another potential issue to note is that the concentration of HS could impact the kinetics of the reduction. The concentration observed for all these experiments was 100 mg/L. A higher concentration of HS could have a longer reduction time frame.

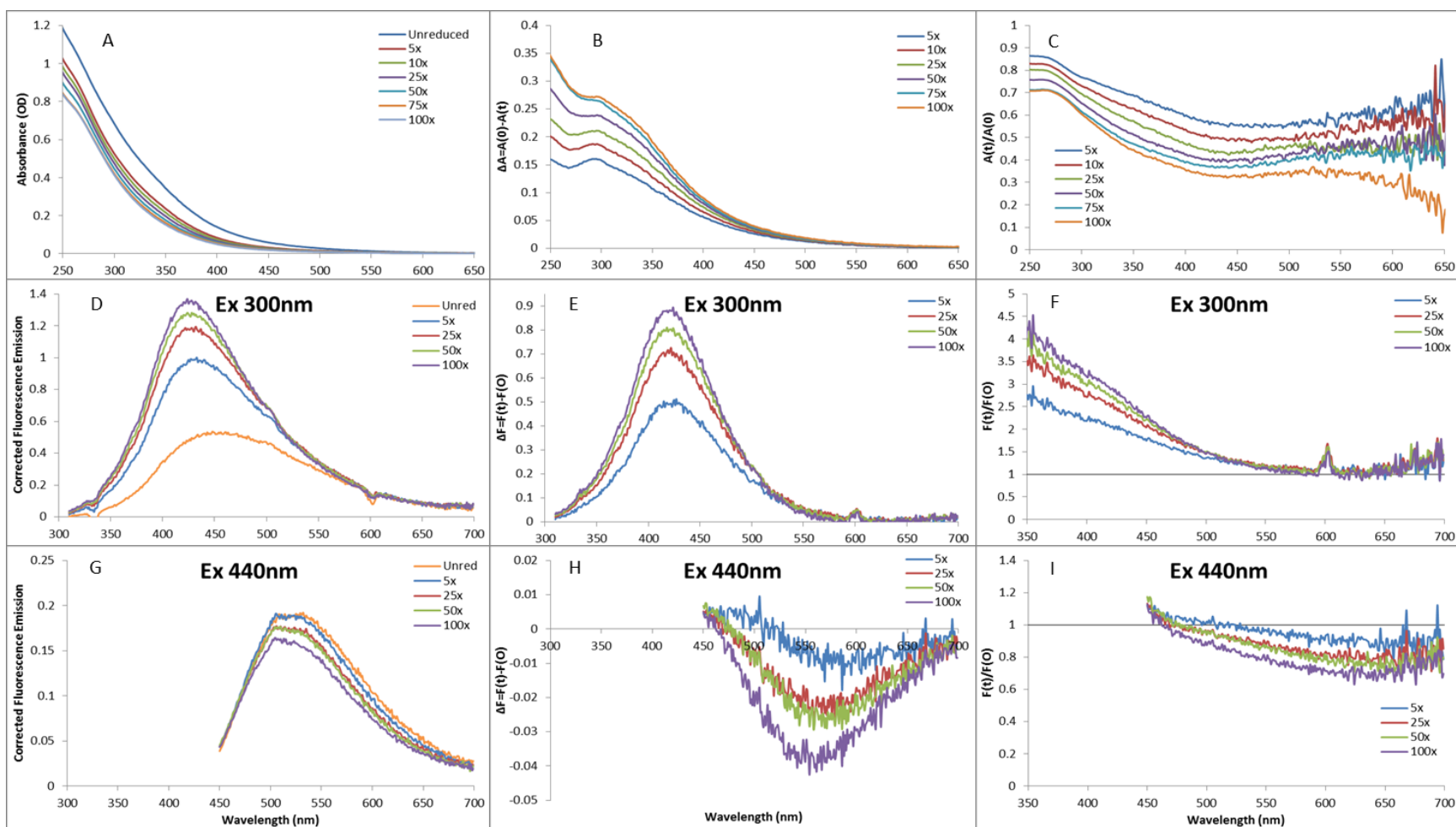


Figure 7. Optical changes upon reduction for SRFA adjusted to pH 7. Left panel, from top to bottom: Absorbance (A); Fluorescence emission spectra (D, excitation 300 nm; G, excitation 440 nm). Middle panel, from top to bottom, ΔA (B), where $\Delta A > 0$ indicates a loss in absorbance; ΔF (E, excitation 300 nm; H, excitation 440 nm), where $\Delta F > 0$ represents a gain in fluorescence signal while $\Delta F < 0$ represents a loss in fluorescence signal. Right panel, from top to bottom, $A(t)/A(0)$ (C), < 1 indicates a loss in absorbance; $F(t)/F(0)$ (F, excitation 300 nm; I, excitation 440 nm), where > 1 represents a gain in fluorescence signal while < 1 represents a loss in fluorescence signal.

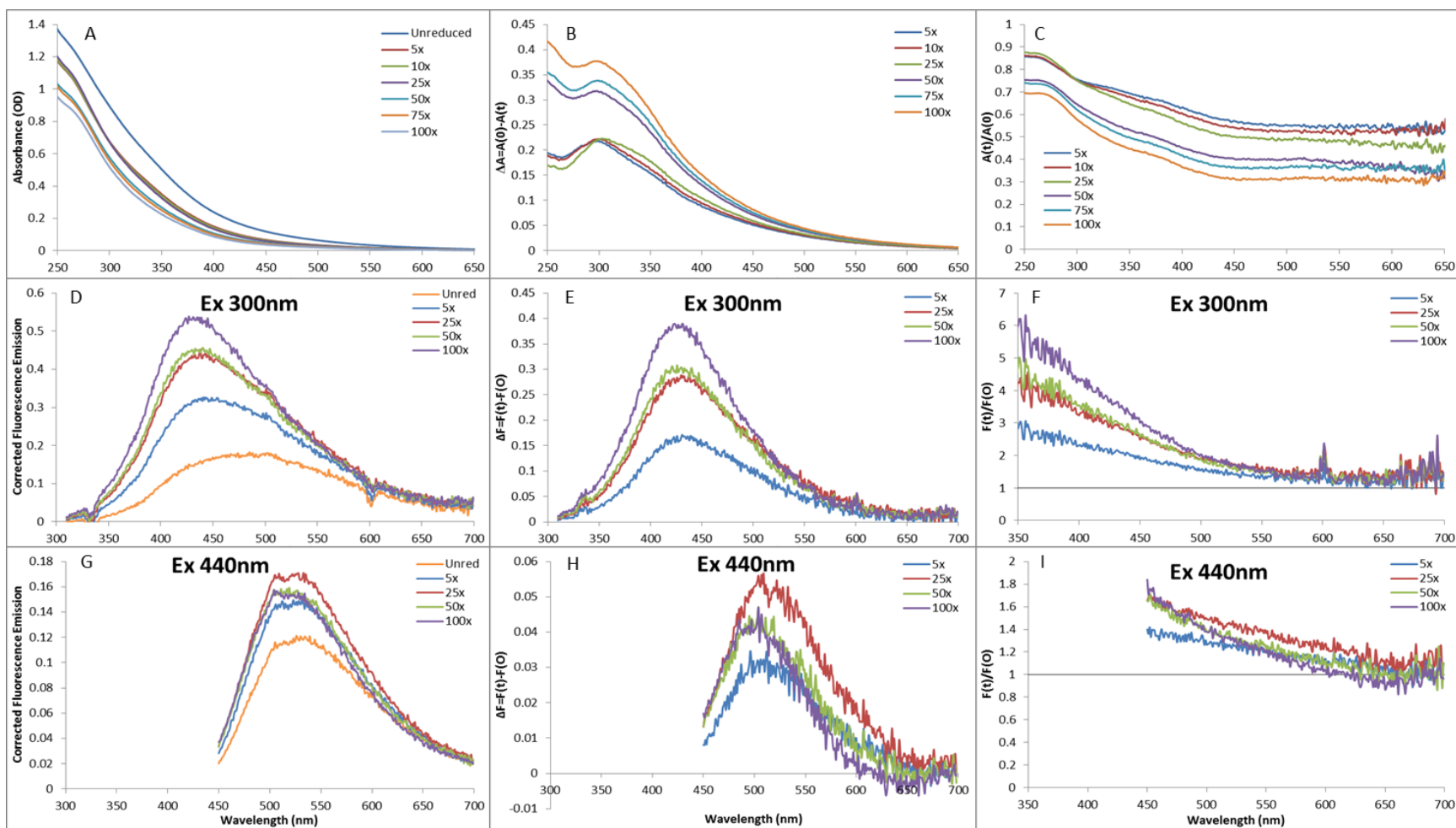


Figure 8. Optical changes upon reduction for SRHA adjusted to pH 7. Left panel, from top to bottom: Absorbance (A); Fluorescence emission spectra (D, excitation 300 nm; G, excitation 440 nm). Middle panel, from top to bottom, ΔA (B), where $\Delta A > 0$ indicates a loss in absorbance; ΔF (E, excitation 300 nm; H, excitation 440 nm), where $\Delta F > 0$ represents a gain in fluorescence signal while $\Delta F < 0$ represents a loss in fluorescence signal. Right panel, from top to bottom, $A(t)/A(0)$ (C), < 1 indicates a loss in absorbance; $F(t)/F(0)$ (F, excitation 300 nm; I, excitation 440 nm), where > 1 represents a gain in fluorescence signal while < 1 represents a loss in fluorescence signal.

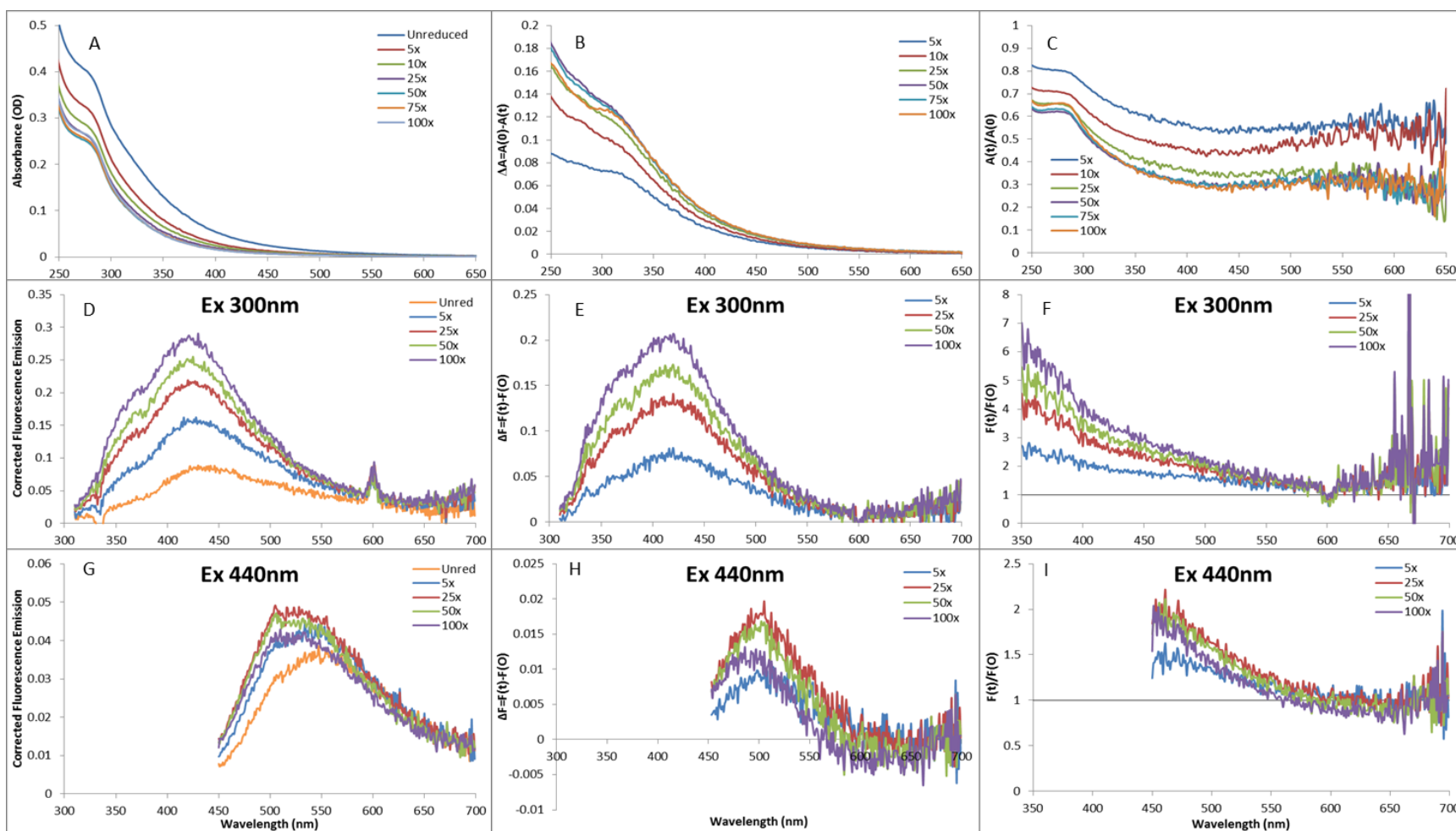


Figure 9. Optical changes upon reduction for LAC adjusted to pH 7. Left panel, from top to bottom: Absorbance (A); Fluorescence emission spectra (D, excitation 300 nm; G, excitation 440 nm). Middle panel, from top to bottom, ΔA (B), where $\Delta A > 0$ indicates a loss in absorbance; ΔF (E, excitation 300 nm; H, excitation 440 nm), where $\Delta F > 0$ represents a gain in fluorescence signal while $\Delta F < 0$ represents a loss in fluorescence signal. Right panel, from top to bottom, $A(t)/A(0)$ (C), < 1 indicates a loss in absorbance; $F(t)/F(0)$ (F, excitation 300 nm; I, excitation 440 nm), where > 1 represents a gain in fluorescence signal while < 1 represents a loss in fluorescence signal.

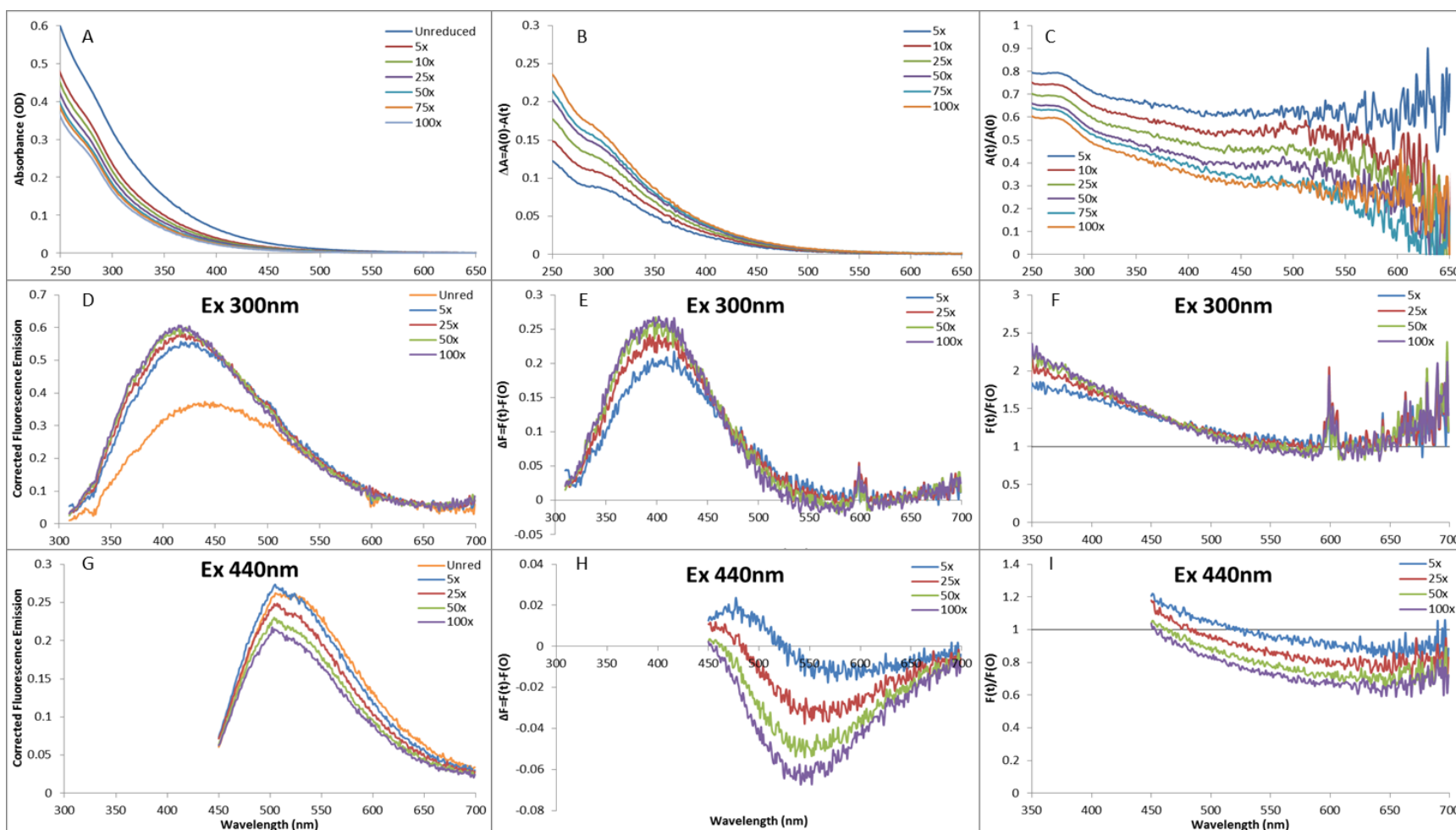


Figure 10. Optical changes upon reduction for PLFA adjusted to pH 7. Left panel, from top to bottom: Absorbance (A); Fluorescence emission spectra (D, excitation 300 nm; G, excitation 440 nm). Middle panel, from top to bottom, ΔA (B), where $\Delta A > 0$ indicates a loss in absorbance; ΔF (E, excitation 300 nm; H, excitation 440 nm), where $\Delta F > 0$ represents a gain in fluorescence signal while $\Delta F < 0$ represents a loss in fluorescence signal. Right panel, from top to bottom, $A(t)/A(0)$ (C), < 1 indicates a loss in absorbance; $F(t)/F(0)$ (F, excitation 300 nm; I, excitation 440 nm), where > 1 represents a gain in fluorescence signal while < 1 represents a loss in fluorescence signal.

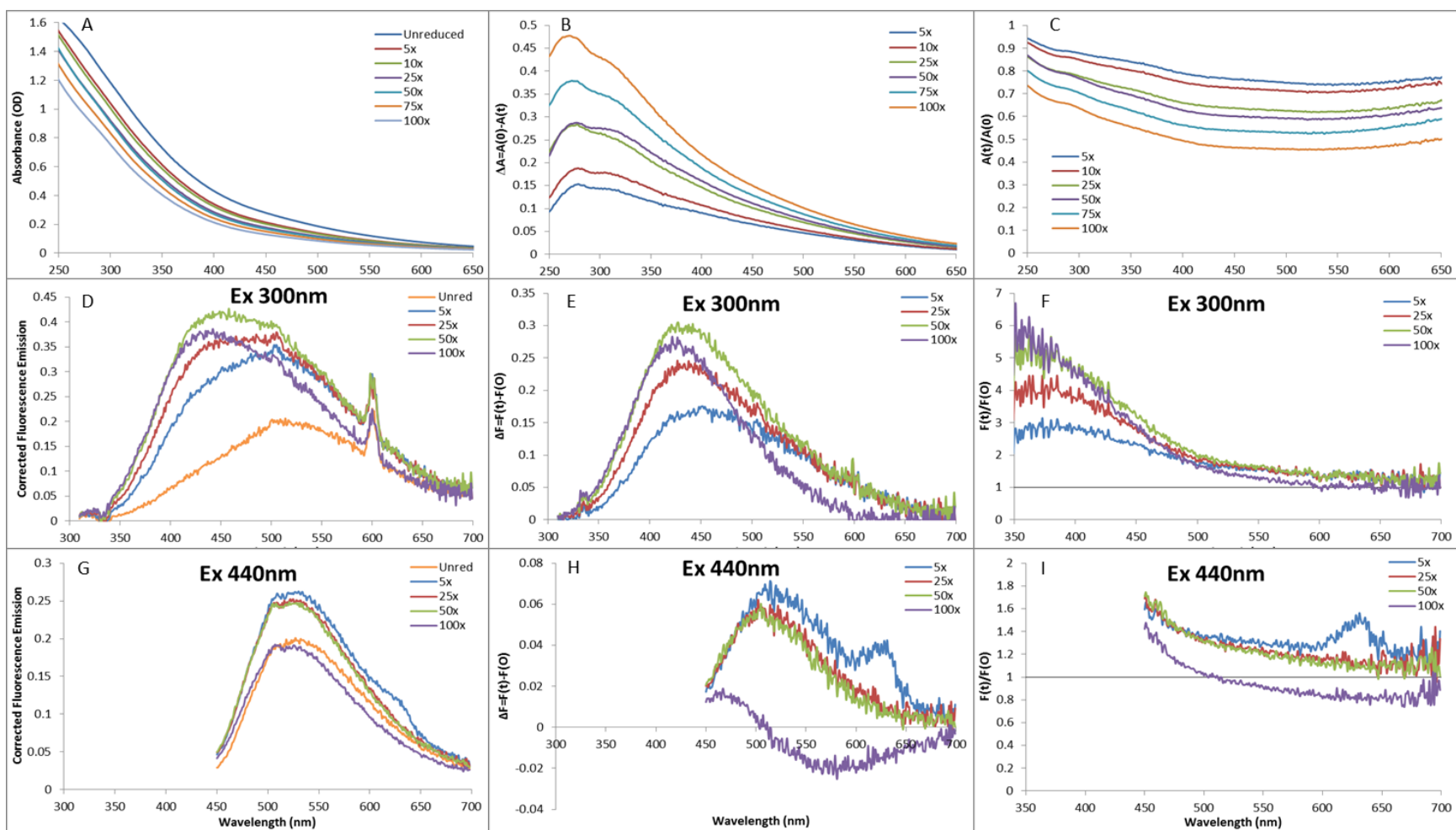


Figure 11. Optical changes upon reduction for LHA adjusted to pH 7. Left panel, from top to bottom: Absorbance (A); Fluorescence emission spectra (D, excitation 300 nm; G, excitation 440 nm). Middle panel, from top to bottom, ΔA (B), where $\Delta A > 0$ indicates a loss in absorbance; ΔF (E, excitation 300 nm; H, excitation 440 nm), where $\Delta F > 0$ represents a gain in fluorescence signal while $\Delta F < 0$ represents a loss in fluorescence signal. Right panel, from top to bottom, $A(t)/A(0)$ (C), < 1 indicates a loss in absorbance; $F(t)/F(0)$ (F, excitation 300 nm; I, excitation 440 nm), where > 1 represents a gain in fluorescence signal while < 1 represents a loss in fluorescence signal.

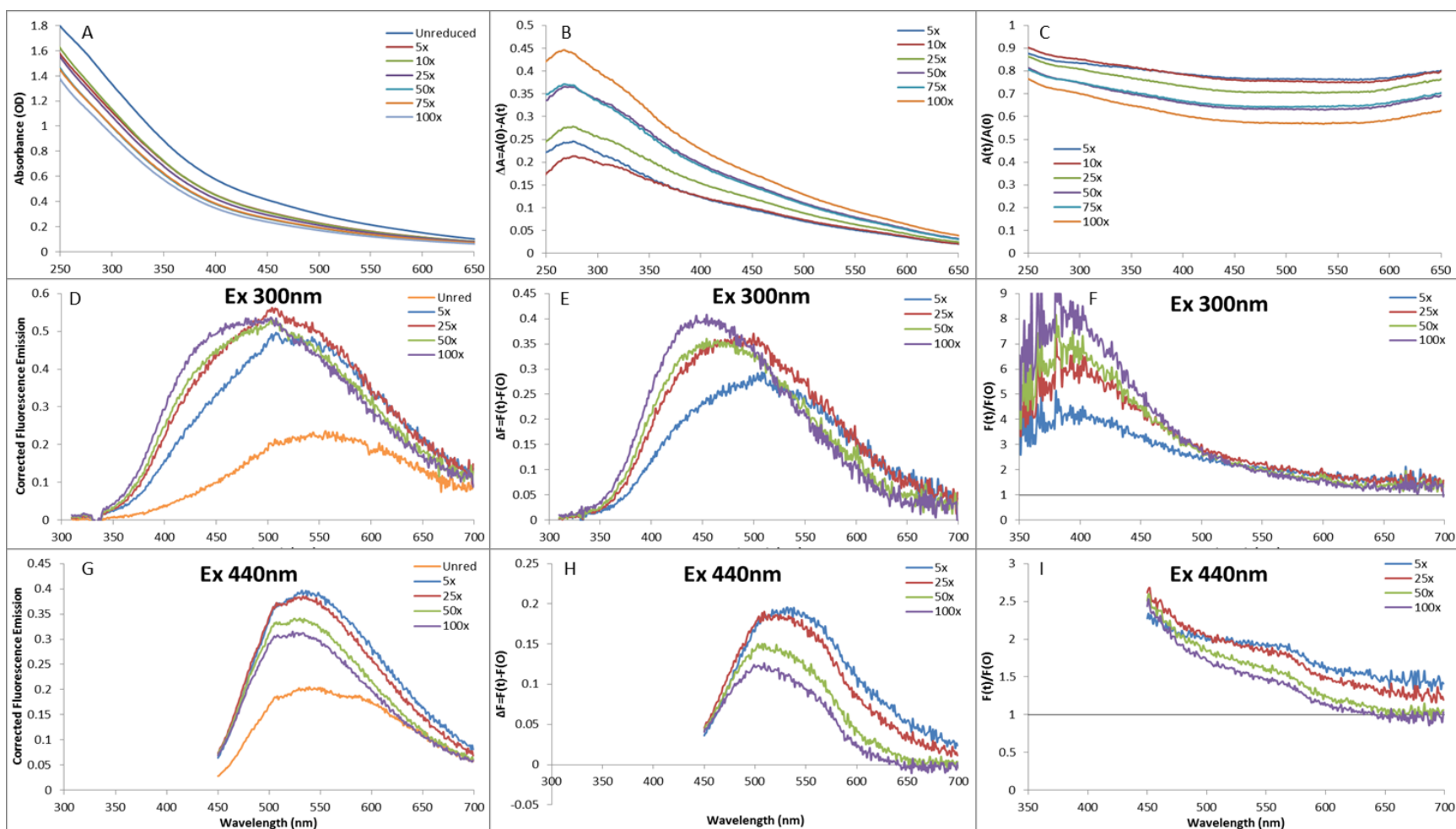


Figure 12. Optical changes upon reduction for EHA adjusted to pH 7. Left panel, from top to bottom: Absorbance (A); Fluorescence emission spectra (D, excitation 300 nm; G, excitation 440 nm). Middle panel, from top to bottom, ΔA (B), where $\Delta A > 0$ indicates a loss in absorbance; ΔF (E, excitation 300 nm; H, excitation 440 nm), where $\Delta F > 0$ represents a gain in fluorescence signal while $\Delta F < 0$ represents a loss in fluorescence signal. Right panel, from top to bottom, $A(t)/A(0)$ (C), < 1 indicates a loss in absorbance; $F(t)/F(0)$ (F, excitation 300 nm; I, excitation 440 nm), where > 1 represents a gain in fluorescence signal while < 1 represents a loss in fluorescence signal.

As with the absorbance data, the fluorescence emission showed a logarithmic increase in intensity with increasing NaBH_4 reduction that plateaued at the 25-fold mass excess (Fig. 13). Since the fluorescence emission data follows the same trend as the absorbance data for each HS, it further supports the conclusion that the 25-fold mass excess reduction is a sufficient reduction amount. The fluorescence increase is consistent with the partial elimination of the quenching of the donors by removal of the acceptors as proposed through the charge-transfer model.

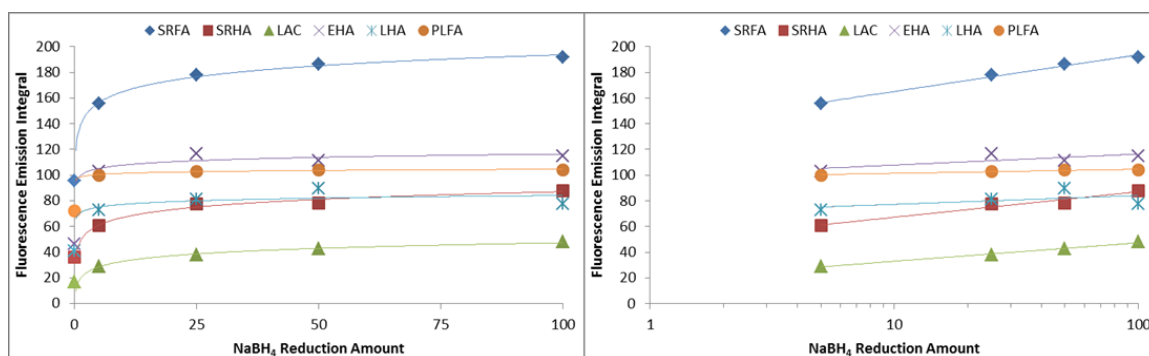


Figure 13. Logarithmic dependence of the fluorescence emission gain (excitation 300 nm, integrated over the 300-700 nm range) based on NaBH_4 reduction amount for humic substance at pH 7. Left: x-axis displayed on a linear scale. Right: x-axis displayed on a logarithmic scale.

Conclusions

Previous research focused mainly on a one to one mass ratio of NaBH_4 to HS as the ideal reduction amount with a 33-fold mass excess being the furthest extent of reduction possible.^{11,16,19} While these chemical reductions seemed to plateau after the 5-fold mass excess addition of NaBH_4 , electrochemical reductions seem to lead to a further reduction in the HS.^{20,21,22} Further, while the HS optical properties were significantly modified by NaBH_4 reduction under a 5-fold mass excess, they were not completely eliminated.

In this work, we showed that a 25-fold mass excess of NaBH_4 was sufficient to induce significant and irreversible losses of absorbance in the visible (~60 %) and gain in fluorescence at the edge of the visible region without compromising the solutions with excess borate. Thereafter, the optical properties of reduced samples continued to change with the increasing amount of NaBH_4 (up to 100-fold mass excess) at a much slower rate. Given the information on the reduction process, the use of the columns, and the overall asymptotical relationship of the absorption and fluorescence data after the reduction is complete, a 25-fold mass excess reduction is considered the ideal standard amount for reduction. There is little benefit gained from further reducing the samples with NaBH_4 and the process to remove the excess borate remaining is substantially more time consuming and less efficient.

In addition, these results are consistent with the charge-transfer model in that reduction showed a decrease in absorption in the visible region and an increase in blue-shifted fluorescence emission. The 25-fold mass excess reduction showed a further increase in reduction effects versus the 5-fold mass excess previously used. The results show that the decrease in absorption at wavelengths greater than 450 nm and increase in fluorescence are consistent with the removal of the charge-transfer interactions that occur between the chromophores in the untreated samples.

The recommended protocol to reduce HS through a standard method would be the use a 25-fold mass excess reduction amount (15 moles NaBH_4/C) of the alkaline solution of NaBH_4 to HS mass. Allow this reduction to run for 72 hours to ensure that the reduction is complete and fully reduced/reoxidized. After the reduction is complete, bring the samples pH back to 7 using concentrated HCl or HClO_4 and run the sample through a

Sephadex G-10 10 cm column. The G-10 column will remove any borate salts in the sample from the reduction, leaving behind a borate free reduced sample that can be used for further analysis.

Chapter 3: Dependence of the Optical Properties of Humic Substances on pH and Borohydride Reduction

Introduction

Different methods have been used in an attempt to define and quantify the relative amount of functional groups present in humic substances (HS). Based on previous studies, it is known that carboxylic acids and phenolic functional groups account for a significant portion of the carbon found in dissolved organic matter (DOM).¹² One set of studies used models such as a modified Henderson-Hasselbach model to determine the ratio of carboxyl to phenolic functional groups in direct acid/base titrations and compared the results to indirect titration models.¹² They determined that the phenolic moieties content was similar for humic and fulvic acids, but aquatic HS had greater amounts of phenolic groups than terrestrial HS.^{8,12} On the other hand, carboxylic acid groups were greater in fulvic acids than humic acids.^{8,12} In addition, while the carboxylic acid contents were consistent between the indirect and the direct titrations, the phenolic groups content was reported as much higher in the indirect method versus the direct method.¹²

Other studies have used pH titrations coupled with the acquisition of absorbance difference spectra to de-convolve the contributions of specific acid/base moieties to the optical properties of HS.^{23, 13} Korshin, et al. showed that absorbance difference spectra could be used as a means to study the chemical nature of species participating in light absorption and emission.¹³ Absorption changes were specifically noted over pK_a ranges corresponding to phenolic moieties and carboxylic acid moieties. Thus, the effect of pH

on various HS can be employed to determine the contribution of specific moieties to the optical properties.^{23, 12, 13}

In this study, pH titrations were conducted on six different HS in both their original and sodium borohydride (NaBH₄) reduced forms, with the changes in optical properties monitored. First, both carboxylic acids and phenolic groups exhibited a pH dependence that extended into the visible, thus suggesting their coupling to charge-transfer interactions. Next, a far greater change in HS optical properties at pH values > 8 could be noted, indicating a possible increase in charge-transfer interactions due to the deprotonation of phenols to phenolate anions, which are better electron donors.⁵ Further, the reduced samples show much less change in the optical properties as compared with the untreated samples, which can be explained as a decrease in charge-transfer interactions following reduction of acceptors. Last, while the carboxylic acids contribution is about uniform among HS and is unaffected by reduction (except for the visible absorption), the phenolic moieties contribution varies more substantially among samples and with reduction. All of these observations are consistent with the charge-transfer model of the optical properties of these materials.

Material and Methods

Materials. Suwannee River fulvic and humic acid (SRFA; Lot 2S101F and SRHA; Lot 2S101H), Pony Lake fulvic acid (PLFA; Lot 1R109F), Leonardite humic acid (LHA; Lot 1S104H-5), and Elliot Soil humic acid (EHA; Lot 1S102H) were obtained from the International Humic Substances Society (IHSS). Alkali-extracted and carboxylated lignin (LAC; Lot 19714 DS) was obtained from Sigma-Aldrich. Sodium borohydride (NaBH₄;

Lot 083480B) was obtained from Fisher Scientific. Sephadex G-10 (Lot SLBF7082V) was obtained from Sigma-Aldrich. Fluka Analytical Trace Select sodium hydroxide solution (NaOH; 30%; Lot BCBK1724V) was obtained from Sigma-Aldrich. ACS grade perchloric acid (HClO₄; Lot 117272) was obtained from Fisher Scientific. Quinine sulfate (QS) was obtained from MC/B. Water was obtained from a Milli-Q Plus purification system (Millipore). Tumeric Analytical Test Strips were obtained from Scientific Equipment of Houston (Lot 4012).

Apparatus. A Shimadzu UVPC 2401 spectrophotometer was employed to acquire UV-visible absorption spectra. An Aminco-Bowman AB-2 luminescence spectrometer was employed for the fluorescence measurements (monochromator excitation and emission band-passes set to 4 nm). A Thermoscientific micro pH electrode coupled to an Orion 4 Star pH ISE bench top meter was employed for the pH measurements.

Optical Measurements. Absorption spectra were recorded using 1-cm quartz cuvettes over the range from 190 to 820 nm against air and were MQ subtracted afterward. Fluorescence emission spectra were collected over the 280 to 600 nm excitation range, while the absorbance was kept at < 0.05-0.1 OD at the excitation wavelength.⁷ Emission spectra were MQ subtracted and corrected for the instrument response applying correction factors provided by the manufacturer.

Borohydride (NaBH₄) reductions. Three milliliters of 100 mg/L concentrations of SRFA, SRHA, LAC, PLFA, LHA, and EHA in MQ adjusted to pH 7 were transferred to 1-cm cuvettes. Solid NaBH₄ was added at a 5-fold, 25-fold, and 50-fold mass excess of NaBH₄ to HS. Samples were treated in the dark under aerated conditions. Due to the

large amounts of borate remaining after the reduction process, a G-10 column was used to adjust the pH back down to approximately 7 and remove the excess salt (see chap 2).¹¹

pH Titration. The pH meter was calibrated with pH 1.68, 4.01, 7.00, 10.01, and 12.46 buffer solutions prior to running any titrations each day with a calibration R^2 greater than 98%. In addition, the pH 7.00 buffer was checked prior to each sample titration to ensure an accurate calibration. HClO_4 (0.25 M) and NaOH (0.25 M and 0.125 M) were used to control the pH of the solutions.¹³ The untreated and the 25-fold reduced samples were brought down to pH 2 using the HClO_4 (0.25 M) and their absorbance was recorded. NaOH (0.25 M) was then added to the pH 2 samples to increase the pH to 12, taking the absorbance of each sample at approximately 1-pH unit intervals. From approximately pH 5 to approximately pH 9, NaOH (0.125 M) was used to ensure the pH did not rise too quickly. Additionally, to test whether the extent of reduction had an effect on the pH titration, the pH dependence of the optical properties was investigated for SRFA reduced at the 5-fold, 25-fold, and 50-fold mass excess following the above procedures. All of the samples were corrected for dilution effects from the acid and base additions prior to processing the data.

Results and Discussion

Optical properties of HS. The absorption and fluorescence properties of untreated and NaBH_4 -reduced HS were investigated at neutral pH (~ 7). Consistent with previous studies, untreated SRFA and SRHA show absorption spectra that have no discernable absorbance bands and decrease exponentially with increasing wavelength (Fig. 14, inset).^{7,10,9} Similarly, untreated EHA, LHA, PLFA and LAC also show featureless

spectra (Fig. 14, inset). However, at equivalent mass concentrations, untreated EHA and LHA absorb farther into the visible than the other HS examined in this study.

As previously reported, untreated SRFA, SRHA and LAC exhibited fluorescence emission maxima that remained constant (at ~ 450 nm) for excitation < 350 nm.¹⁰ Thereafter, the emission maxima continuously red-shifted and decreased in intensity with increasing excitation wavelength. Further, the emission spectra at longer excitation wavelengths always fell within the emission spectra acquired at shorter excitation wavelengths (Fig. 14). Untreated PLFA exhibited similar fluorescence properties, although it showed slightly blue-shifted emission maxima (at ~ 425 nm) for excitation < 350 nm (Fig. 14). In contrast, terrestrial HS exhibited much greater Stokes shifts and longer wavelength emission maxima (at ~ 500 and 550 nm for LHA and EHA, respectively) that were also constant for excitation < 450 nm. Thereafter, the emission maxima continuously red-shifted and decreased in value with increasing excitation wavelength (Fig. 14).

The emission spectra reported herein for untreated HS (Fig. 14) were collected at approximately the same absorbance values at 300 nm (Appendix 11). Despite the similar absorbance values, the fluorescence emission decreased in intensity as follow: SRFA>PLFA>SRHA~LHA~EHA>LAC, indicating greater quantum yields for fulvic than humic acids, consistent with other work.⁷ A similar trend was observed for the emission maxima, which showed larger degree in the red shift of emission with increasing excitation wavelength for PLFA, SRFA, and LAC versus SRHA, LHA, and EHA.

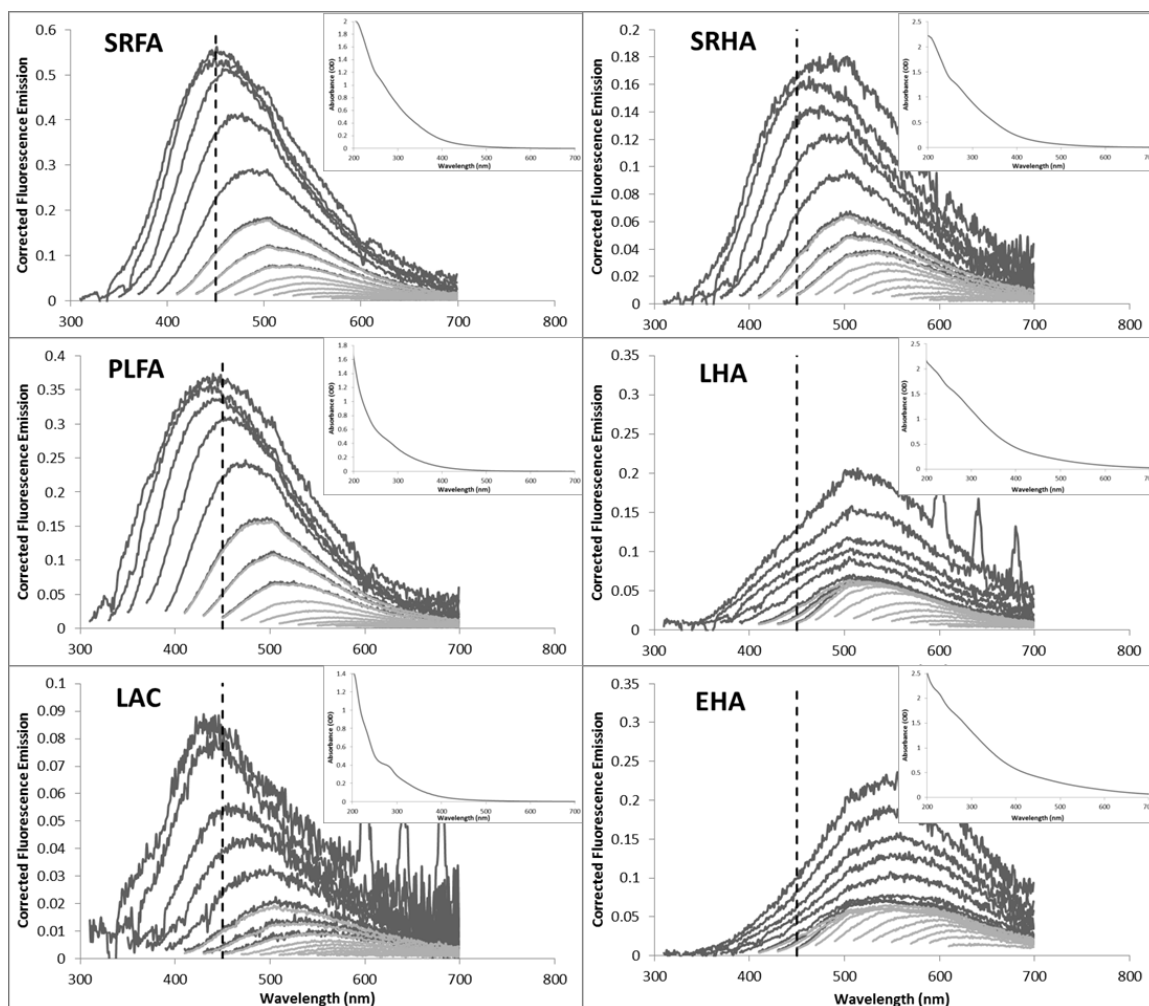


Figure 14. Fluorescence emission spectra at pH 7 for excitation 300-440 nm (black) and 400-600 nm (gray), exciting every 20 nm at the concentrations reported below and the corresponding absorbance for each HS at 100 mg/L pH 7 inset. SRFA was 25 mg/L, SRHA was 16 mg/L, PLFA and LAC were 40 mg/L and EHA and LHA were 10 mg/L for the visible region. SRFA, PLFA and LAC were 10 mg/L, SRHA was 5 mg/L, and EHA and LHA were 3 mg/L for the UV region.

Upon NaBH_4 reduction, the HS optical properties were significantly altered consistent with previous work and with the charge-transfer model.¹¹ As noted in chapter 2, a substantial and mostly irreversible decrease in absorption more significant over the visible range (~60 % at > 450 nm for the 25-fold mass excess reduction) was observed for SRFA, SRHA, LAC and PLFA, with much smaller losses observed for LHA and EHA (~35 % at > 450 nm for the 25-fold mass excess reduction). All HS exhibited a blue-shifted emission that was enhanced by 2- to 3-fold. LHA and EHA exhibited the

largest blue shift (~50 nm), while SRFA, SRHA, and PLFA were intermediate (~30 nm), and LAC was the smallest (~10 nm) (Fig. 15; Appendix 13). For all of the samples, while the absorbance decreased with reduction over the visible wavelengths, the fluorescence increased in the far visible and decreased in the visible.

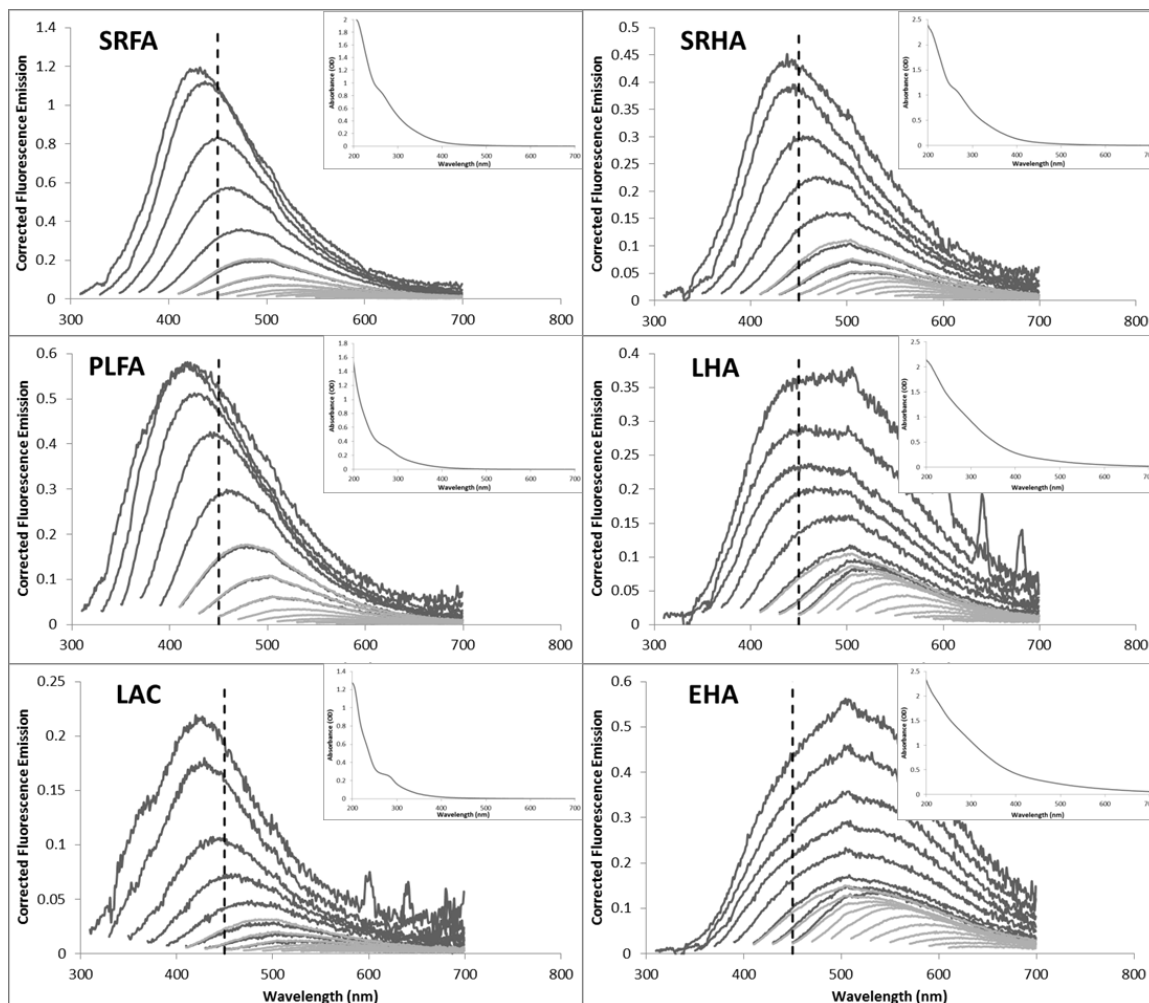


Figure 15. Fluorescence emission spectra at pH 7 for a 25-fold mass of borohydride for excitation 300-440 nm (black) and 400-600 nm (gray), exciting every 20 nm with concentrations reported below and the corresponding absorbance for each reduced HS pH 7 inset. SRFA was 25 mg/L, SRHA was 16 mg/L, PLFA and LAC were 40 mg/L and EHA and LHA were 10 mg/L for the visible region. SRFA, PLFA and LAC were 10 mg/L, SRHA was 5 mg/L, and EHA and LHA were 3 mg/L for the UV region.

pH dependence of the optical properties of untreated HS. As reported above,

the HS within this study exhibited broad and featureless absorption spectra that decreased

approximately exponentially with increasing wavelength; this spectral shape was maintained across the entire pH range investigated (pH 2-12) (Fig. 16; Appendix 14). However, as the pH increases, the absorbance increases throughout the entire range, but particularly in the visible region,¹³ with the higher pH producing a greater increase in this absorbance. Of all the samples examined, PLFA exhibited the least pH dependence across the entire wavelength range.

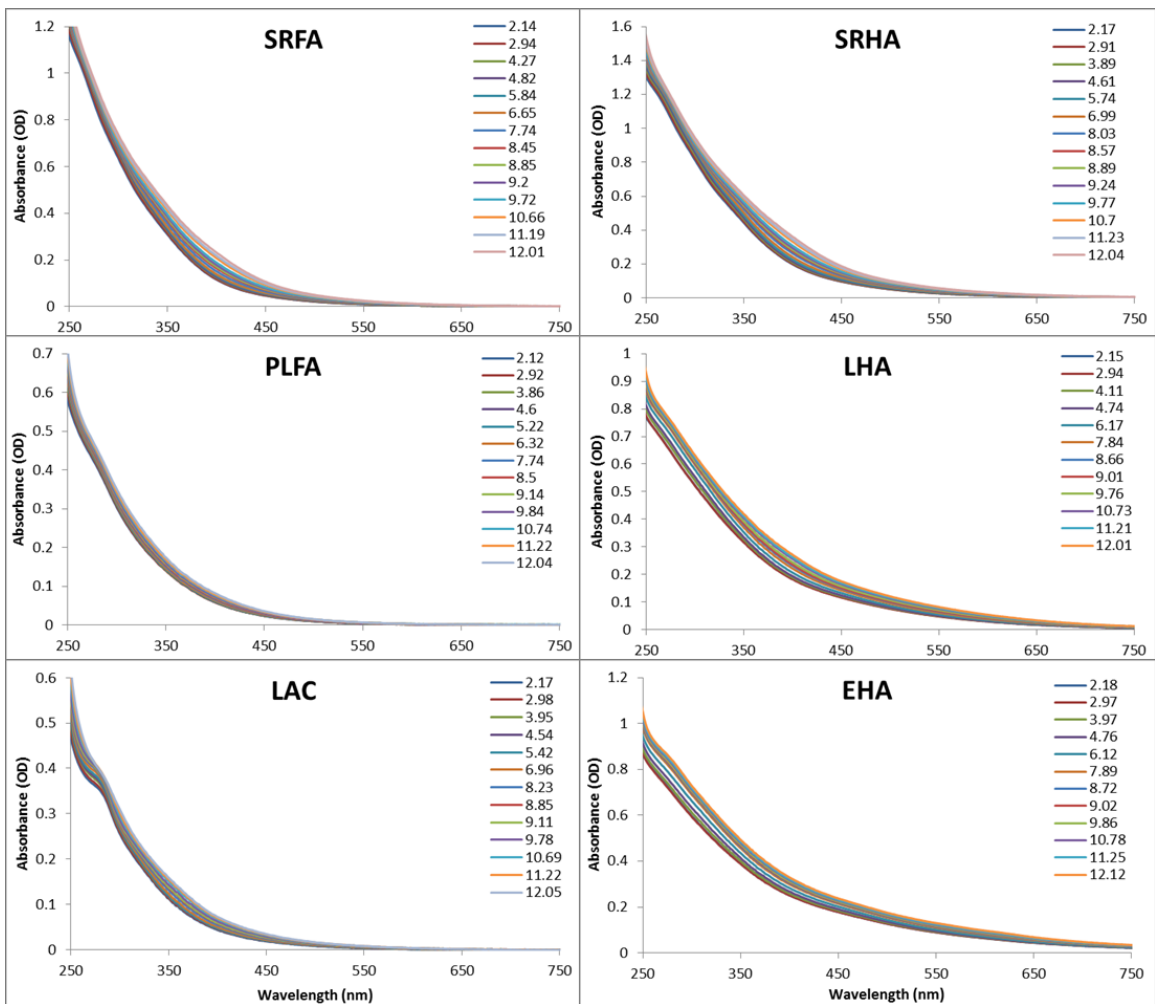


Figure 16. Dependence of the absorption spectra on pH following corrections for dilution. SRFA and SRHA were 50 mg/L, LAC was 43 mg/L, PLFA was 44 mg/L, and LHA and EHA were 25 mg/L.

A general trend was noted in each of the titrations conducted; the pH stabilized quickly in the range from 2 to 5 and from 9 to 12, taking about 15 seconds to stabilize and then remaining constant. However, from 5 to 9, the pH took longer to stabilize (a couple of minutes). A similar response was noted by Ritchie and Perdue in their study of HS.¹² While the origin of this effect is still unknown, the leading hypothesis is that the proton dissociation is coupled with a slower secondary reaction, and thus is not a simple acid dissociation.¹²

Because the absorbance was greatest at pH 12, the pH 12 spectrum was used as a reference to calculate the fractional absorption loss with decreasing pH (Fig. 17; Table 5). While there was a substantial decrease in absorption from pH 12 to pH 6 (~15-50 % depending on the HS and wavelength), very little changes occurred from pH 6 to pH 2 (~10 %). In all cases, the largest losses were observed across the visible wavelengths. While SRFA, SRHA, LAC and PLFA exhibited minimal absorption loss at short wavelengths, (< 10 % at < 300 nm) the loss significantly increased with increasing wavelength (> 50 % at > 400 nm). EHA and LHA exhibited less loss that was more uniform with wavelength and that never exceeded ~30%.

The increase in absorbance at long wavelengths at higher pH is consistent with an enhancement of charge-transfer interactions. At pH > 8, the phenolic groups would be deprotonated. Because the corresponding phenolate anions are better electron donors⁵, an increase in charge-transfer interactions could be expected and would produce an increase in absorbance over long wavelengths.

Table 5. Loss in absorbance due to pH for untreated HS

	SRFA	SRHA	LAC	PLFA	LHA	EHA
Wavelength	450 300	450 300	450 300	450 300	450 300	450 300
pH 10	22% 5%	17% 4%	16% 8%	13% 5%	10% 3%	5% 3%
pH 8	40% 7%	30% 6%	29% 10%	23% 8%	19% 6%	9% 5%
pH 6	48% 8%	40% 7%	41% 13%	28% 10%	24% 8%	15% 9%
pH 4	52% 10%	45% 11%	42% 14%	33% 11%	31% 14%	22% 16%
pH 2	56% 14%	48% 14%	46% 17%	35% 13%	32% 17%	25% 18%

Note: pH 12 is used as the reference sample.

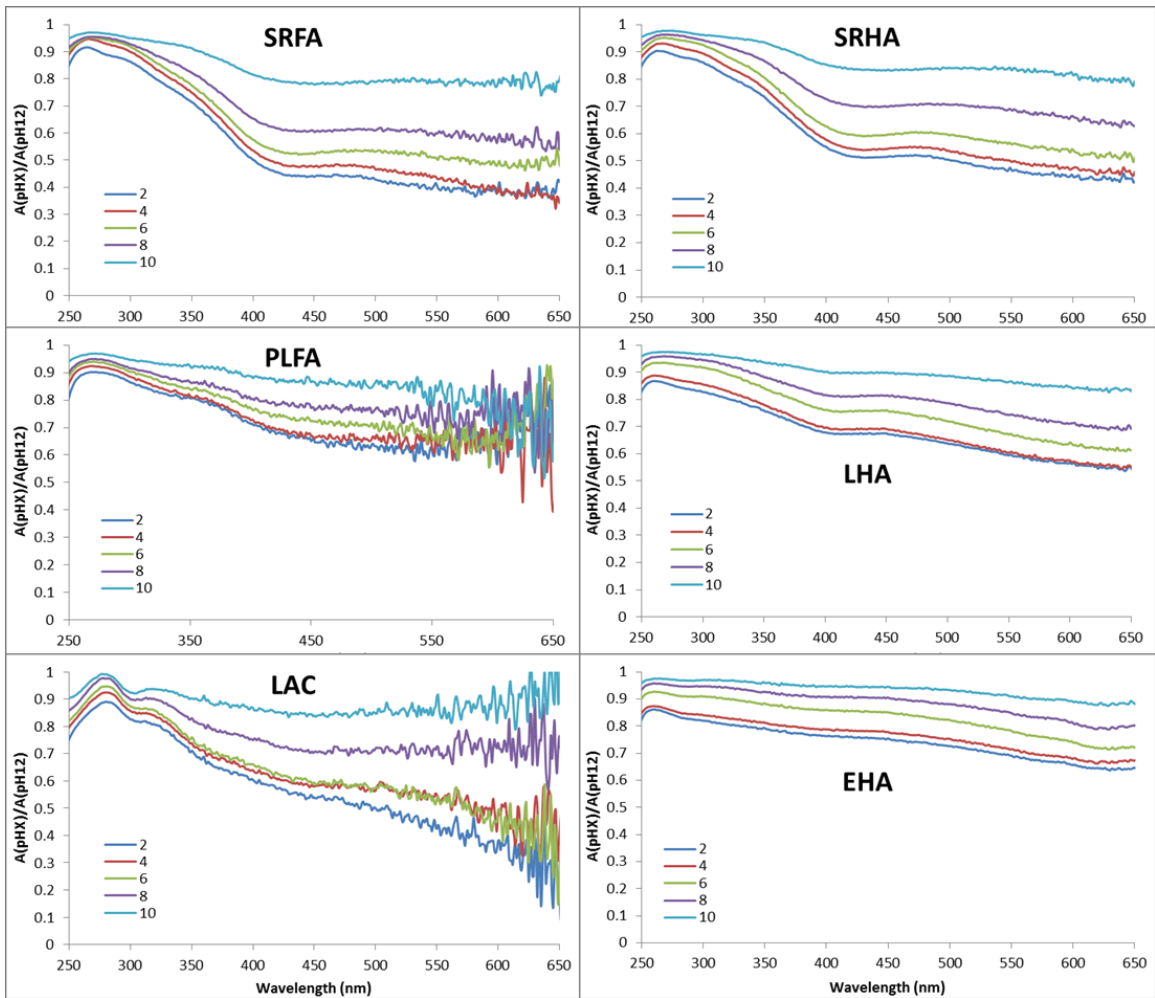


Figure 17. Fractional loss of absorbance due to change in pH, relative to pH 12.

In an effort to gain more insight into the moieties producing the spectral changes, the absorbance difference spectra were analyzed. Following the procedures presented previously by Dryer et. al.¹³, the samples were mass normalized and the absorption difference spectra were calculated. Three difference spectra were acquired. The first was the total difference spectra, which used the pH 2 absorbance as the reference absorbance and encompassed the entire range up to pH 12. The second and third spectra looked at the specific contributions over the pH ranges corresponding to the deprotonation of the carboxylic acids and phenolic moieties. Previous data has shown that the pK_a range for carboxylic acids is between approximately 3 and 5, while the phenolic groups pK_a range is greater than 8.¹² Thus, the reference absorbance spectrum for the carboxylic acid groups was the spectrum at pH 3 and for the phenolic groups was that at pH 8.¹³

The total difference spectra for all HS studied exhibited contributions from both carboxylic acids and phenolic groups (Fig. 18).¹³ Similar to results from previous studies, at pH < 6, all the difference spectra show a peak at approximately 280 nm attributed to the deprotonation of aromatic carboxylic acids that extended into the visible (Fig. 19).²³ At pH > 8, a broad peak at approximately 300-400 nm that also extended into the visible was noted for all HS (Fig. 20). These results show that there are two distinct sets of chromophores that contribute to the optical properties of these samples at different pHs. While the pH dependence of the absorbance at short wavelength can be directly attributed to individual chromophores, specifically the carboxylic acids and phenolic groups as they absorb in the UV, the absorbance at longer wavelength cannot be attributed to individual chromophores and possibly arises from charge-transfer interactions between donors (aromatic carboxylic acids and phenol moieties) and acceptors (carbonyls). The

carboxylic acids content based on optical properties is larger for humic acids than for fulvic acids, despite the fact that there are less carboxylic acids in humic acids than fulvic acids (Fig. 19).¹² Contrarily, the content of phenol moieties (based on optical measurements) is fairly constant among different samples, with the exception of LAC and PLFA (Fig. 20; Appendices 16 and 18).

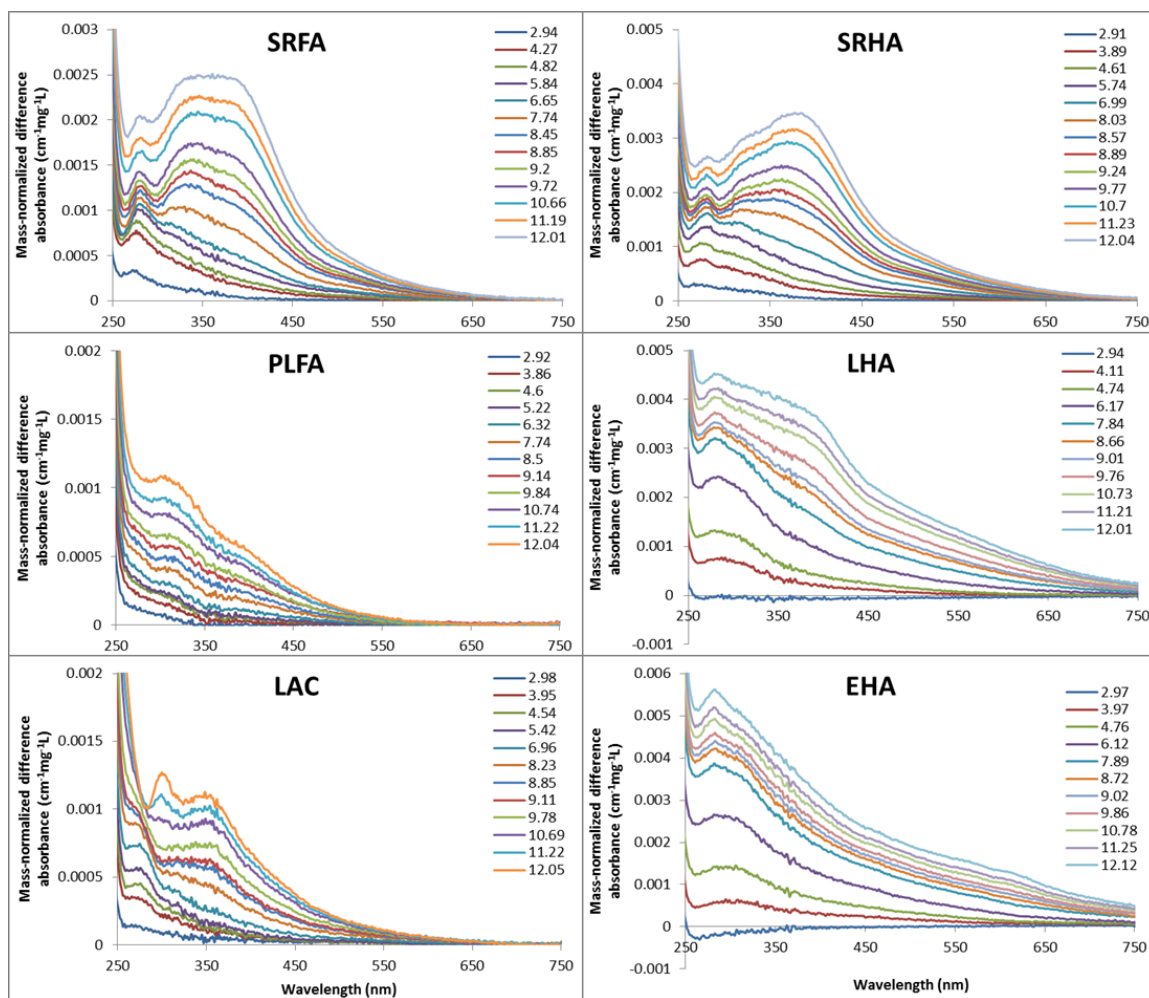


Figure 18. Mass normalized total difference spectra for each untreated HS. The pH 2 spectra serve as the reference spectra for each sample. SRFA and SRHA were 50 mg/L, LAC was 43 mg/L, PLFA was 44 mg/L, and LHA and EHA were 25 mg/L.

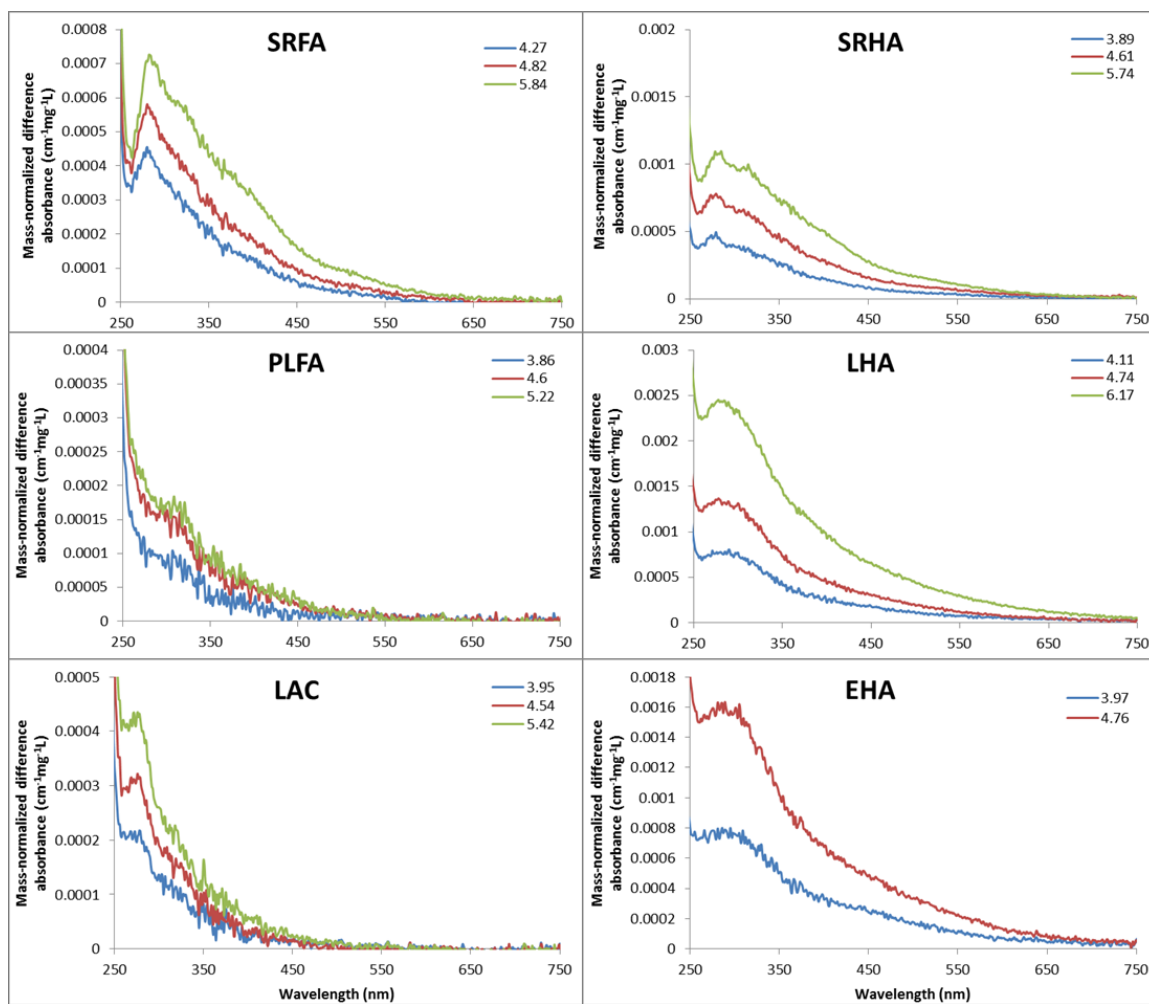


Figure 19. Mass normalized carboxylic acids difference spectra for each untreated HS over the carboxylic acids pK_a range. The pH 3 spectra serve as the reference spectra for each sample. SRFA and SRHA were 50 mg/L, LAC was 43 mg/L, PLFA was 44 mg/L, and LHA and EHA were 25 mg/L.

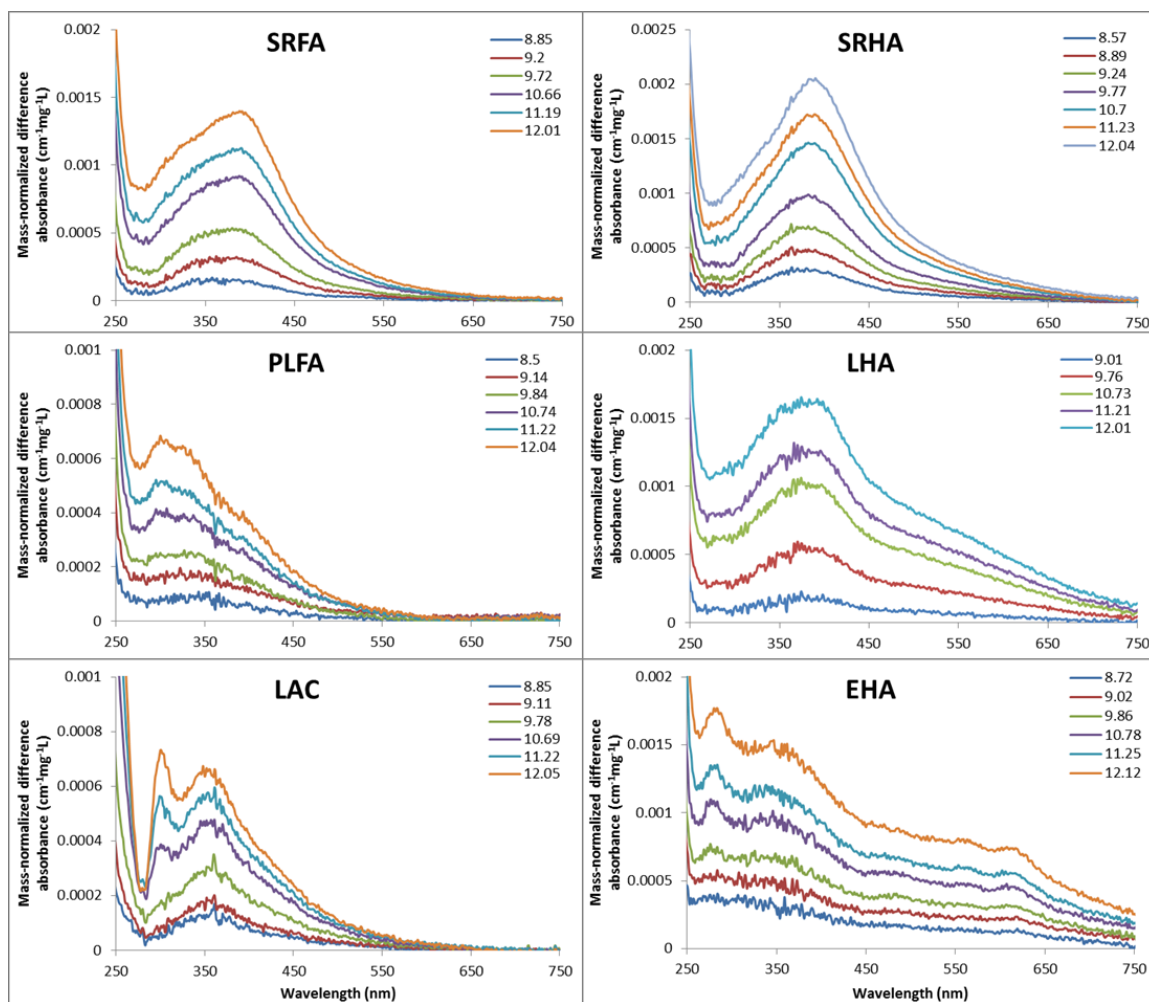


Figure 20. Mass normalized phenolic groups difference spectra for each untreated HS over the phenolic groups pK_a range. The pH 8 spectra serve as the reference spectra for each sample. SRFA and SRHA were 50 mg/L, LAC was 43 mg/L, PLFA was 44 mg/L, and LHA and EHA were 25 mg/L.

pH dependence of the optical properties of borohydride-reduced HS. As previously noted, borohydride reduction preferentially removes the long wavelength absorption relative to the untreated samples due to the removal of one class of possible acceptors (aromatic ketones/aldehydes), which results in the loss of the charge-transfer interactions (Fig. 21; Table 6; Appendices 14 and 15).

Table 6. Loss in absorbance due to pH for reduced HS

	SRFA	SRHA	LAC	PLFA	LHA	EHA
Wavelength	450 300	450 300	450 300	450 300	450 300	450 300
pH 10	18% 6%	15% 5%	14% 13%	3% 5%	8% 4%	4% 3%
pH 8	35% 9%	27% 7%	27% 17%	11% 8%	15% 6%	7% 5%
pH 6	38% 10%	33% 9%	40% 21%	12% 9%	19% 8%	9% 6%
pH 4	43% 13%	37% 12%	41% 23%	19% 10%	25% 14%	16% 13%
pH 2	45% 17%	40% 16%	45% 26%	17% 11%	25% 15%	18% 16%

Note: pH 12 is used as the reference sample.

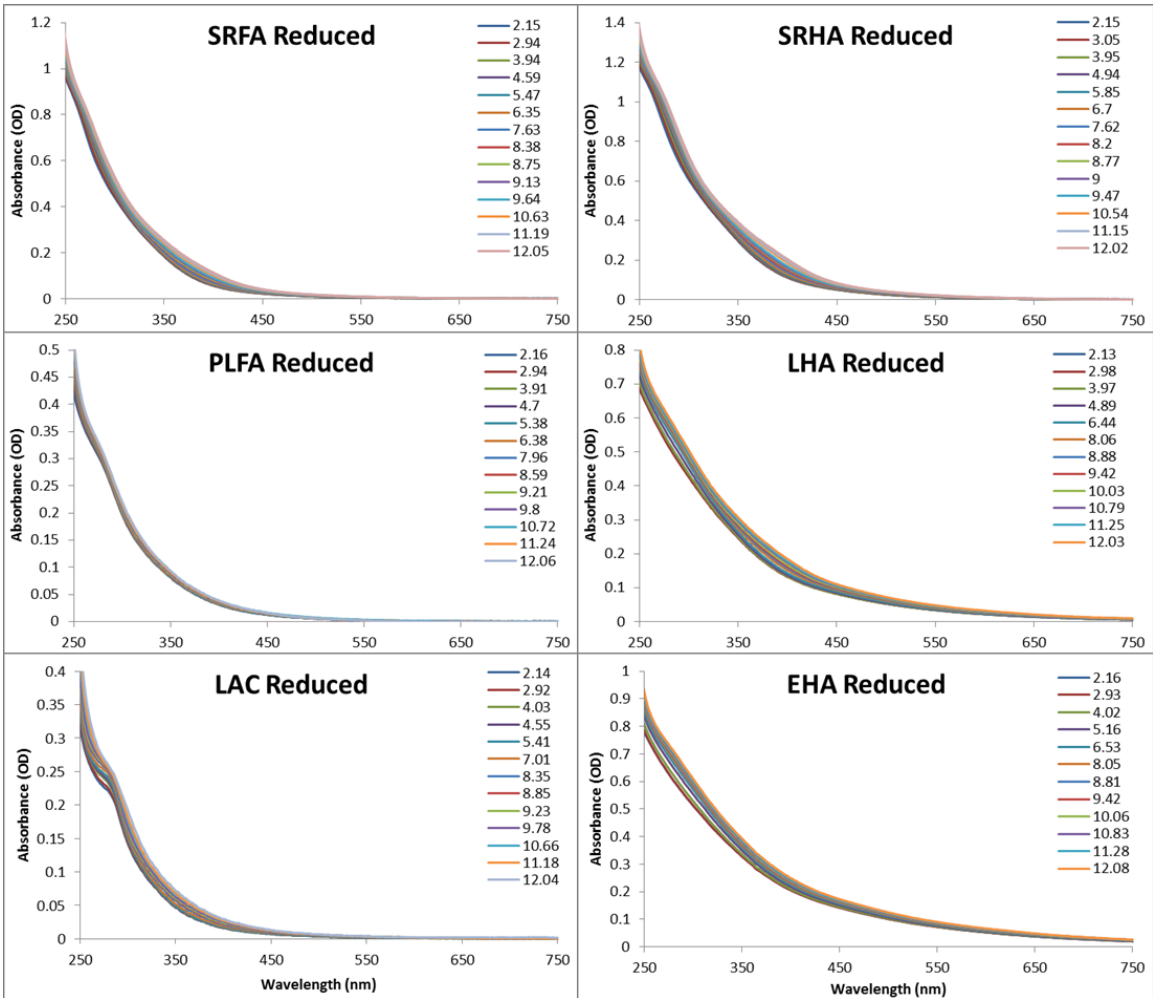


Figure 21. Dependence of the absorption spectra on pH following corrections for dilution for the reduced HS sample. SRFA and SRHA were 50 mg/L, LAC was 43 mg/L, PLFA was 44 mg/L, and LHA and EHA were 25 mg/L.

As anticipated, at low pH values reduction does not impact the 280 nm peak, its relative intensity for each HS remains the same between untreated and reduced samples (Figs. 18, 22 and 23). However, the long wavelength absorption at low pH values is lost, particularly for PLFA (Fig. 22). Similarly, at higher pH values, the absorbance over the phenolic groups pK_a range slightly decreases over the short wavelength (~ 300 nm) and significantly decreases over the long wavelength range (Fig. 24; Appendices 17 and 18). Altogether, these results support that the long wavelength absorbance arises from the charge-transfer between carbonyl species and donor molecules (aromatic carboxylic acids and phenol moieties) and not from individual chromophores.

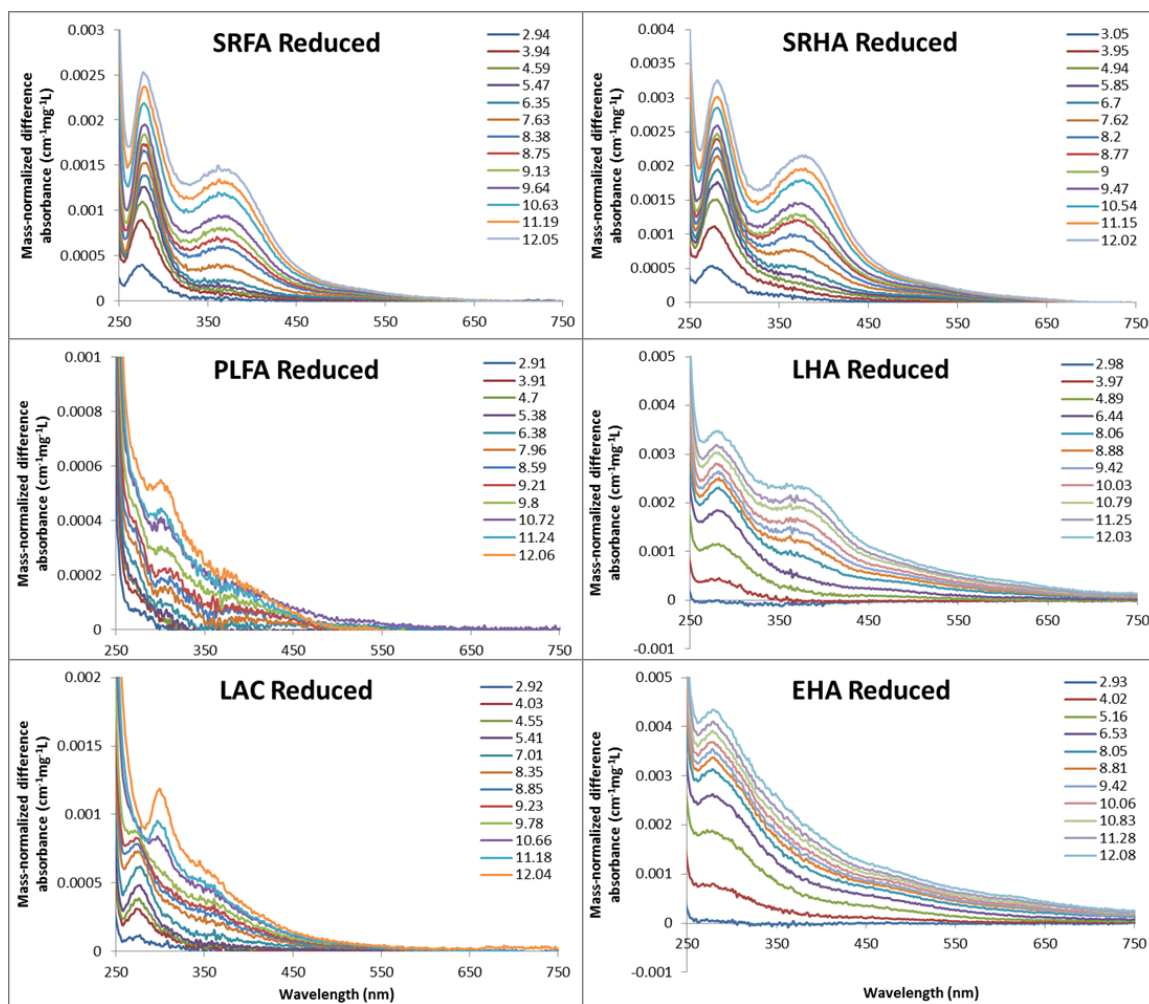


Figure 22. Mass normalized total difference spectra for 25-fold mass excess borohydride reduced HS. The pH 2 spectra serve as the reference spectra for each sample. SRFA and SRHA were 50 mg/L, LAC was 43 mg/L, PLFA was 44 mg/L, and LHA and EHA were 25 mg/L.

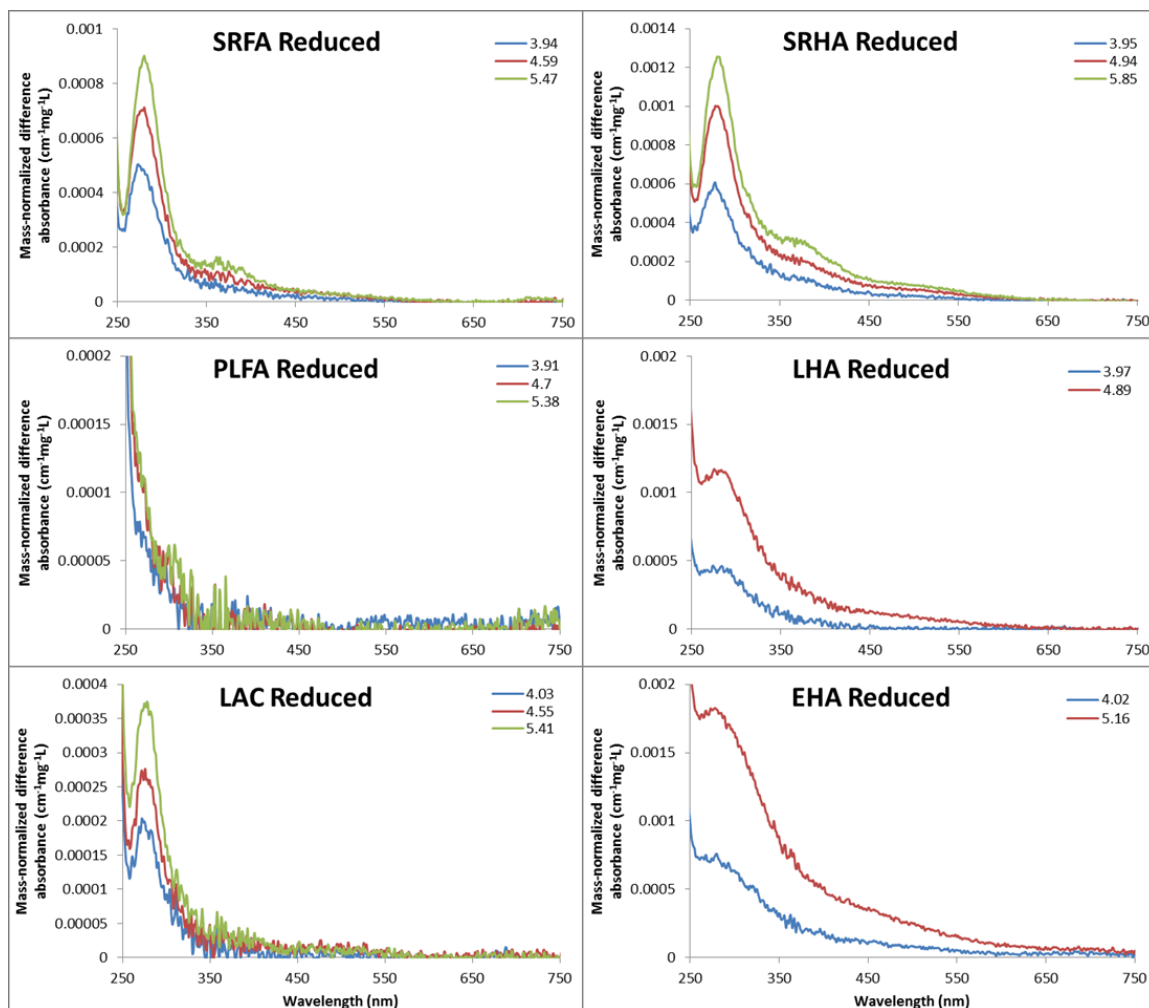


Figure 23. Mass normalized carboxylic acids difference spectra for 25-fold mass excess borohydride reduced HS over the carboxylic acids pK_a range. The pH 3 spectra serve as the reference spectra for each sample. SRFA and SRHA were 50 mg/L, LAC was 43 mg/L, PLFA was 44 mg/L, and LHA and EHA were 25 mg/L.

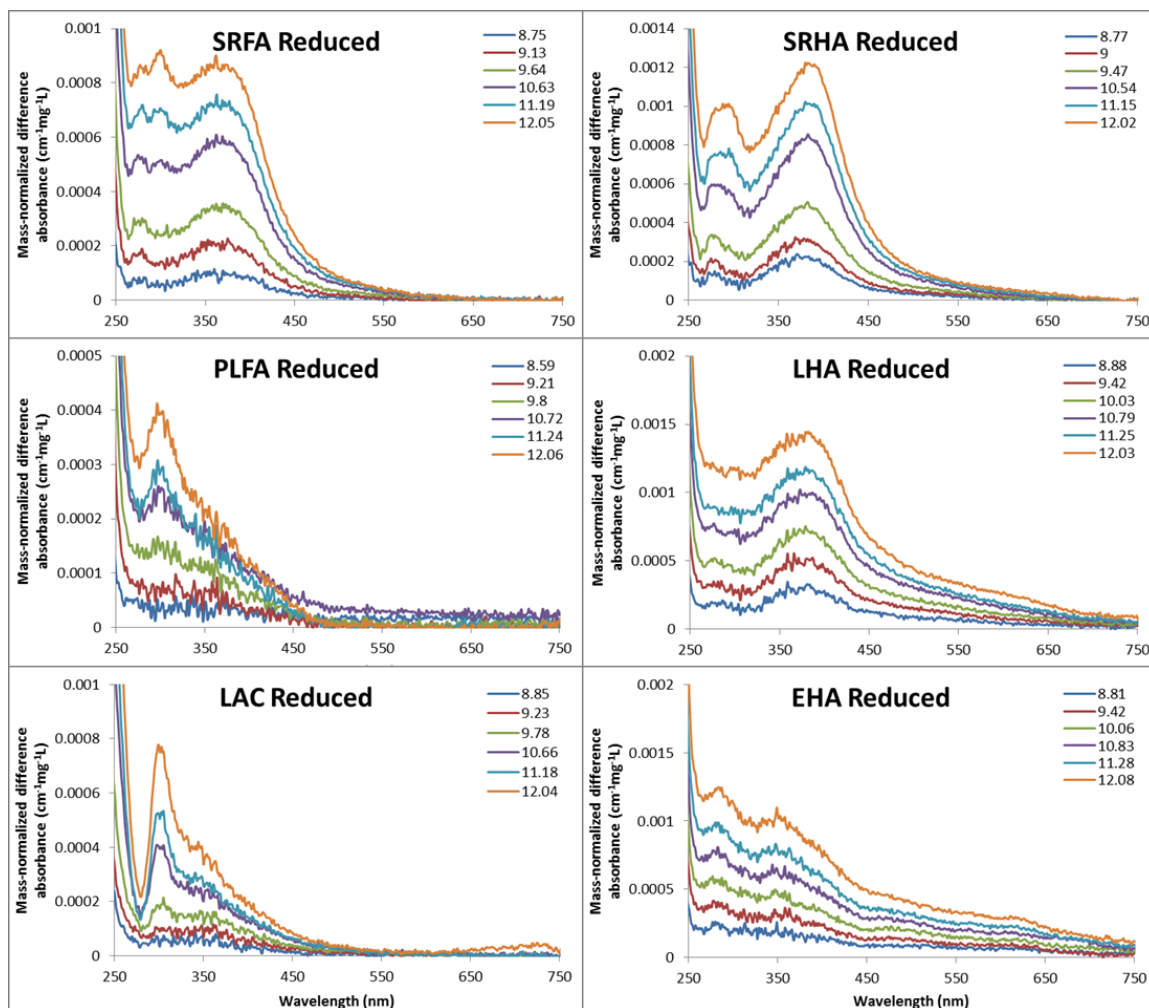


Figure 24. Mass normalized phenolic groups difference spectra for 25-fold mass excess borohydride reduced HS over the phenolic groups pK_a range. The pH 8 spectra serve as the reference spectra for each sample. SRFA and SRHA were 50 mg/L, LAC was 43 mg/L, PLFA was 44 mg/L, and LHA and EHA were 25 mg/L.

The difference absorbance at specific wavelengths was investigated relative to the pH for the untreated and reduced HS. While 300 nm shows both carboxylic acid groups ($pH < 5$) and phenolic groups ($pH > 8$), 400 nm only shows phenolic moieties contributions (Figs. 25 and 26; Appendix 20). These data show the same information previously presented and further shows that the difference in absorbance at 400 nm at low pH is much smaller than at the high pH, highlighting the assumption that phenolic groups contribute more to the charge-transfer interactions than aromatic carboxylic acids. Upon

reduction, this also suggests that at long wavelengths, there remains some charge-transfer interactions since there is not a complete removal of long wavelength absorption, i.e. not all of the potential acceptors have been removed from the material.

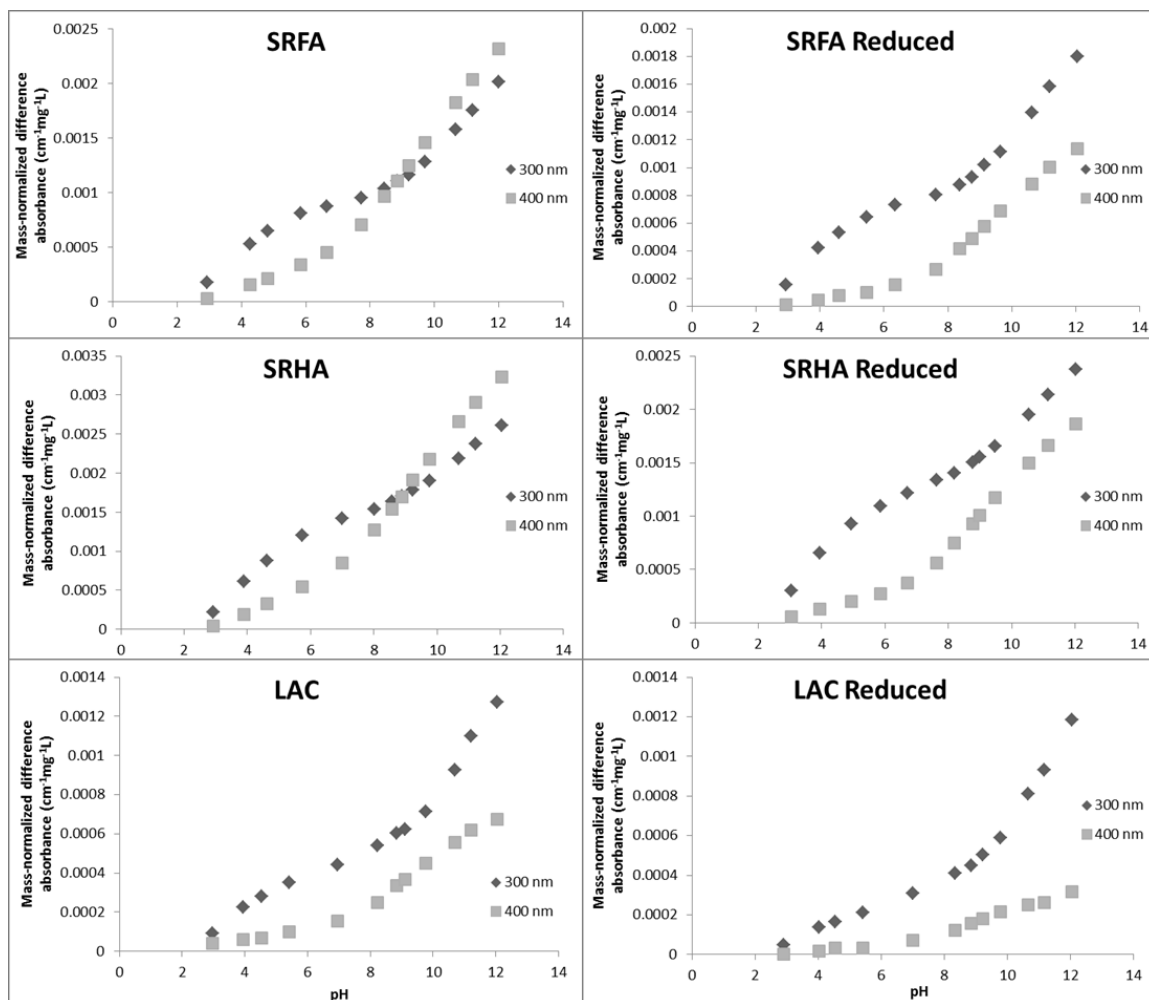


Figure 25. Comparison of the unreduced versus 25-fold mass excess reduced SRFA, SRHA, and LAC at 300 and 400 nm.

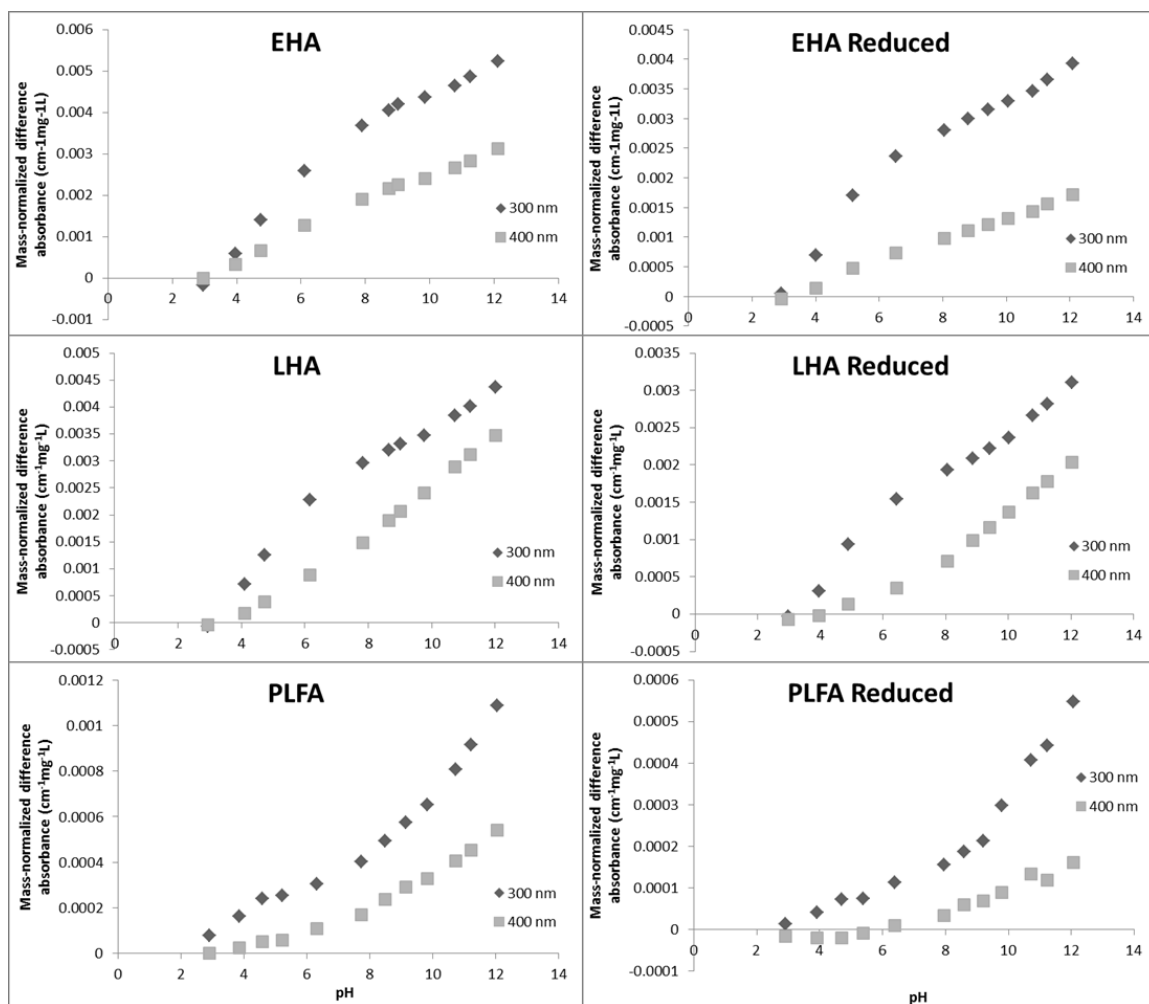


Figure 26. Comparison of the unreduced versus 25-fold mass excess reduced EHA, LHA, and PLFA at 300 and 400 nm.

To examine the pH dependence of the chromophores removed upon reduction, the difference absorbance of the untreated carboxylic acids (or phenolic groups) were subtracted from the difference spectra of the reduced carboxylic acids (or phenolic groups). The remaining spectra show a loss in absorbance when it is above zero and a gain in absorbance below zero. For all of the HS in this study, over the entire pH range, substantial losses of absorbance at wavelengths > 350 nm were observed (Figs. 27 and 28). However, while both the carboxylic acids and phenolic groups contributed to the long wavelength absorbance, there is a much greater contribution from the phenolic

groups (Figs. 27 and 28). In addition, SRFA and SRHA both show a distinct gain in absorbance at ~ 280 nm, which is consistent with an increase and blue shift in absorbance due to the protonation of a chromophore in the carboxylic acids pK_a range (Fig. 27).

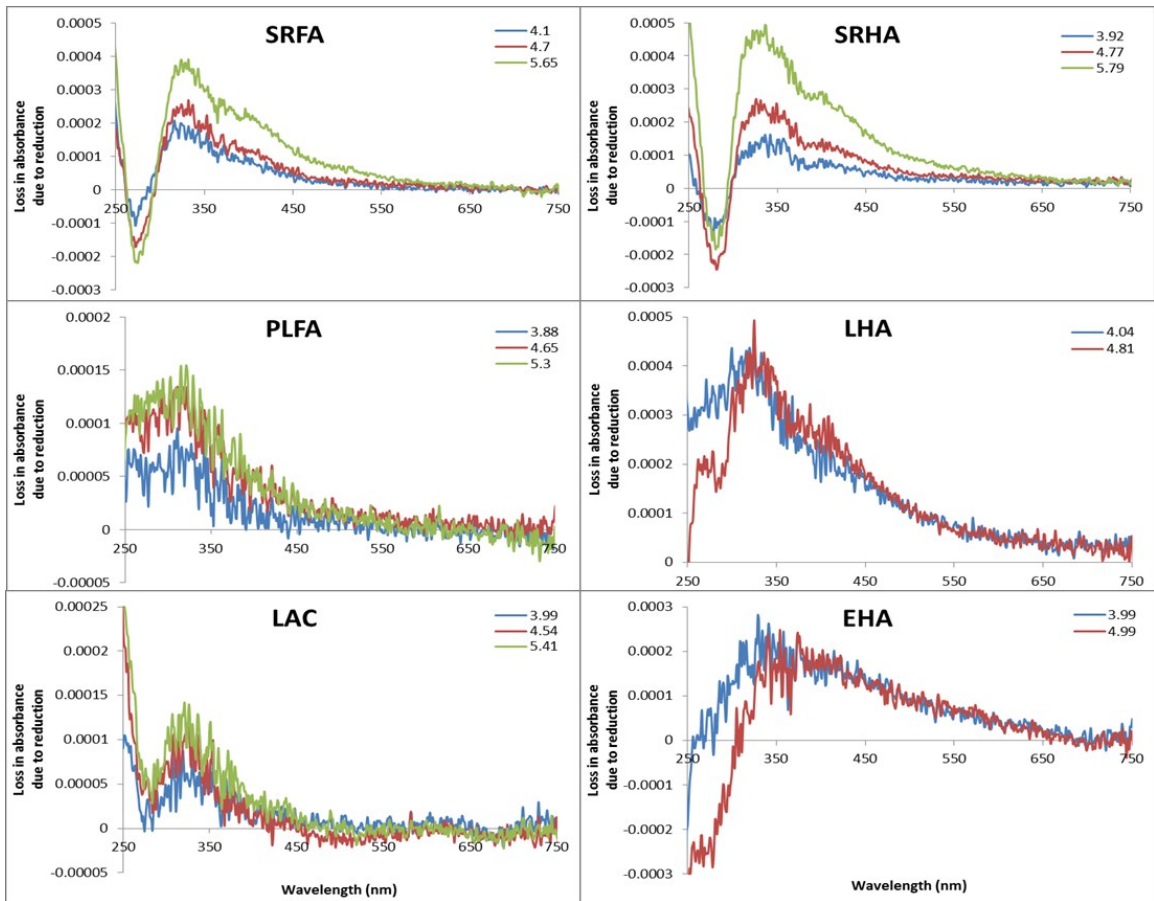


Figure 27. Difference absorbance spectra for the untreated versus reduced samples over the carboxylic acids pK_a range.

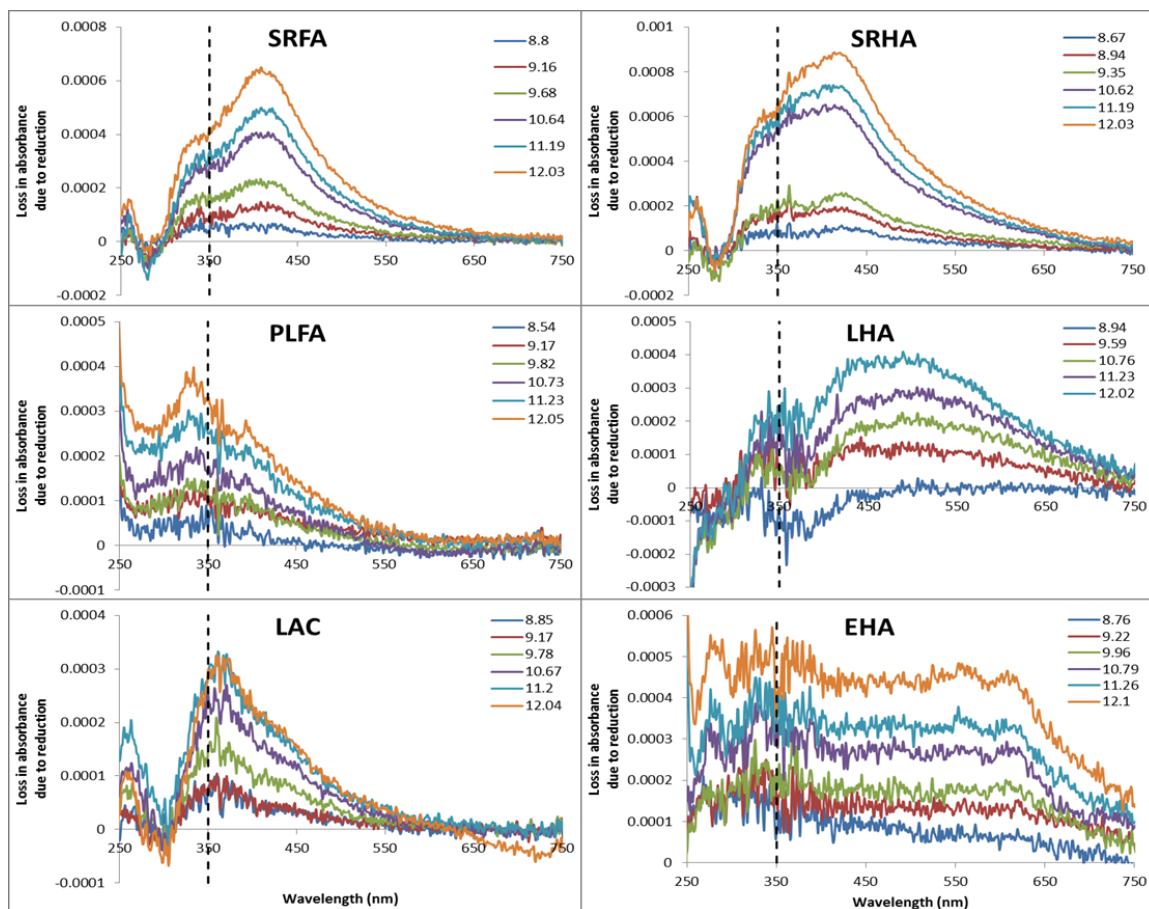


Figure 28. Difference absorbance spectra for the untreated versus reduced samples over the phenolic groups pK_a range.

Increasing the extent of NaBH_4 reduction did not change the pH dependency of absorbance over the carboxylic acids pK_a range to any significant degree (Appendix 21). The 280 nm peak remains constant regardless of the reduction amount and the long wavelength absorbance loss is so minor at a 5-fold mass excess reduction, that any differences with an increase in reduction amount cannot be verified. However, over the phenolic groups pK_a range the long wavelength absorption decreased with an increase in reduction amount. This is consistent with the charge-transfer interaction in that the greater the reduction, the more the acceptors are eliminated, the less the interactions with the donor (phenols), thus a decrease in long wavelength absorbance (Appendix 21).

Conclusions

Throughout this study, a series of general observations could be made that holds true for each HS considered. First, NaBH_4 reduction caused significant and irreversible loss of absorbance mostly at longer wavelengths and caused a blue shift and increase in emission as noted in chapter 2. This change in the optical properties can be explained by the loss of the electron acceptors (aromatic ketones/aldehydes) upon reduction, eliminating or greatly reducing the charge-transfer interactions and causing a decrease in absorbance, particularly over the long wavelength regime.

Second, the untreated samples at low pH values (carboxylic acids region), showed a short wavelength band (280 nm) coupled to long wavelength absorbance. At high pH values (phenolic groups region), a broad band at approximately 300-400 nm is observed, coupled to long wavelength absorbance as seen in the low pH spectra. The short wavelength absorbance can be explained by the individual chromophores. The long wavelength absorbance for both moieties can be explained by the charge-transfer model. As the pH is increased, the absorption increases due to the deprotonation of these moieties. At $\text{pH} > 8$, for example, the phenol will be deprotonated to phenolate anion, which is a better electron donor, leading to increased charge-transfer interactions with the electron acceptors and an increase in absorbance.

Finally, at low pH values (carboxylic acids region), the reduced samples continued to show the short wavelength band at 280 nm, but the long wavelength absorbance was decreased. In addition, at high pH values (phenolic groups region), the reduced samples showed a substantial decrease in both the long wavelength absorption and the broad band. The long wavelength absorbance was greatly diminished in both

moieties, showing that the carboxylic acids and phenolic moieties are most likely coupled in some way to the carbonyl groups. Further, while the phenols are still deprotonated at high pH, they do not have many readily available electron acceptors due to their loss during reduction, so there are less charge-transfer interactions that are possible. Overall, there is less pH dependence of the reduced samples versus the untreated samples. All these data support the charge-transfer model and further show that carboxylic acids and phenolic groups are involved in the long wavelength absorbance of HS.

Chapter 4: Conclusion

Conclusion

The first goal of this project was to develop a simple, systematic method for reducing HS through a standard procedure. This reduction method further required a way in which to purify the samples. The protocol developed included starting with the sample at pH 7, using a concentrated solution of NaBH₄ to reduce the sample to a 25-fold mass excess reduction amount, and allowing the reduction to proceed for 96 hours. After the reduction was complete, the samples were passed over a 10 cm Sephadex G-10 column to eliminate excess borate and the pH was adjusted back down to 7 if needed. Following the reduction of a series of HS to distinct reduction amounts, it was determined that a 25-fold mass excess of NaBH₄ induced significant and irreversible losses of absorbance (~60 % at 450 nm) and a gain in fluorescence at the edge of the visible region without compromising the solutions with excess borate. Past the 25-fold mass excess reduction, the samples showed only a minor further decrease in absorbance in the visible.

The second goal was to evaluate the optical properties of both the untreated samples and the NaBH₄ reduced samples in an attempt to obtain further insights into the structural basis of HS. The unreduced samples all showed a broad, featureless absorption spectrum that decreased in intensity with increasing wavelength. According to the charge-transfer model, the long wavelength absorbance is potentially linked to charge-transfer interactions. Thus, the NaBH₄ reduced samples should display a decrease in long wavelength absorbance due to the loss in electron acceptors from the reduction, which would eliminate or partially eliminate the charge-transfer interactions. The results are

consistent with the expected outcome with the 25-fold mass excess reduced samples showing an approximately 30-65 % loss in absorbance at 450 nm depending on the HS.

Last, the effect of pH on the optical properties of both the untreated and the reduced HS samples was analyzed. The pH titrations showed two distinct chromophores, carboxylic acids and phenolic groups, impacted the optical properties of HS. The carboxylic acids dominate when the pH is less than 5 and display a peak at 280 nm that extends into the long wavelengths. The peak does not change upon reduction, however, the long wavelength absorbance is essentially lost upon reduction. The phenolic groups dominate at pH values greater than 8 and show a significant loss in long wavelength absorption upon reduction. While the NaBH₄ reduction results are consistent with the charge-transfer model, the pH titration further shows that the charge-transfer interactions are lost after reduction over both the phenolic groups pK_a range and to a lesser extent the carboxylic acids pK_a range.

Future Work

First, the 50- and 100-fold mass excess reductions with solutions of NaBH₄ need to be further investigated. Currently, it is presumed that the differences noted in the solid NaBH₄ versus the solution of NaBH₄ reduction is that the reduction process takes a longer amount of time with the solution. In addition to further investigating the solution reduction method, higher concentrations of HS should be reduced to determine if they react to the reductions in the same manner as the lower concentrations (100 mg/L). The higher concentrations can also be used to determine if bringing the samples pH down to 7 prior to running the columns will actually help prevent column cracking.

Next, the optical properties of the natural water samples need to be explored as function of reduction and pH dependence. These samples can be reduced, and the untreated and reduced samples can be subjected to pH titrations in the same manner as discussed in Chapter 3. The differences noted between the untreated and reduced samples can be related to the HS samples already examined to determine the similarities and differences between the standards and the natural water samples.

Last, the pH dependence of the fluorescence emission of the samples need to be examined for the HS in this study and any future natural water samples observed to gain further insights into the optical properties of CDOM and HS.

Appendices

Appendix 1. Logarithmic versus Linear Dependency of Absorbance Loss	63
Appendix 2. Reduction Kinetics for Each HS at pH 10	65
Appendix 3. HS Reduction: Pre-column samples at pH 10.....	71
Appendix 4. Effect of Starting pH on Reduction: pH 7 versus pH 10.....	74
Appendix 5. NaBH ₄ Reduction: Solid versus Solution	77
Appendix 6. 100x-200x-300x Mass Excess NaBH ₄ Reduction.....	84
Appendix 7. Dilution Factors for 10cm Column	85
Appendix 8. Column Performance as a Function of Sample pH: pH 7 versus pH 10.....	86
Appendix 9. EHA and LHA: Second G-10 Purification (10 cm Column).....	87
Appendix 10. G-10 Column Length: 10 cm versus 15 cm	88
Appendix 11. Absorbance Values at 300 nm for Fluorescence Samples	89
Appendix 12. HS Reduction Fluorescence Emission: Post-column samples at pH 7	90
Appendix 13. HS Reduction Fluorescence Emission: Unreduced versus 25-fold Mass Excess Reduction	96
Appendix 14. HS pH Titration: Unreduced versus 25-fold Mass Excess Reduction	98
Appendix 15. 25-fold Mass Excess Reduction: Fractional Loss due to pH	100
Appendix 16. Analysis of Difference Spectra for HS.....	101
Appendix 17. Analysis of Difference Spectra for Borohydride Reduced HS	103
Appendix 18. HS pH Titration: Difference Absorbance of Untreated vs. 25-fold Mass Excess Reduced Samples	105
Appendix 19. HS pH Titration: Circumneutral Difference Absorbance of Unreduced versus 25-fold Mass Excess Reduced Samples	111
Appendix 20. HS Reduction: Difference Absorbance versus pH.....	114
Appendix 21. Effects of Extent of NaBH ₄ Reduction on pH Titration	121

Appendix 1.
Logarithmic versus Linear Dependency of Absorbance Loss

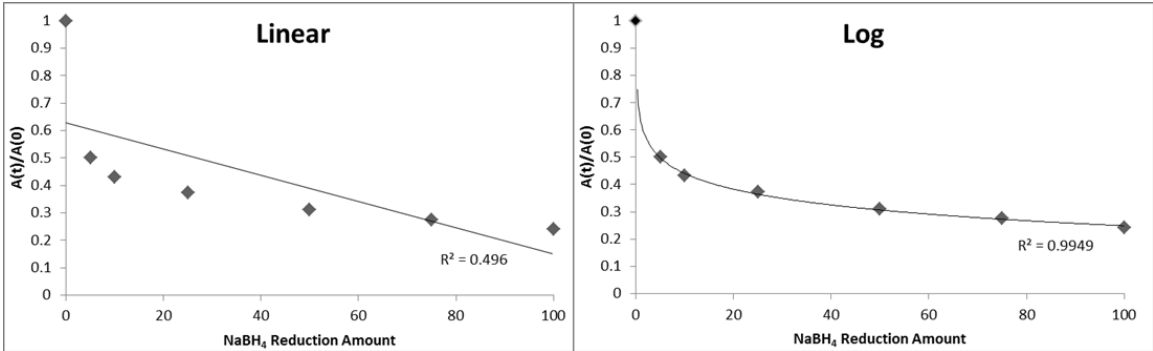


Figure A1-1. Linear (left) and logarithmic (right) dependence of the fractional absorbance loss at 450 nm based on NaBH_4 reduction amount for SRFA at pH 10.

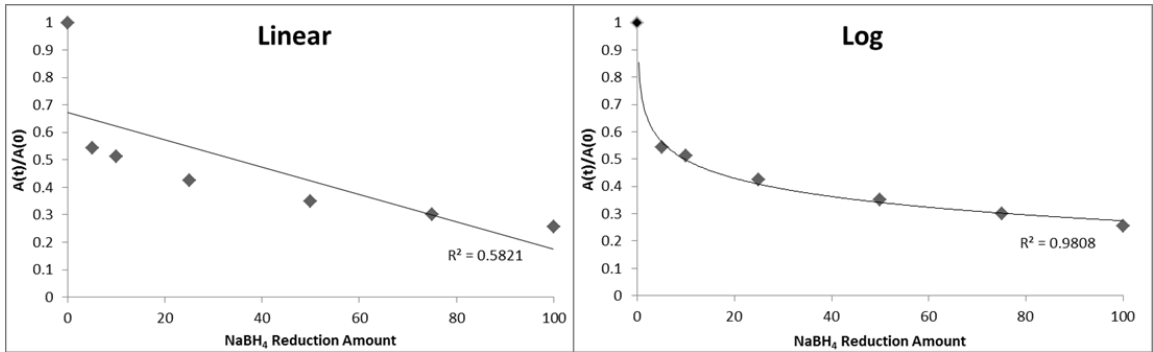


Figure A1-2. Linear (left) and logarithmic (right) dependence of the fractional absorbance loss at 450 nm based on NaBH_4 reduction amount for SRHA at pH 10.

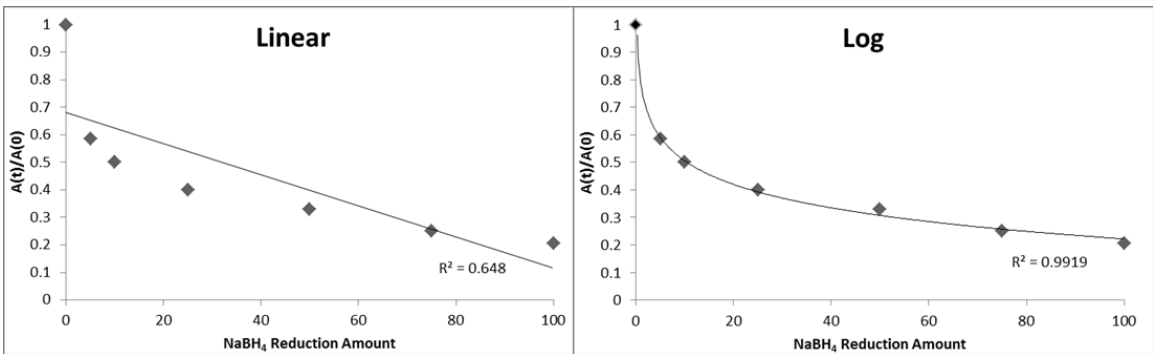


Figure A1-3. Linear (left) and logarithmic (right) dependence of the fractional absorbance loss at 450 nm based on NaBH_4 reduction amount for LAC at pH 10.

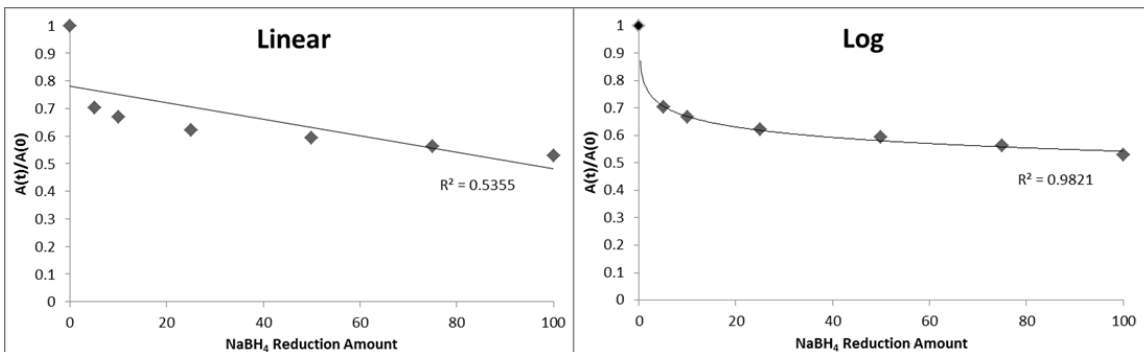


Figure A1-4. Linear (left) and logarithmic (right) dependence of the fractional absorbance loss at 450 nm based on NaBH₄ reduction amount for EHA at pH 10.

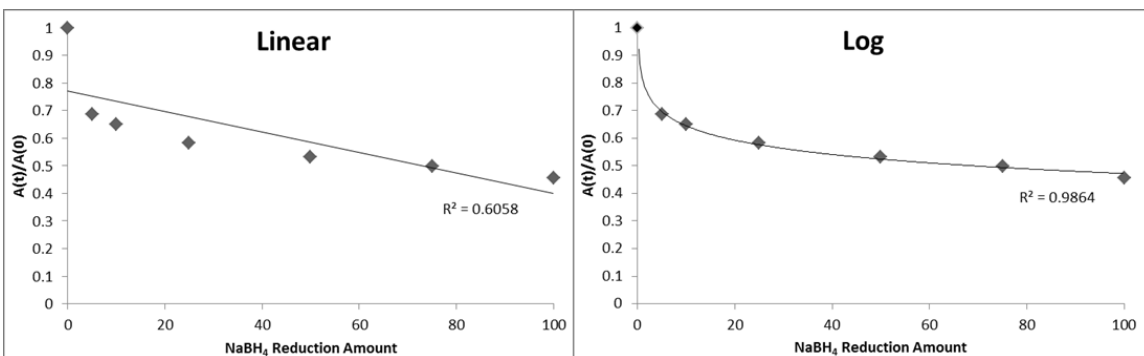


Figure A1-5. Linear (left) and logarithmic (right) dependence of the fractional absorbance loss at 450 nm based on NaBH₄ reduction amount for LHA at pH 10.

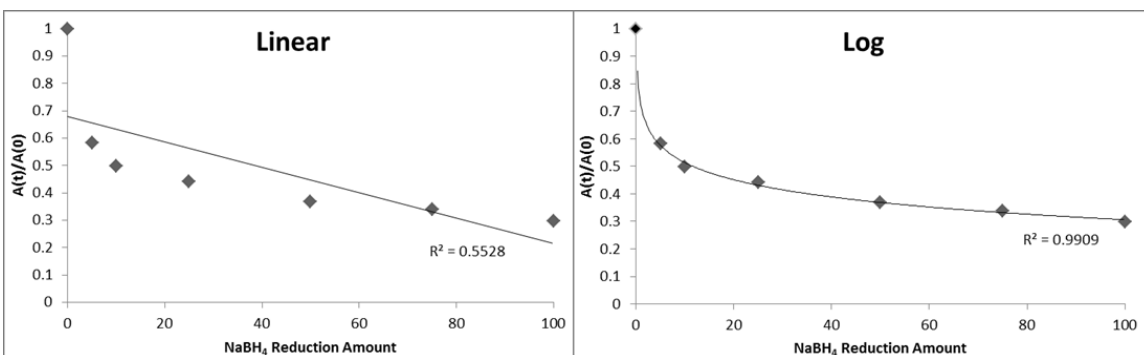


Figure A1-6. Linear (left) and logarithmic (right) dependence of the fractional absorbance loss at 450 nm based on NaBH₄ reduction amount for PLFA at pH 10.

Appendix 2.
Reduction Kinetics for Each HS at pH 10

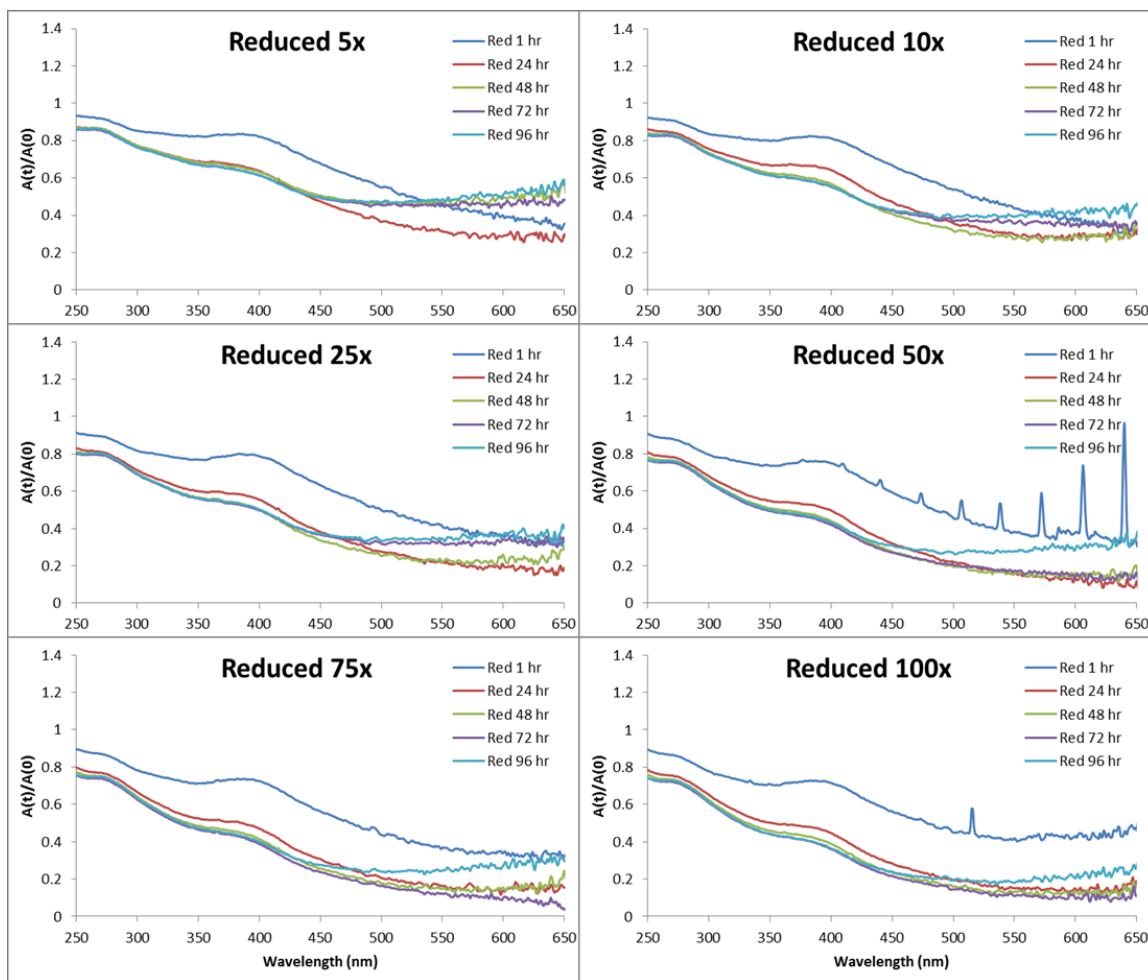


Figure A2-1. Changes in the absorbance of SRFA (100 mg/L, pH 10) following NaBH_4 reduction (5x, 10x, 25x, 50x, 75x, and 100x) from 1 hour after reduction till the reduction was complete at 96 hours. The sharp peaks at 1 hour for the 50-fold and 100-fold mass excess reductions are due to scattering from the hydrogen gas bubbles formed from the reduction process.

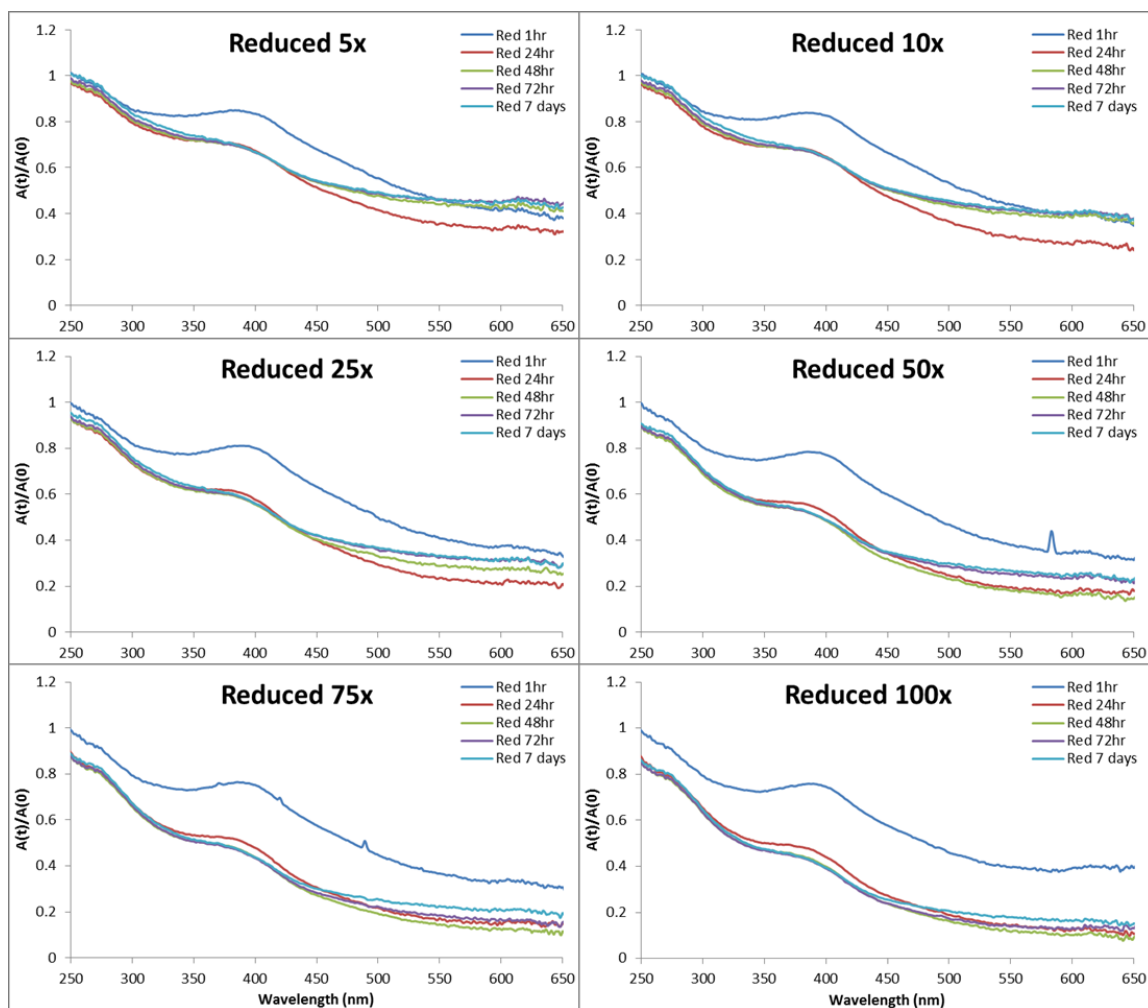


Figure A2-2. Changes in the absorbance of SRHA (100 mg/L, pH 10) following NaBH_4 reduction (5x, 10x, 25x, 50x, 75x, and 100x) from 1 hour after reduction till the reduction was complete at 96 hours. The sharp peaks at 1 hour for the 50-fold and 75-fold mass excess reductions are due to scattering from the hydrogen gas bubbles formed from the reduction process.

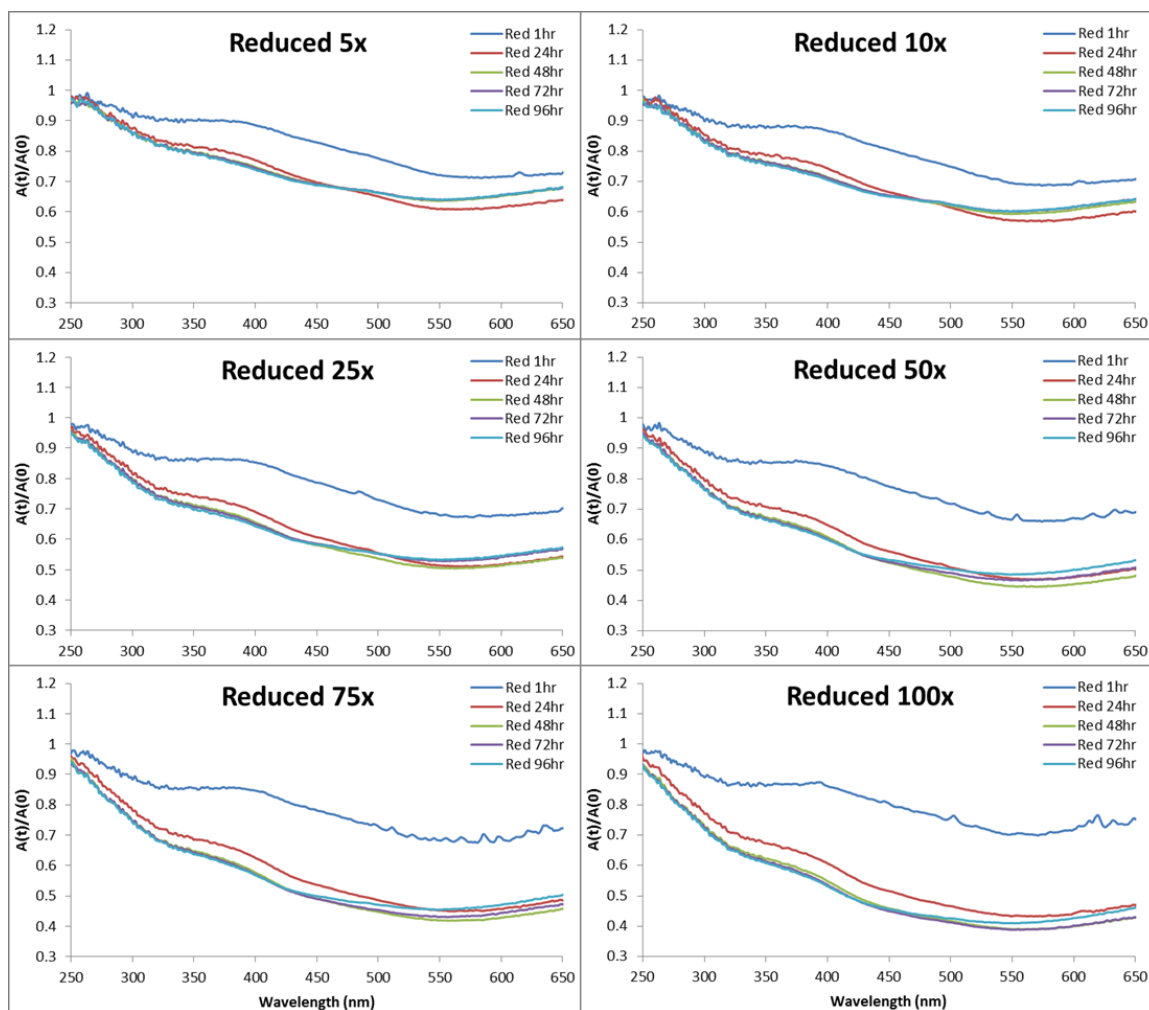


Figure A2-3. Changes in the absorbance of LHA (100 mg/L, pH 10) following NaBH_4 reduction (5x, 10x, 25x, 50x, 75x, and 100x) from 1 hour after reduction till the reduction was complete at 96 hours. The sharp peaks at 1 hour for the 50-fold, 75-fold and 100-fold mass excess reductions are due to scattering from the hydrogen gas bubbles formed from the reduction process.

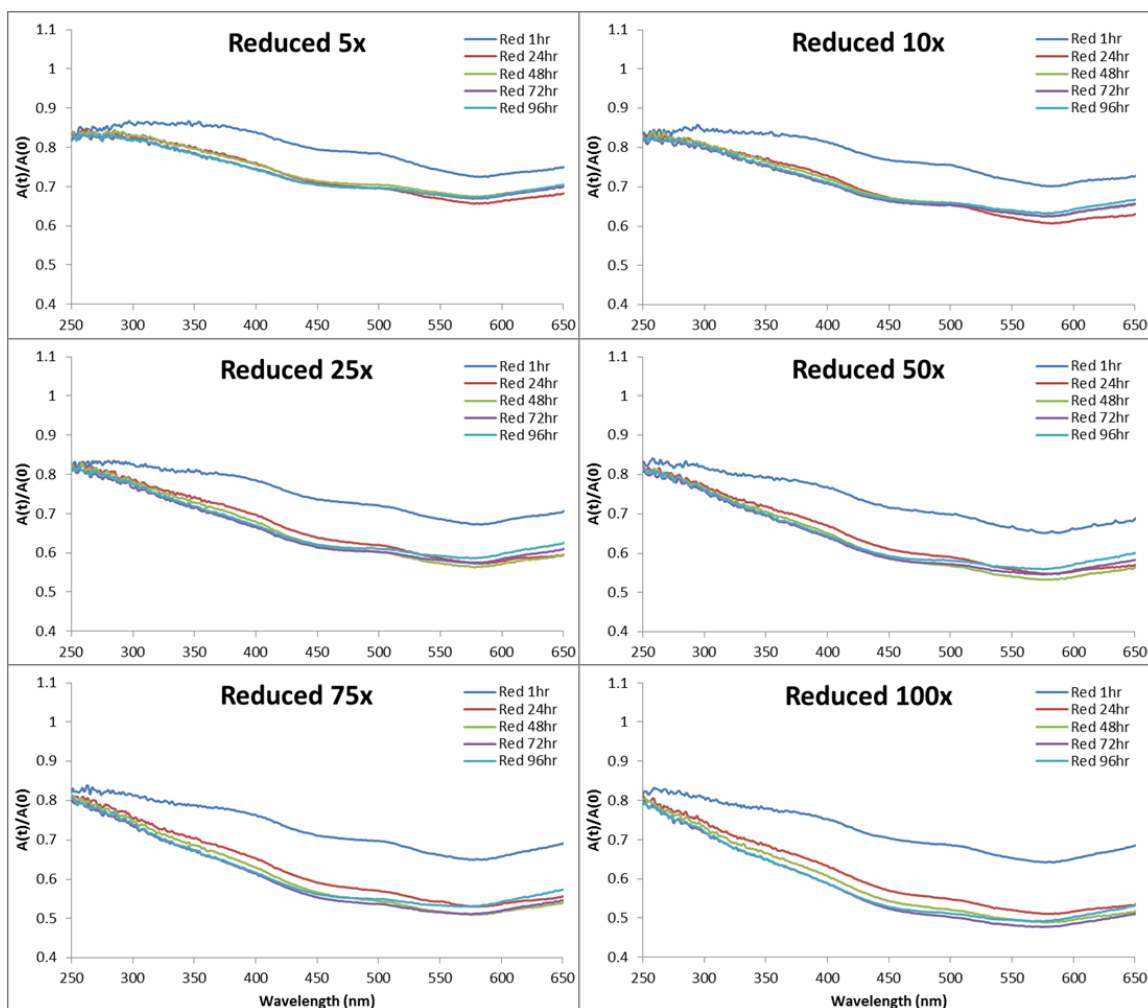


Figure A2-4. Changes in the absorbance of EHA (100 mg/L, pH 10) following NaBH_4 reduction (5x, 10x, 25x, 50x, 75x, and 100x) from 1 hour after reduction till the reduction was complete at 96 hours. The peaks at 1 hour for the 50-fold mass excess reduction are due to scattering from the hydrogen gas bubbles formed from the reduction process.

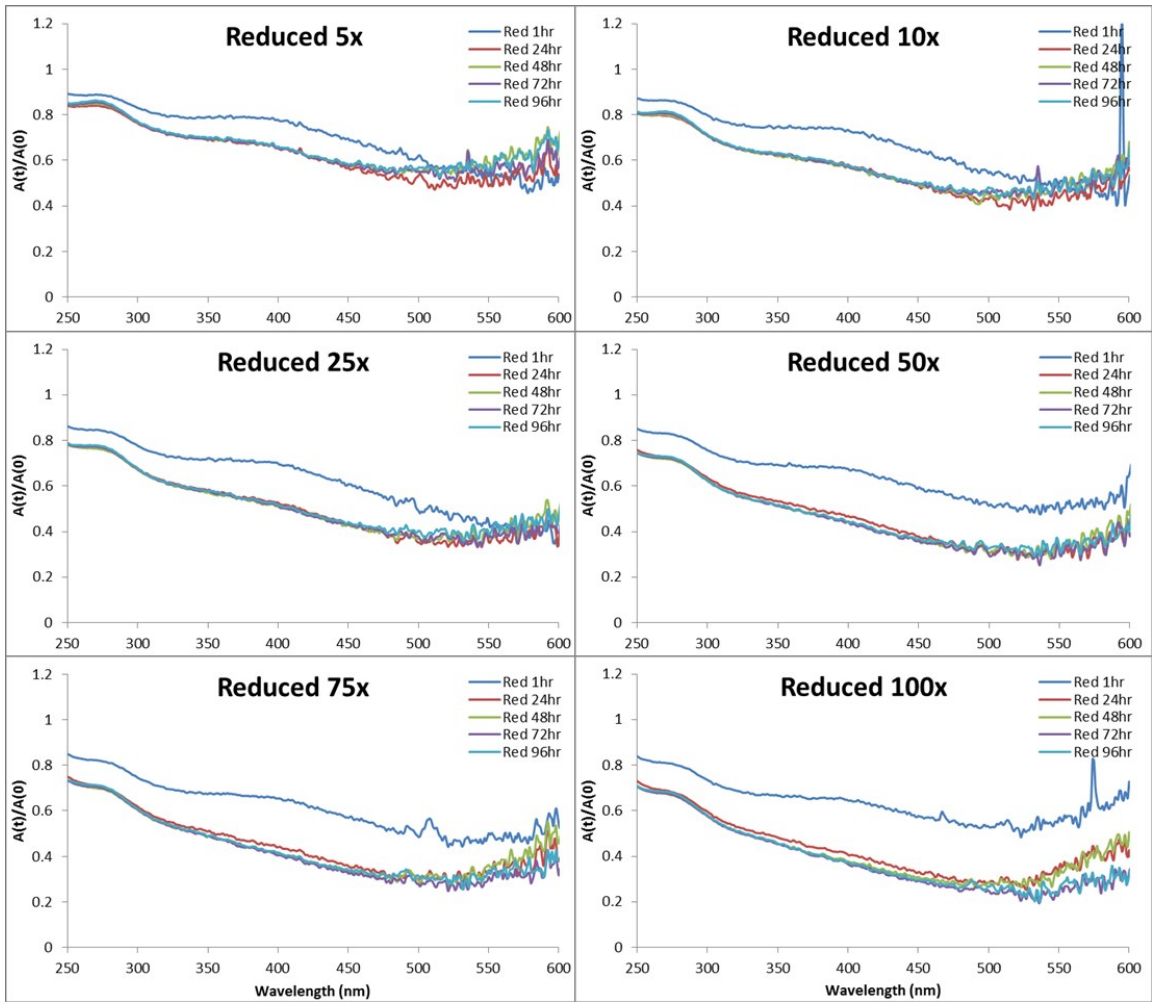


Figure A2-5. Changes in the absorbance of PLFA (100 mg/L, pH 10) following NaBH_4 reduction (5x, 10x, 25x, 50x, 75x, and 100x) from 1 hour after reduction till the reduction was complete at 96 hours. The sharp peaks at 1 hour for the 75-fold and 100-fold mass excess reductions are due to scattering from the hydrogen gas bubbles formed from the reduction process.

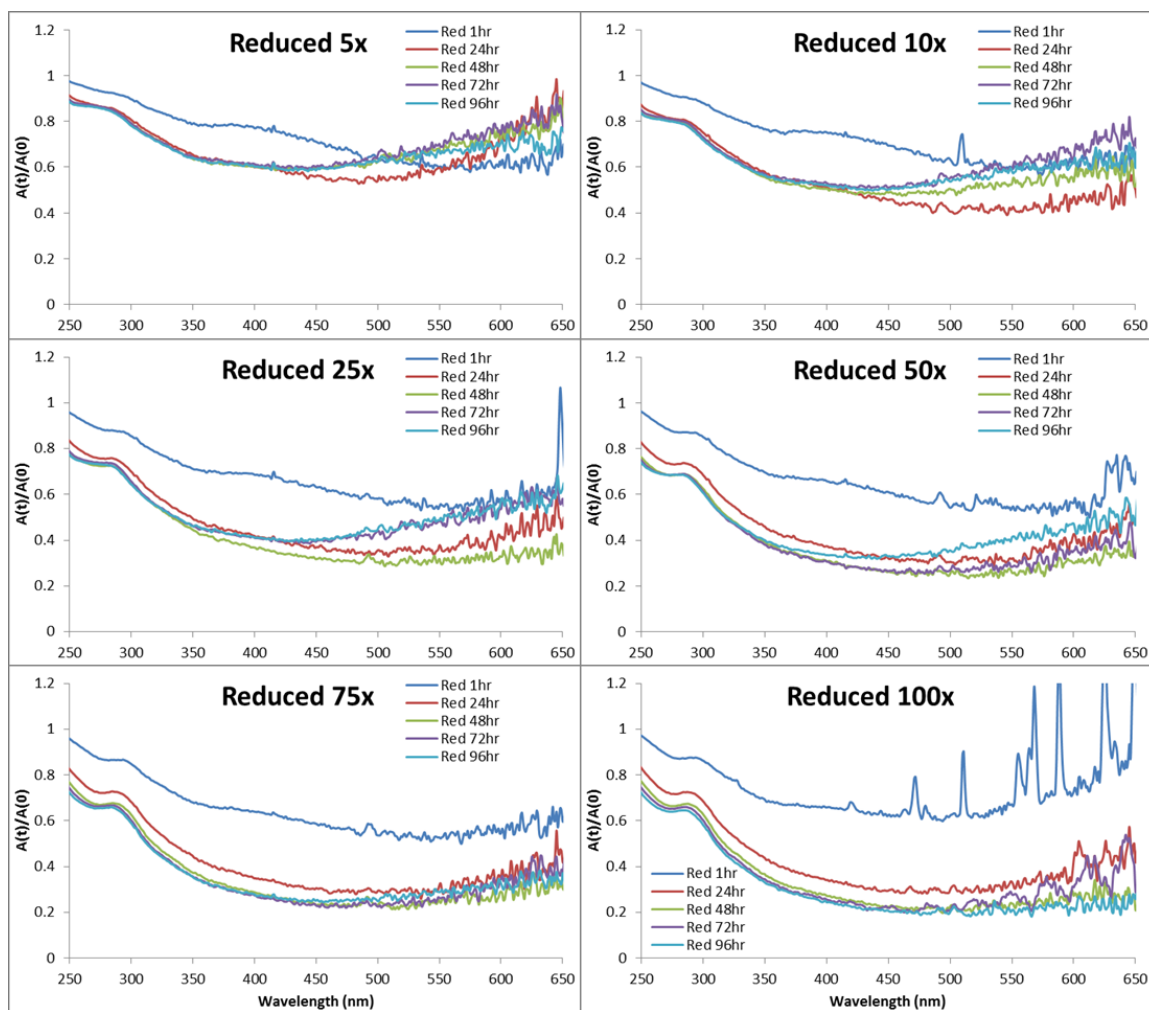


Figure A2-6. Changes in the absorbance of LAC (100 mg/L, pH 10) following NaBH₄ reduction (5x, 10x, 25x, 50x, 75x, and 100x) from 1 hour after reduction till the reduction was complete at 96 hours. The sharp peaks at 1 hour for the 100-fold mass excess reduction are due to scattering from the hydrogen gas bubbles formed from the reduction process.

Appendix 3.
HS Reduction: Pre-column samples at pH 10

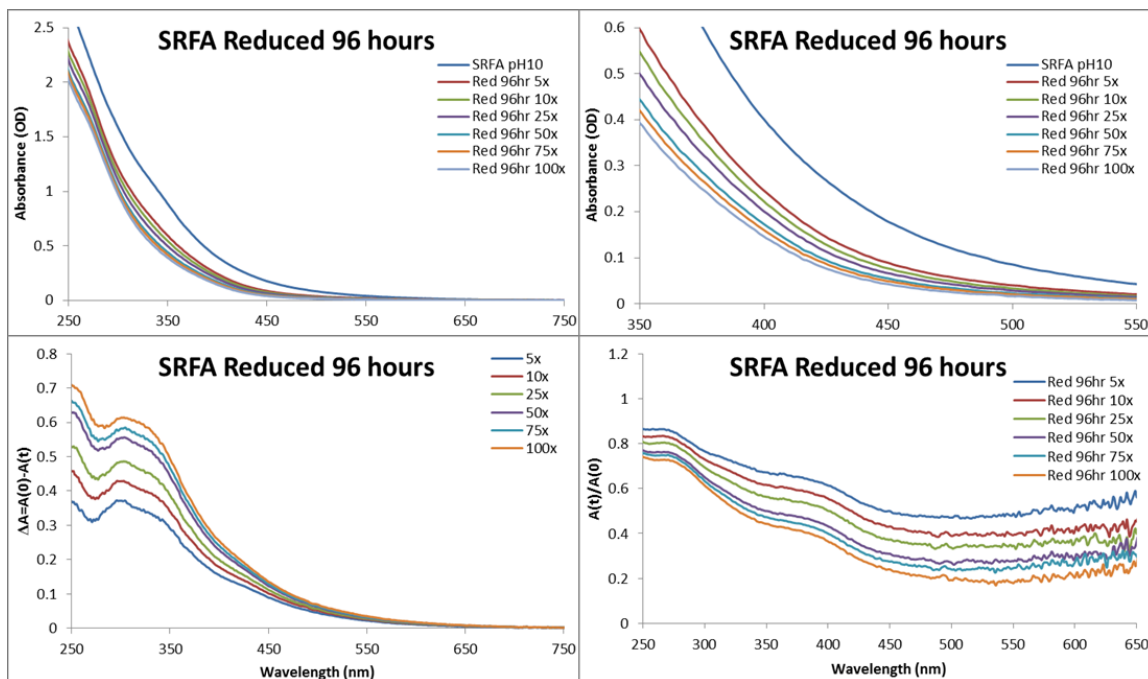


Figure A3-1. Optical changes upon reduction for SRFA prior to and post reduction, pH 10, prior to passing through the column. The top panels show the absorbance of SRFA over the full range (left) and an inset (right). The bottom panels show the ΔA (left) and the fractional absorbance loss (right). $\Delta A > 0$ and $A(t)/A(0) < 1$ indicate a loss in absorbance.

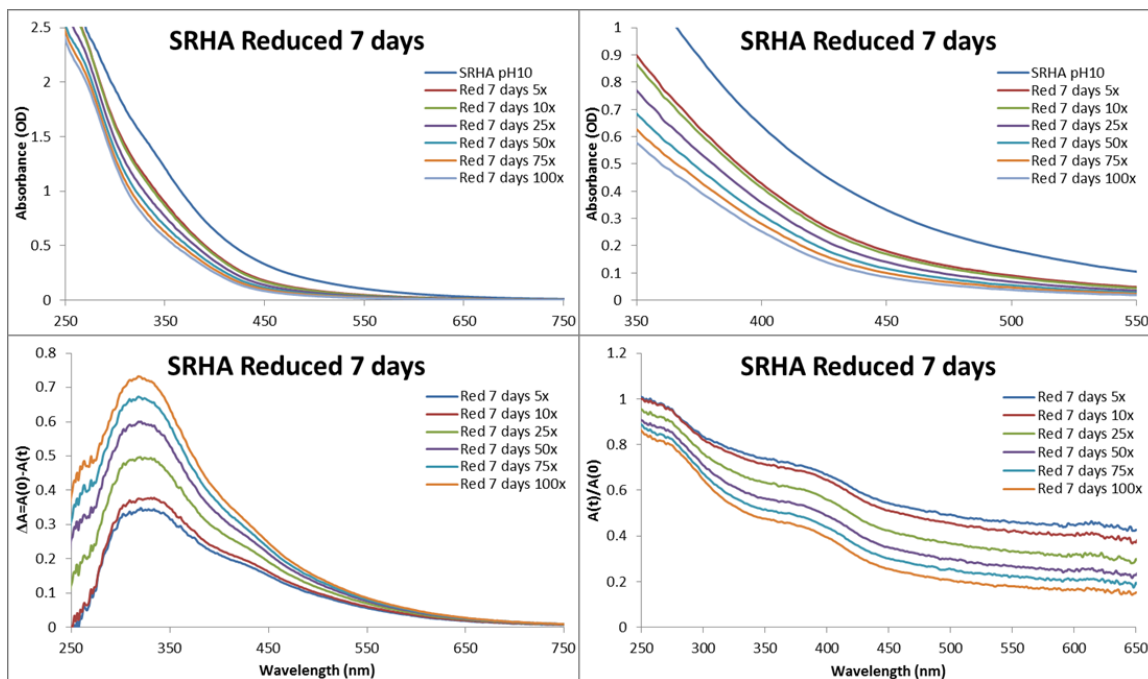


Figure A3-2. Optical changes upon reduction for SRHA prior to and post reduction, pH 10, prior to passing through the column. The top panels show the absorbance of SRHA over the full range (left) and an inset (right). The bottom panels show the ΔA (left) and the fractional absorbance loss (right). $\Delta A > 0$ and $A(t)/A(0) < 1$ indicate a loss in absorbance.

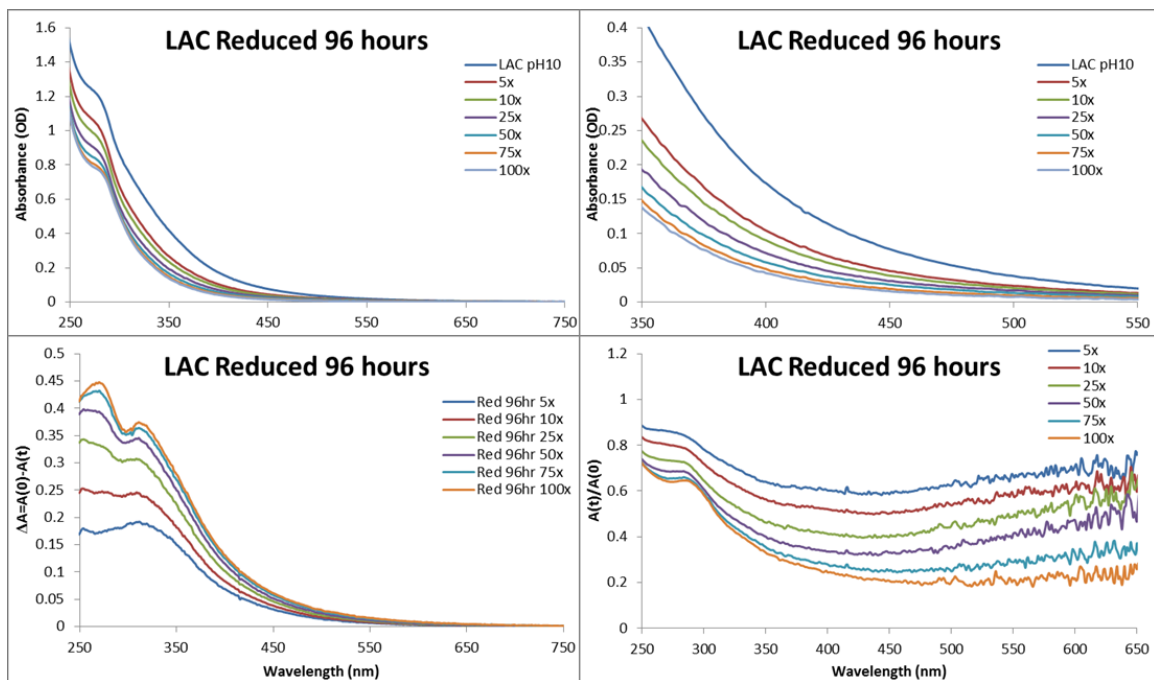


Figure A3-3. Optical changes upon reduction for LAC prior to and post reduction, pH 10, prior to passing through the column. The top panels show the absorbance of LAC over the full range (left) and an inset (right). The bottom panels show the ΔA (left) and the fractional absorbance loss (right). $\Delta A > 0$ and $A(t)/A(0) < 1$ indicate a loss in absorbance.

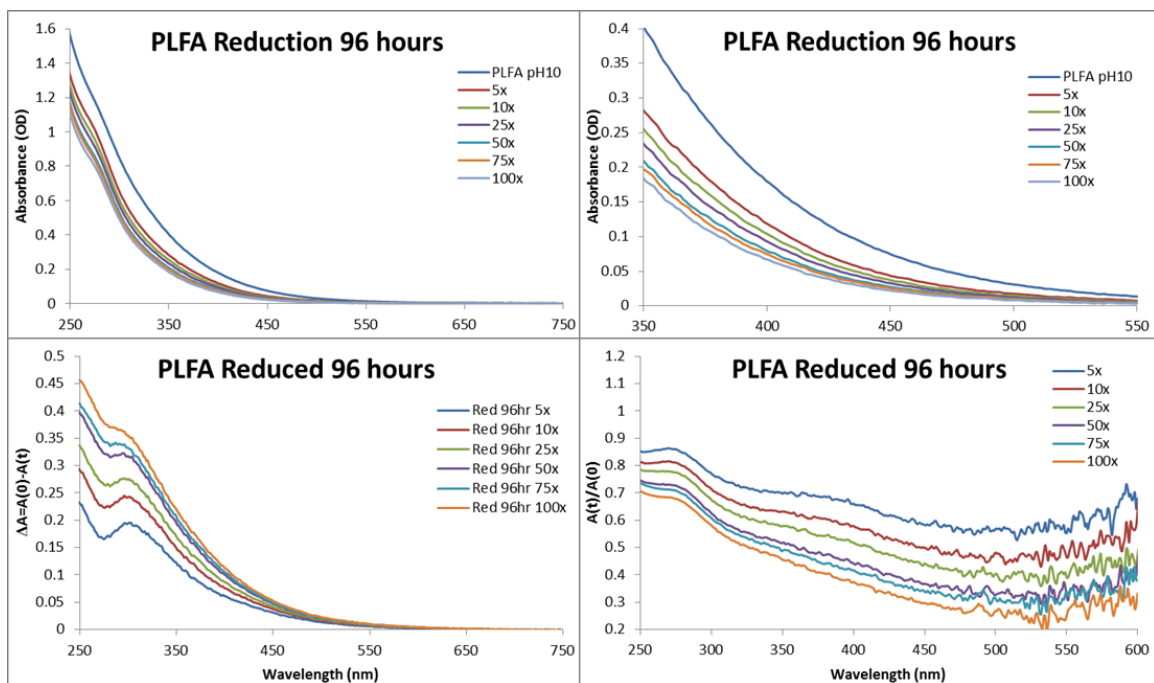


Figure A3-4. Optical changes upon reduction for PLFA prior to and post reduction, pH 10, prior to passing through the column. The top panels show the absorbance of PLFA over the full range (left) and an inset (right). The bottom panels show the ΔA (left) and the fractional absorbance loss (right). $\Delta A > 0$ and $A(t)/A(0) < 1$ indicate a loss in absorbance.

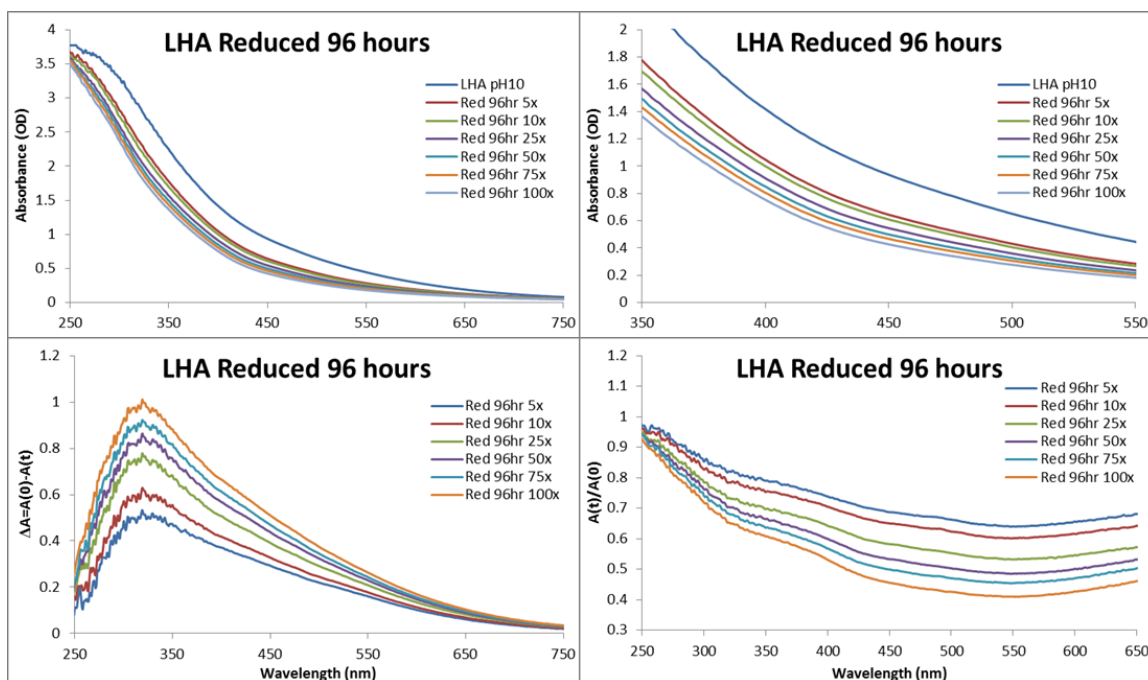


Figure A3-5. Optical changes upon reduction for LHA prior to and post reduction, pH 10, prior to passing through the column. The top panels show the absorbance of LHA over the full range (left) and an inset (right). The bottom panels show the ΔA (left) and the fractional absorbance loss (right). $\Delta A > 0$ and $A(t)/A(0) < 1$ indicate a loss in absorbance.

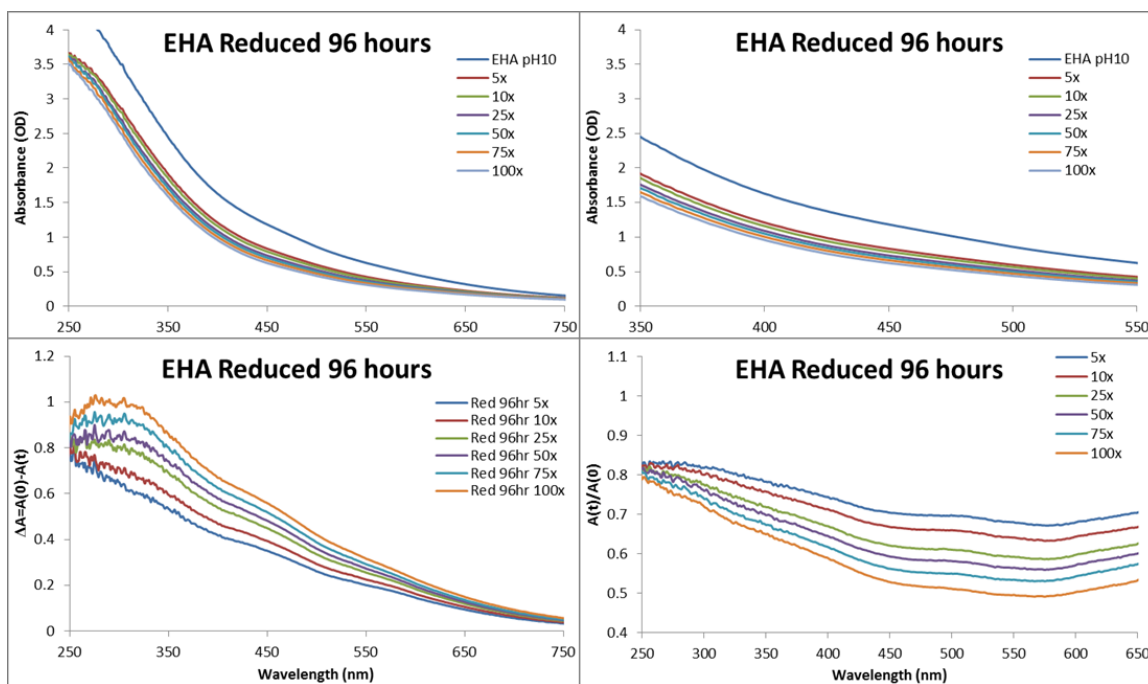


Figure A3-6. Optical changes upon reduction for EHA prior to and post reduction, pH 10, prior to passing through the column. The top panels show the absorbance of EHA over the full range (left) and an inset (right). The bottom panels show the ΔA (left) and the fractional absorbance loss (right). $\Delta A > 0$ and $A(t)/A(0) < 1$ indicate a loss in absorbance.

Appendix 4.
Effect of Starting pH on Reduction: pH 7 versus pH 10

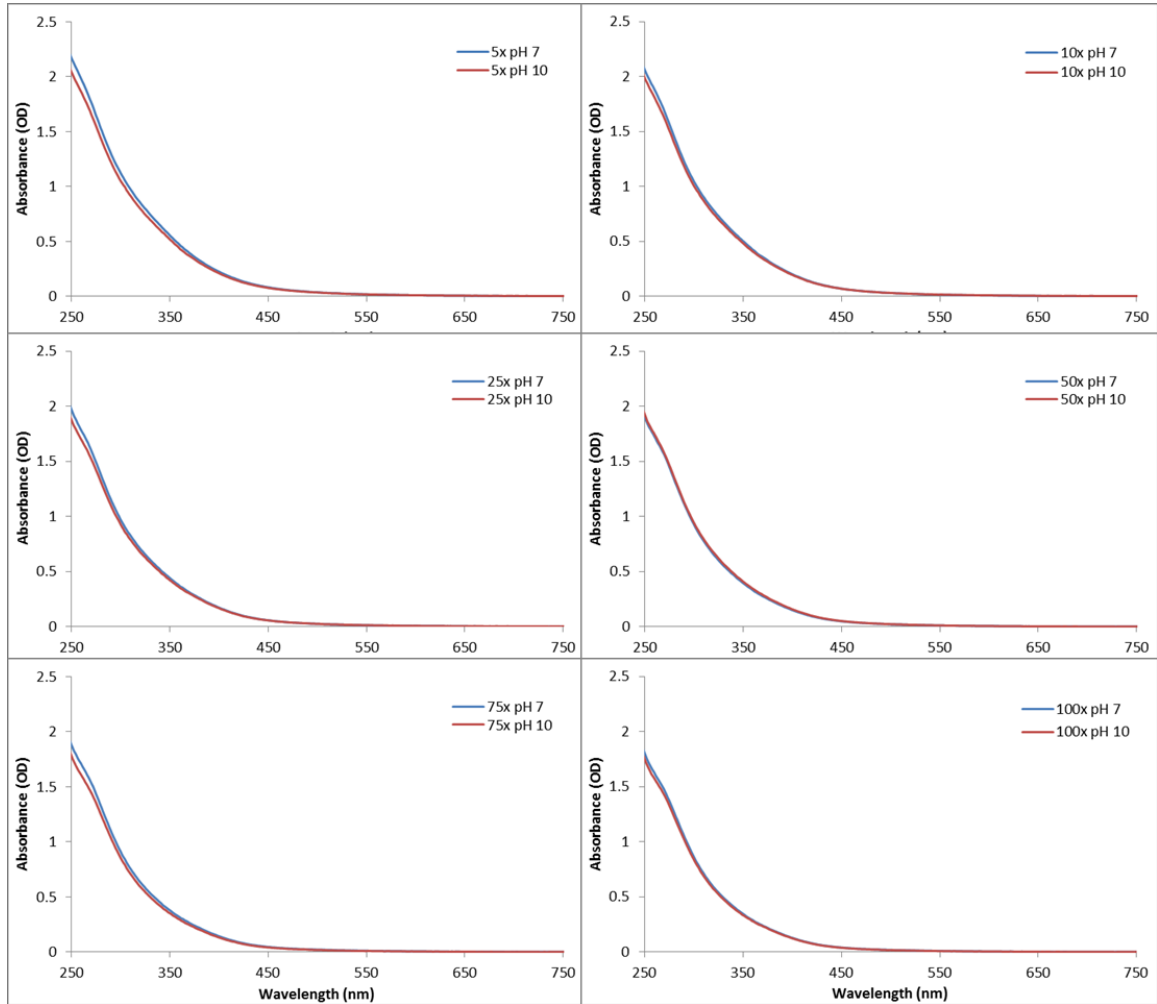


Figure A4-1. Absorbance of SRFA after 96 hours of reduction with a starting pH 7 (blue) or pH 10 (red). The pH of all the samples after reduction was ~10 despite the starting pH.

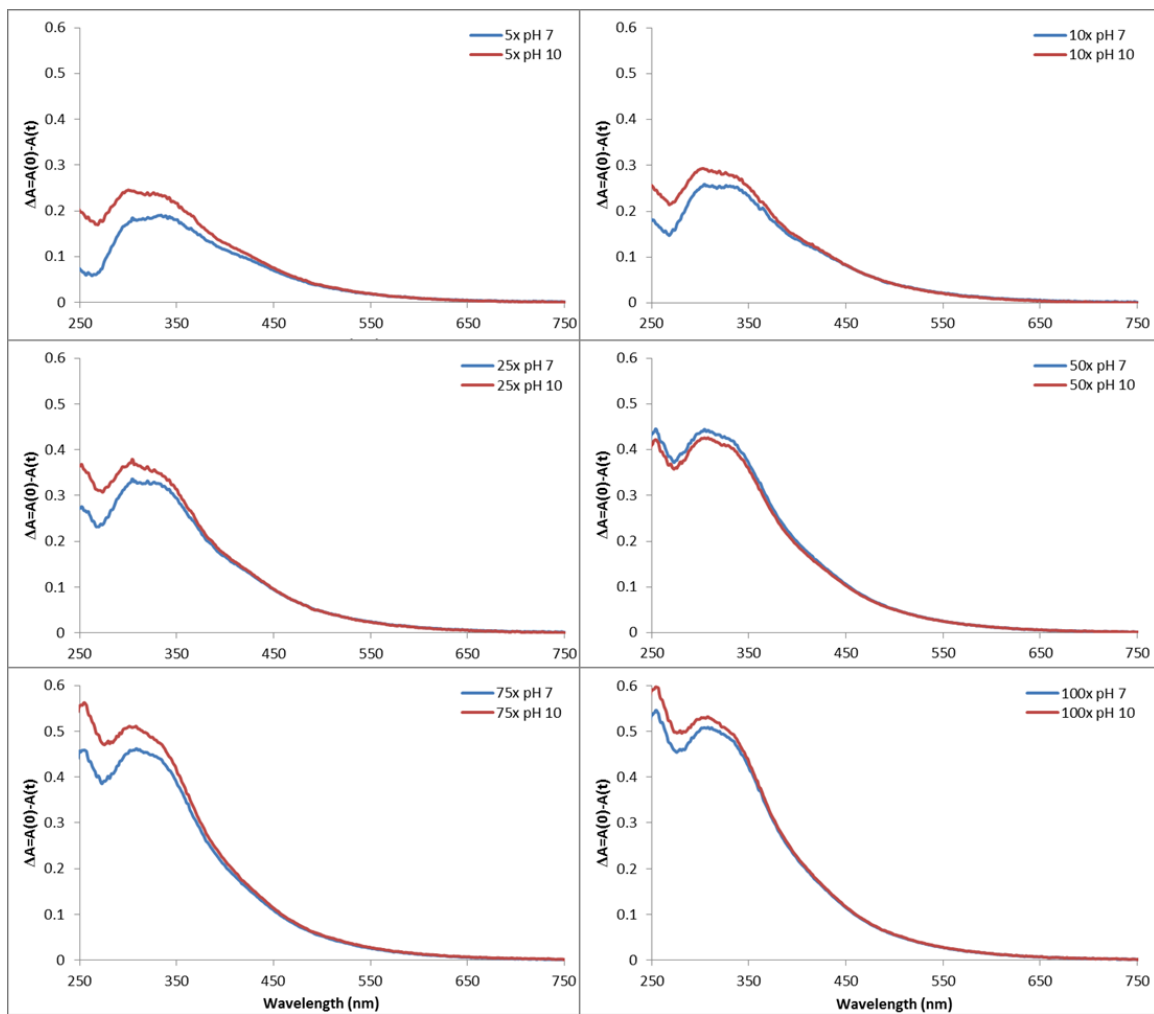


Figure A4-2. ΔA after 96 hours of reduction for SRFA with a starting pH 7 (blue) and pH 10 (red).

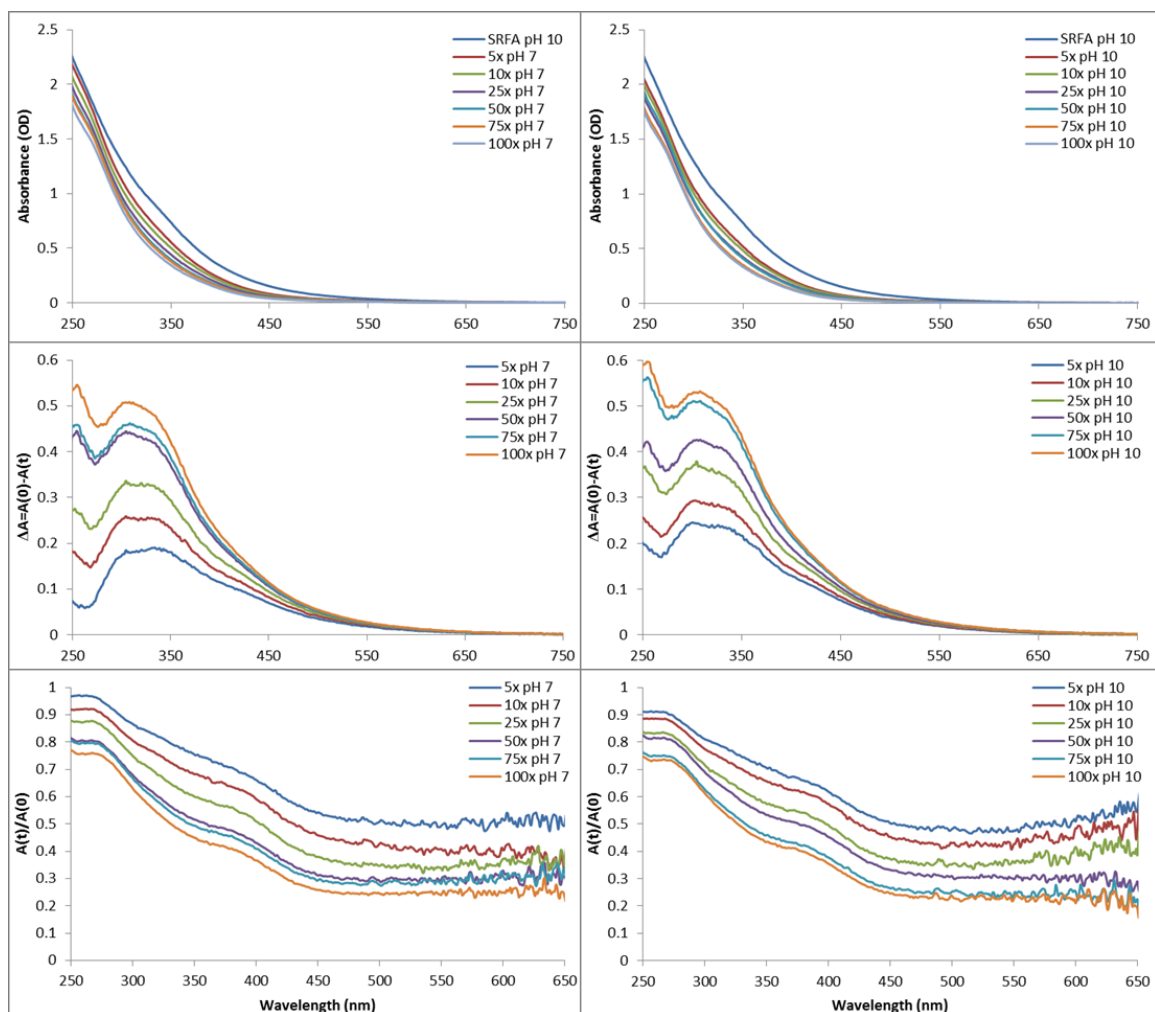


Figure A4-3. Comparison of the effects of initial pH on reduction. The left panel shows the initial pH 7 reduction series while the right panel shows the initial pH 10 reduction series. Both series use unreduced SRFA pH 10 as their reference sample since all the reduced samples were at a pH of approximately 10 after reduction despite their initial pH.

Appendix 5.
NaBH₄ Reduction: Solid versus Solution

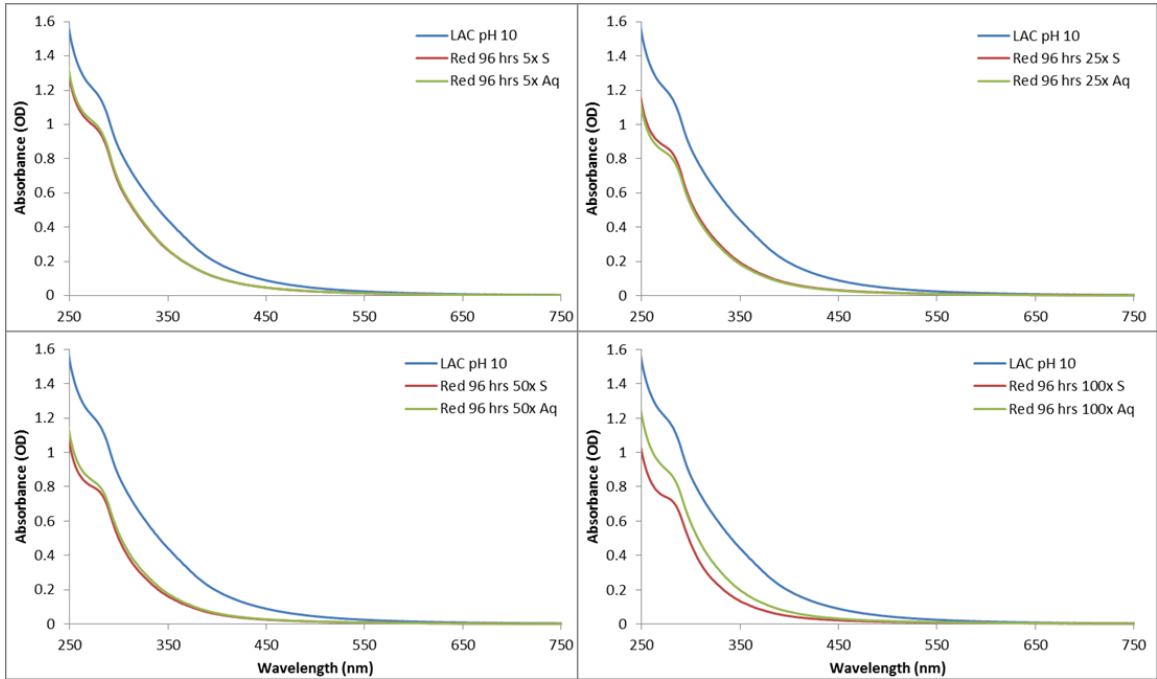


Figure A5-1. Absorbance of LAC after 96 hours for solid NaBH₄ (red) versus NaBH₄ in solution (green) for the first trial. The samples had a starting pH 7 and all reduced to a pH of ~10. A distinct difference can be noted in the 50-fold and 100-fold mass excess reductions.

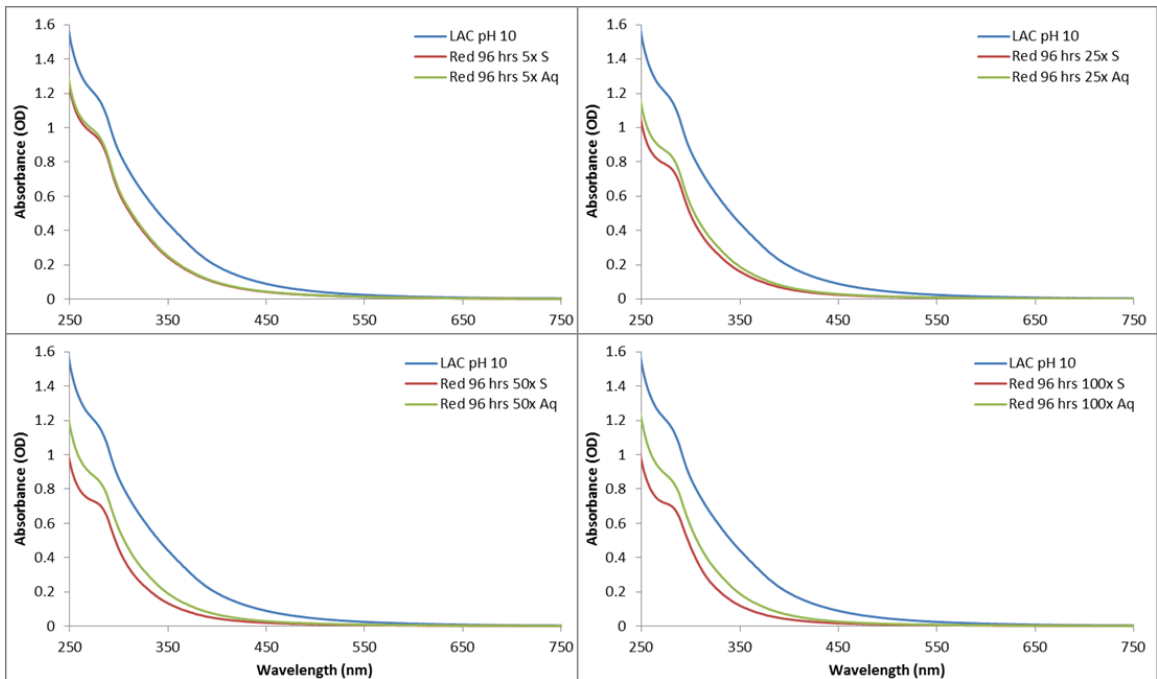


Figure A5-2. Absorbance of LAC after 96 hours for solid NaBH₄ (red) versus NaBH₄ in solution (green) for the second trial. The samples had a starting pH 7 and all reduced to a pH of ~10. A distinct difference can be noted in the 50-fold and 100-fold mass excess reductions.

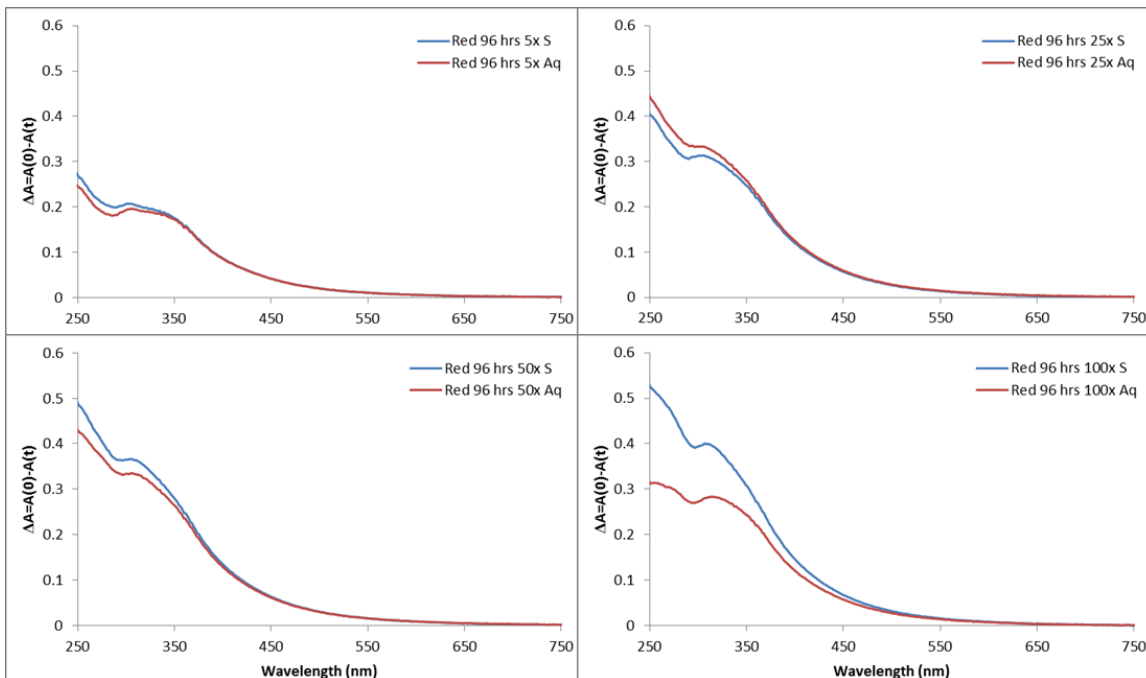


Figure A5-3. ΔA after 96 hours of reduction for solid phase (blue) and solution (red) reduction methods for the first trial.

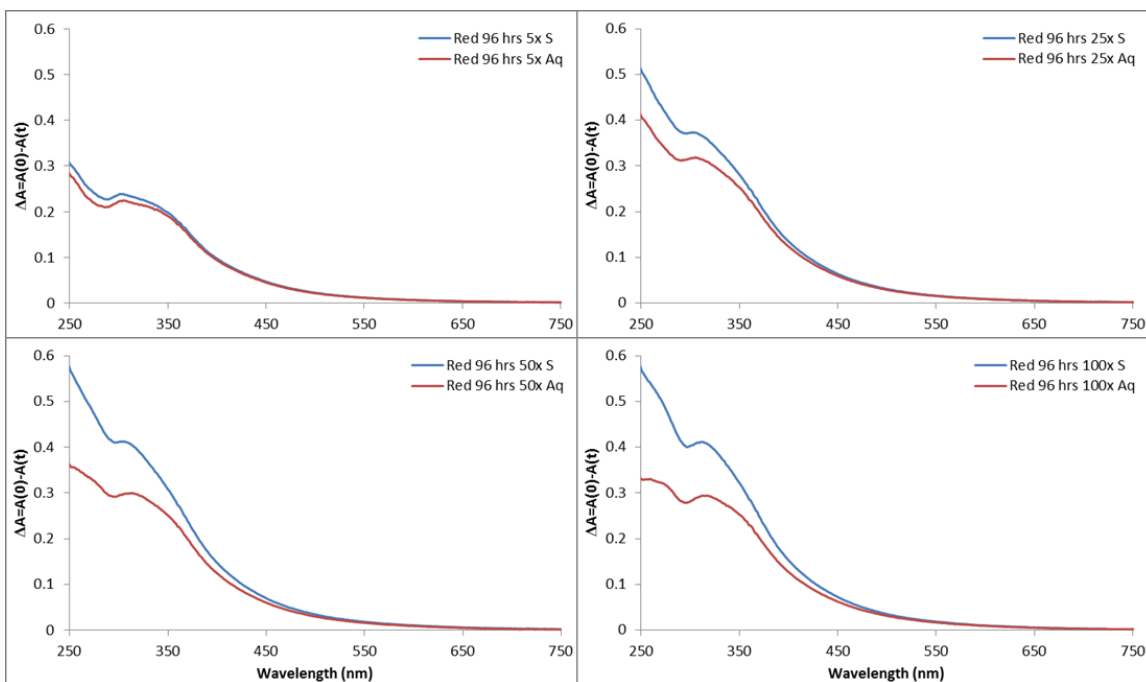


Figure A5-4. ΔA after 96 hours of reduction for solid phase (blue) and solution (red) reduction methods for the second trial.

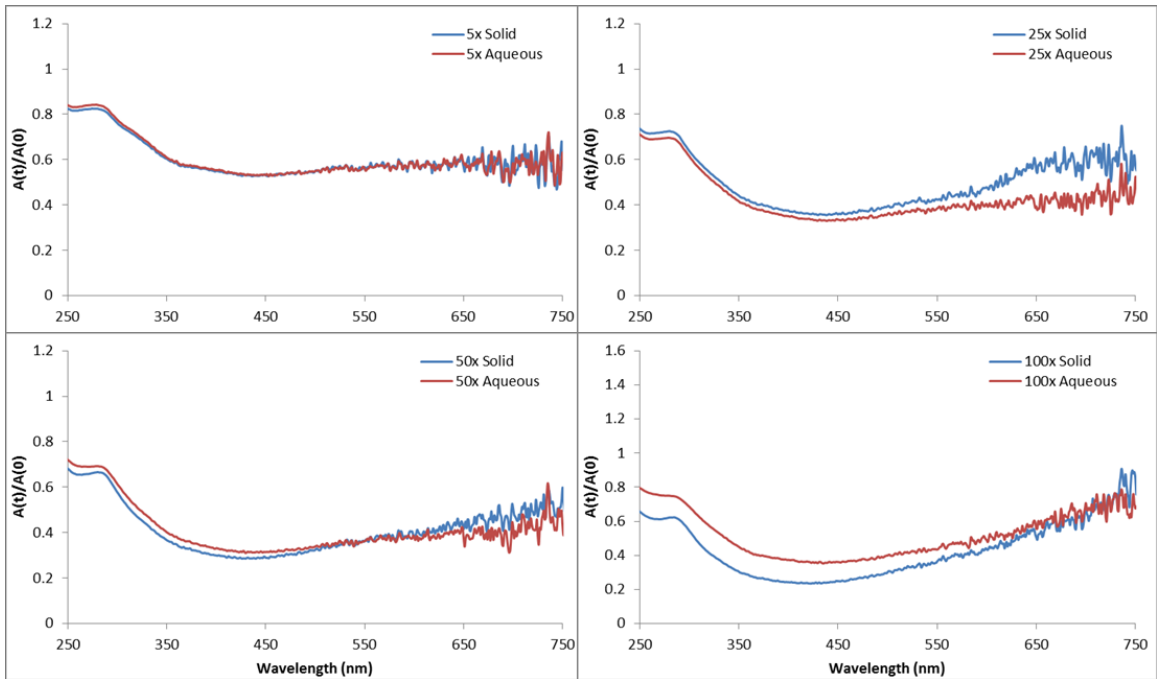


Figure A5-5. Fractional loss in absorbance after 96 hours of reduction for solid phase (blue) and solution (red) reduction methods for the first trial.

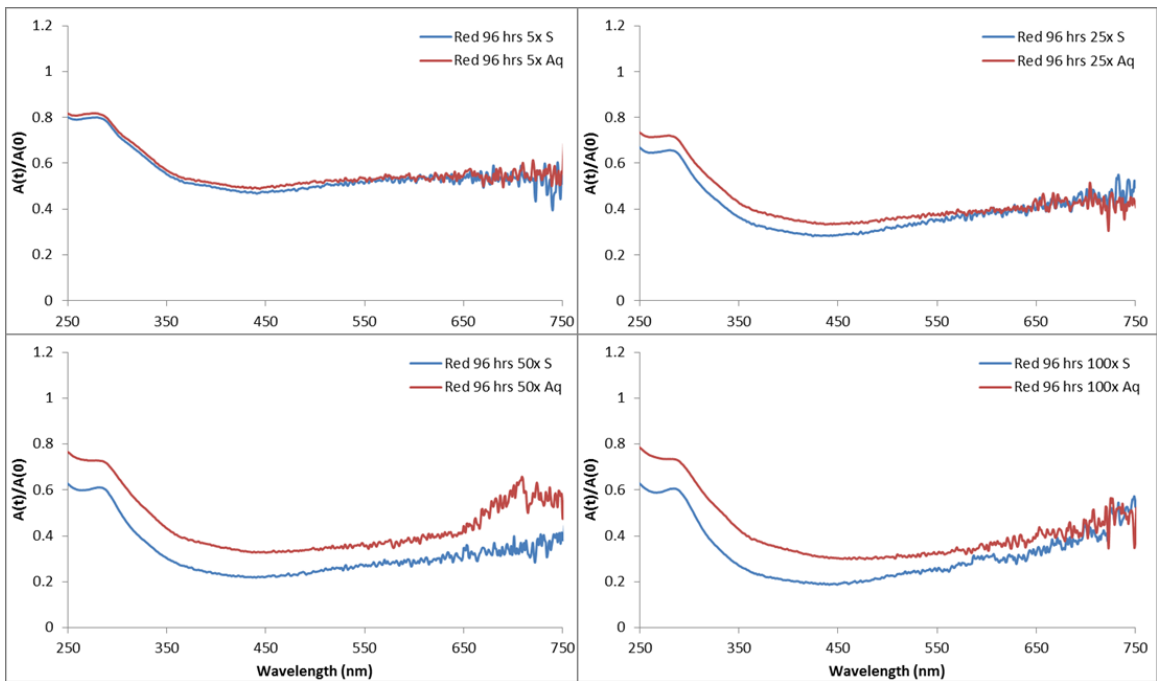


Figure A5-6. Fractional loss in absorbance after 96 hours of reduction for solid phase (blue) and solution (red) reduction methods for the second trial.

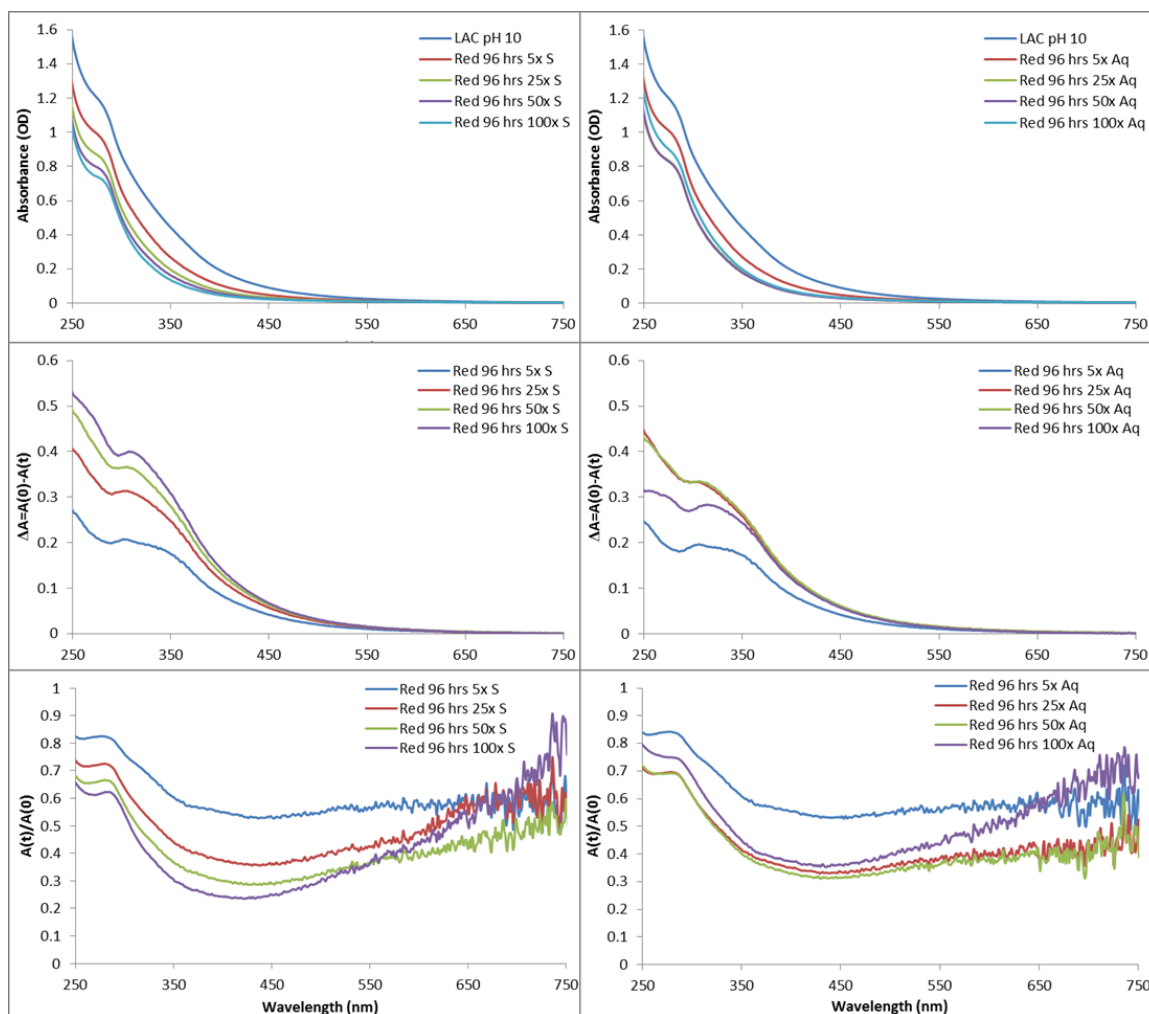


Figure A5-7. Comparison of the effects of NaBH_4 phase on reduction for the first trial. The left panel shows the solid phase reduction series while the right panel shows the solution reduction series. An increase in absorbance (above the unreduced absorbance in the visible) can be noted in the higher reduction amounts. This was not previously seen and could account for the difference noted in the solid versus solution reductions. In addition, the 100-fold mass excess hrs reduced sample does not lose as much absorbance as the 25-fold and 50-fold mass excess reductions, so it most likely either did not have enough NaBH_4 added or there was another, outside influence on the reduction.

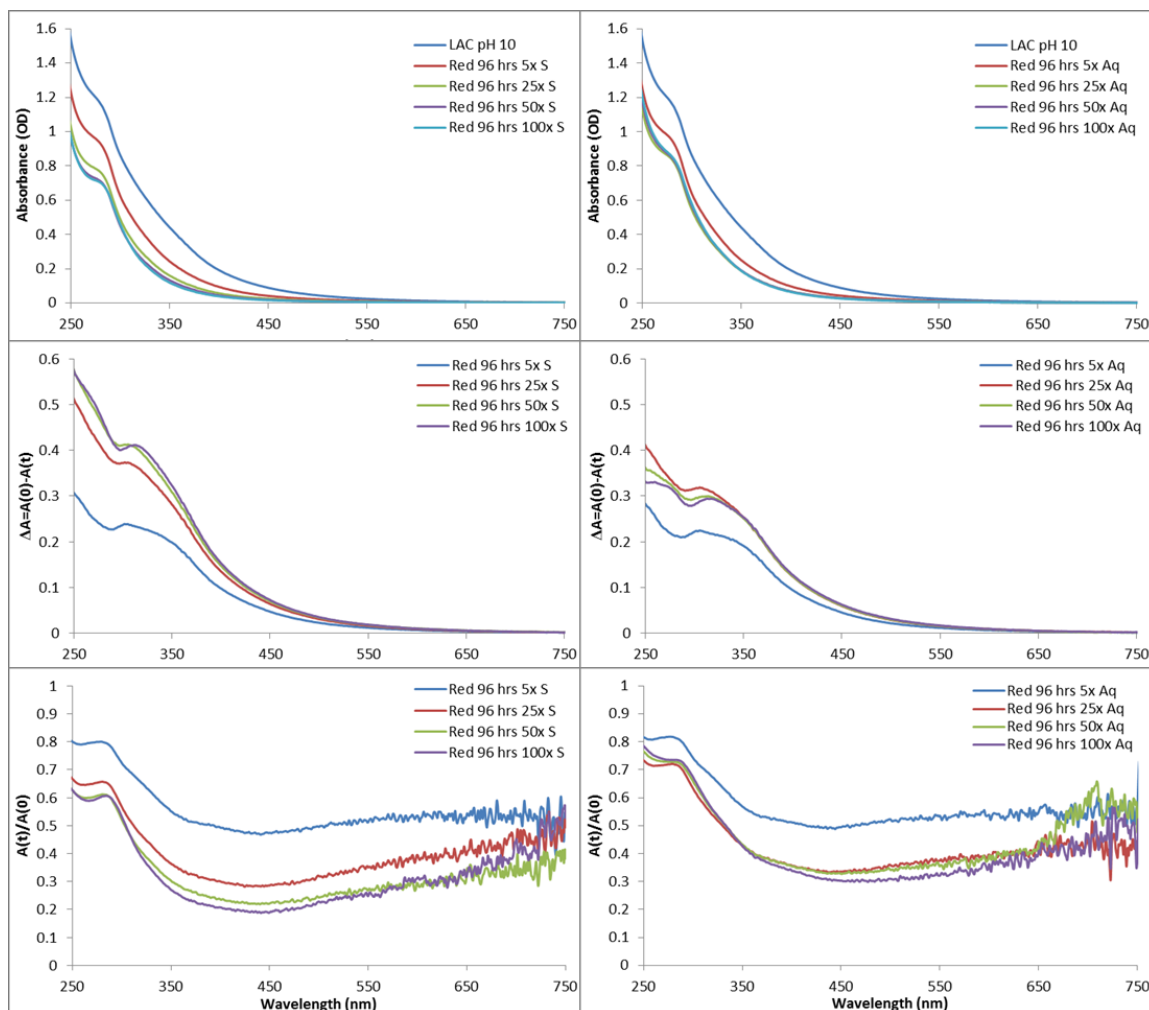


Figure A5-8. Comparison of the effects of NaBH_4 phase on reduction for the second trial. The left panel shows the solid phase reduction series while the right panel shows the solution reduction series. A smaller, but still noticeable increase in absorbance can be observed in both the solid and solution.

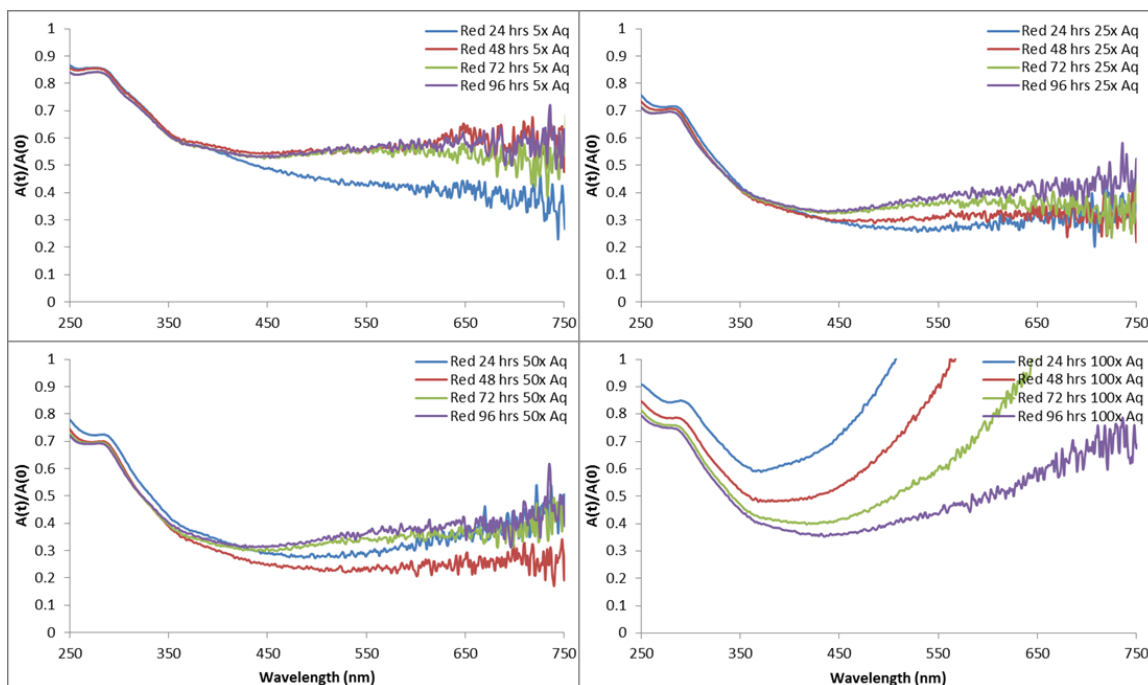


Figure A5-9. Changes in absorbance of LAC (100 mg/L, pH 10) following solution NaBH_4 reduction (5x, 25x, 50x, and 100x) from 24 hours after reduction till the reduction was thought to be complete at 96 hours for the first trial. While hydrogen gas bubbles were not as prevalent in the solution reduction, micro bubbles could be seen in the 100-fold reduced sample, creating a hazy solution, which increased absorbance due to scattering, leading to an absorbance that was initially greater than the unreduced sample.

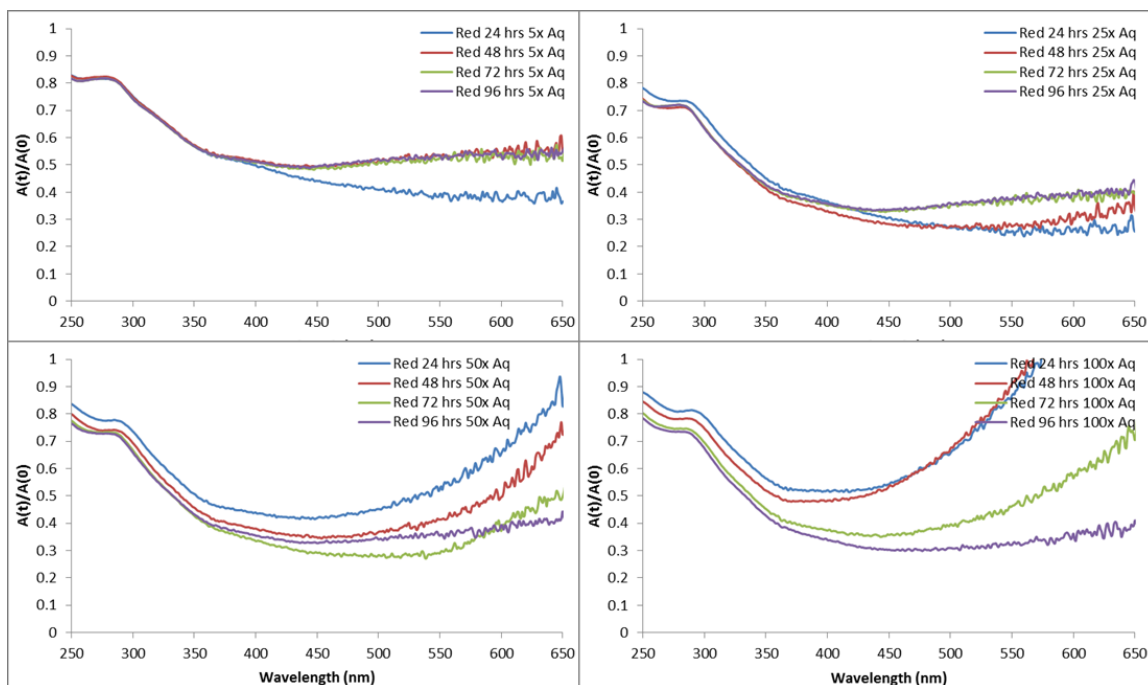
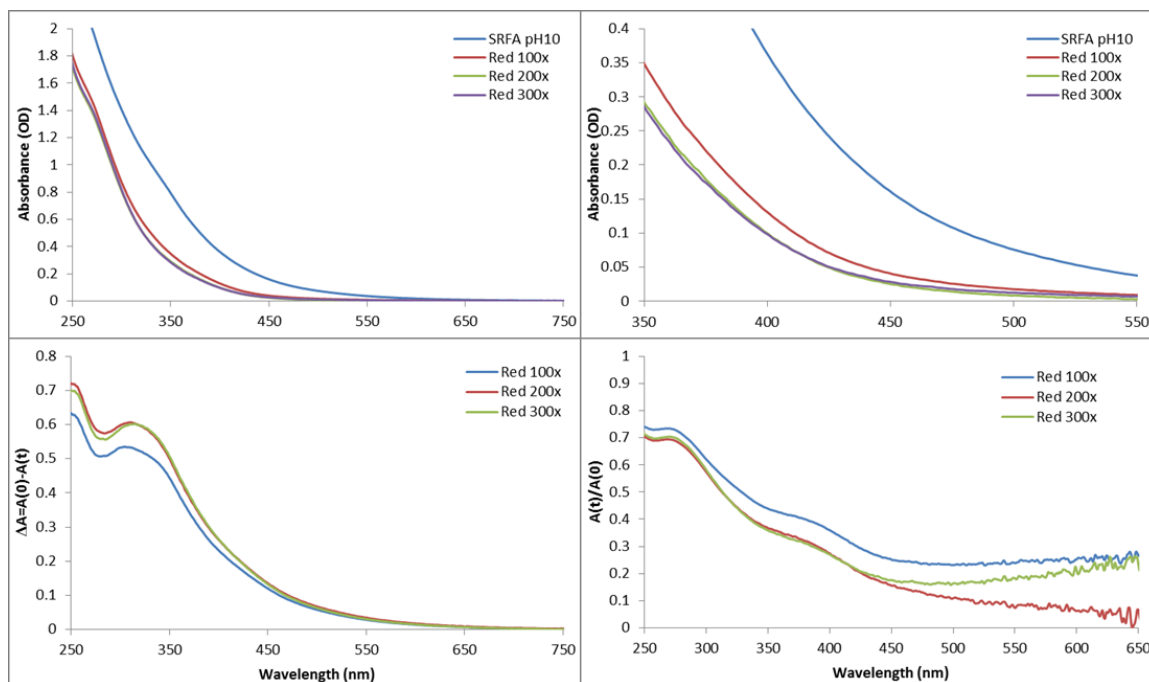


Figure A5-10. Changes in absorbance of LAC (100 mg/L, pH 10) following solution NaBH_4 reduction (5x, 25x, 50x, and 100x) from 24 hours after reduction till the reduction was thought to be complete at 96 hours for the second trial. While hydrogen gas bubbles were not as prevalent in the solution reduction, micro bubbles could be seen in the 100-fold reduced sample, creating a hazy solution, which increased absorbance due to scattering, leading to an absorbance that was initially greater than the unreduced sample.

Appendix 6.
100x-200x-300x Mass Excess NaBH₄ Reduction



Appendix A6-1. Optical changes upon reduction for SRFA prior to and post reduction, pH 10, prior to passing through the column. The top panels show the absorbance of SRFA over the full range (left) and an inset (right). The bottom panels show the ΔA (left) and the fractional absorbance loss (right). $\Delta A > 0$ and $A(t)/A(0) < 1$ indicate a loss in absorbance.

Appendix 7.
Dilution Factors for 10cm Column

Table A7-1. Dilution Factors for 10 cm Column

	Dilution Factor
SRFA	2
SRHA	2
LHA	2.1
EHA	2.2
PLFA	2.3
LAC	2.4

The dilution factor for the 10 cm cell was 2 for both SRFA and SRHA, while for EHA and LHA the dilution factor was approximately 2.2 and PLFA and LAC are approximately 2.3. LAC has a high degree of polydispersion, which would account for the increase in the dilution factor. PLFA, on the other hand, most likely has some small molecular interactions that occur with the Sephadex, which would lead to an increase in the spread of the PLFA on the column.

Appendix 8.
Column Performance as a Function of Sample pH: pH 7 versus pH 10

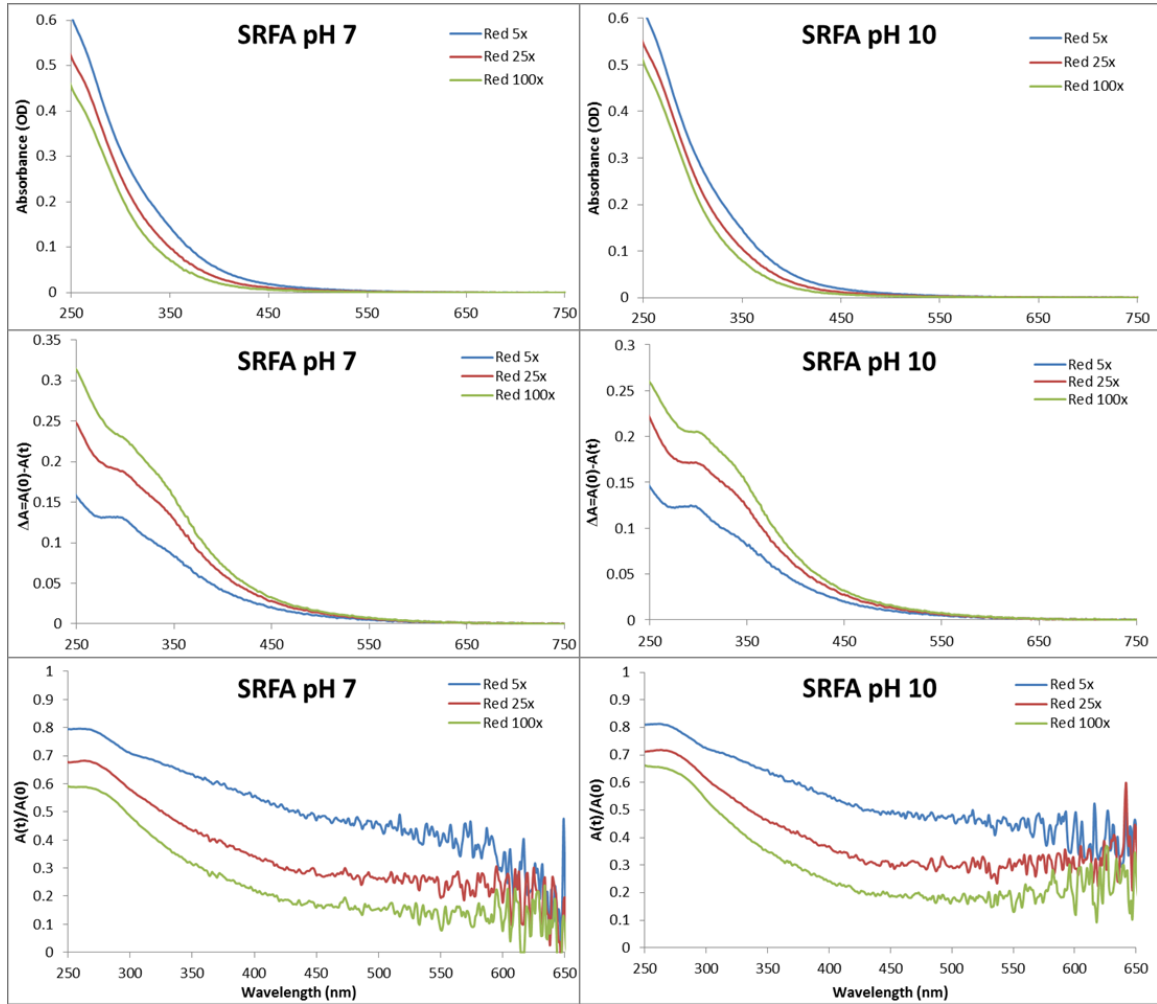


Figure A8-1. Comparison of the effects of the pH of the sample prior to running the column on the column efficiency. The left panel shows the initial pH 7 reduction series while the right panel shows the initial pH 10 reduction series.

Appendix 9.
EHA and LHA: Second G-10 Purification (10 cm Column)

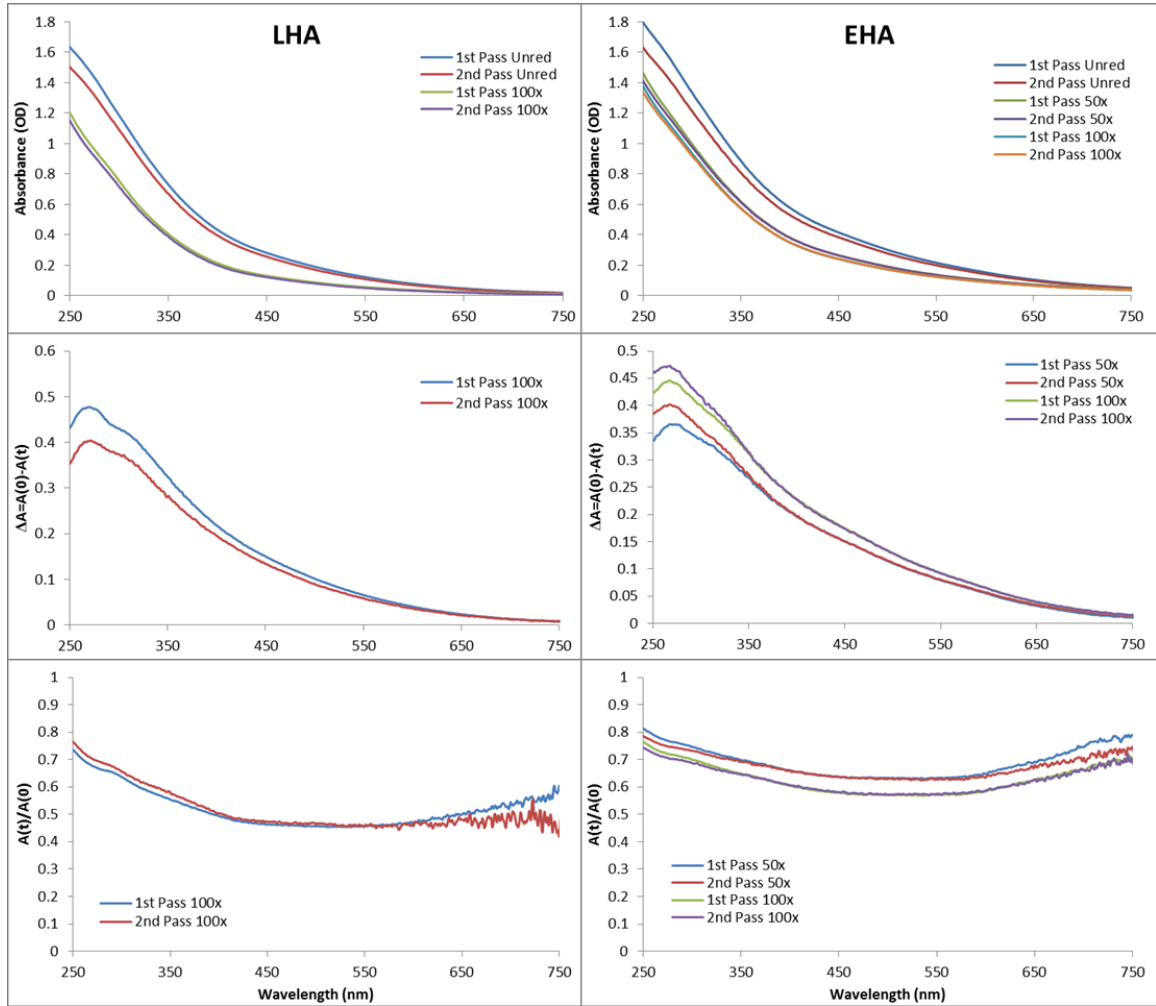


Figure A9-1. Comparison of the effects of the number of 10 cm column runs on the removal of residual borate. The left panel shows the LHA reduction series while the right panel shows the EHA Comparison of the effects of the number of 10 cm column runs on the removal of residual reduction series.

Appendix 10.
G-10 Column Length: 10 cm versus 15 cm

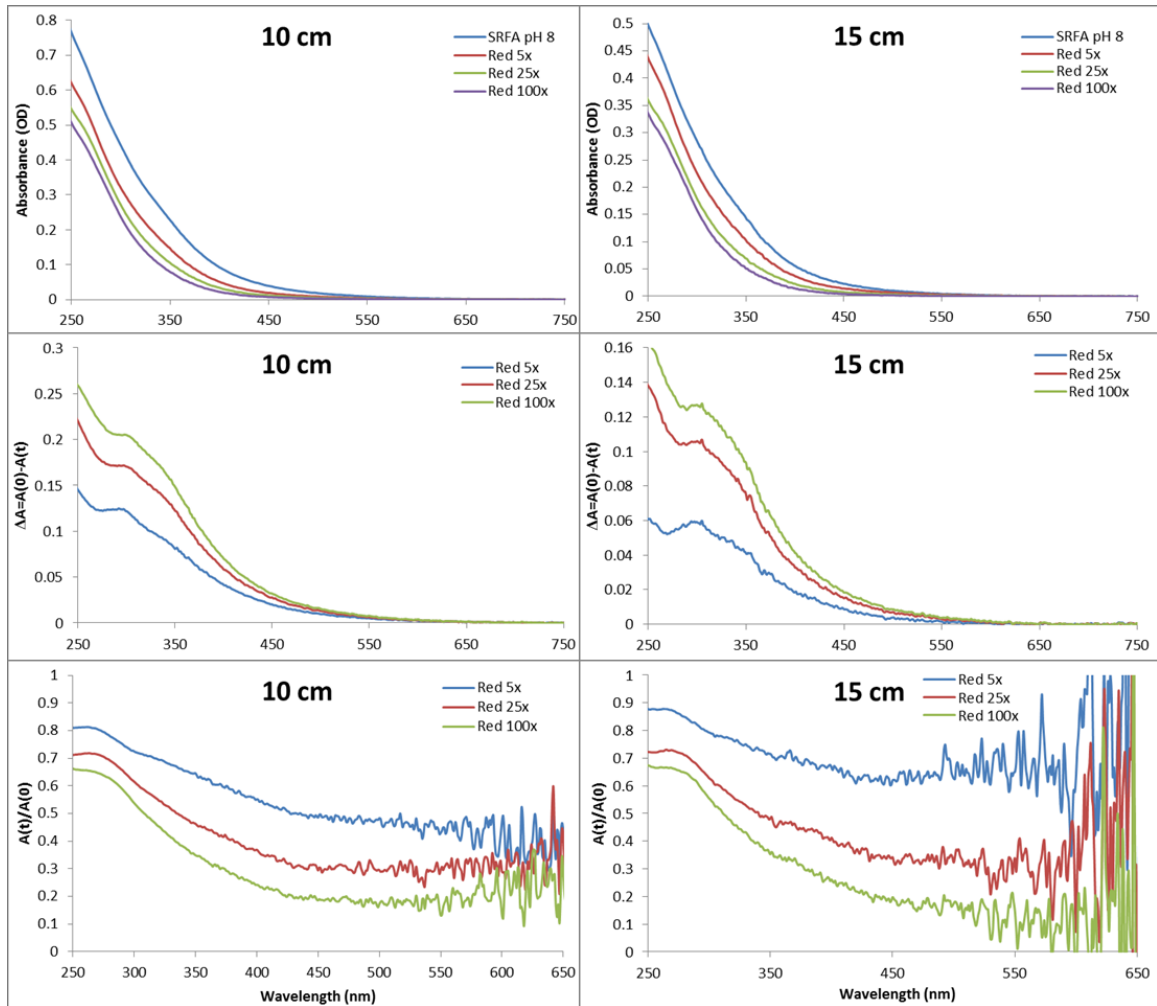


Figure A10-1. Comparison of the effects of the column length on the removal of residual borate. The left panel shows the 10 cm column length reduction series while the right panel shows the 15 cm column length reduction series.

Appendix 11.
Absorbance Values at 300 nm for Fluorescence Samples

Table A11-1. Absorbance Values at 300 nm for Fluorescence Samples

	HS Concentration (mg/L) Vis/UV	Unreduced	25x Reduced
SRFA	25/10	0.13854	0.09626
SRHA	16/5	0.09134	0.06929
LAC	40/10	0.06438	0.03688
PLFA	40/10	0.07357	0.04552
LHA	10/3	0.07417	0.06068
EHA	10/3	0.07392	0.07604

Appendix 12.
HS Reduction Fluorescence Emission: Post-column samples at pH 7

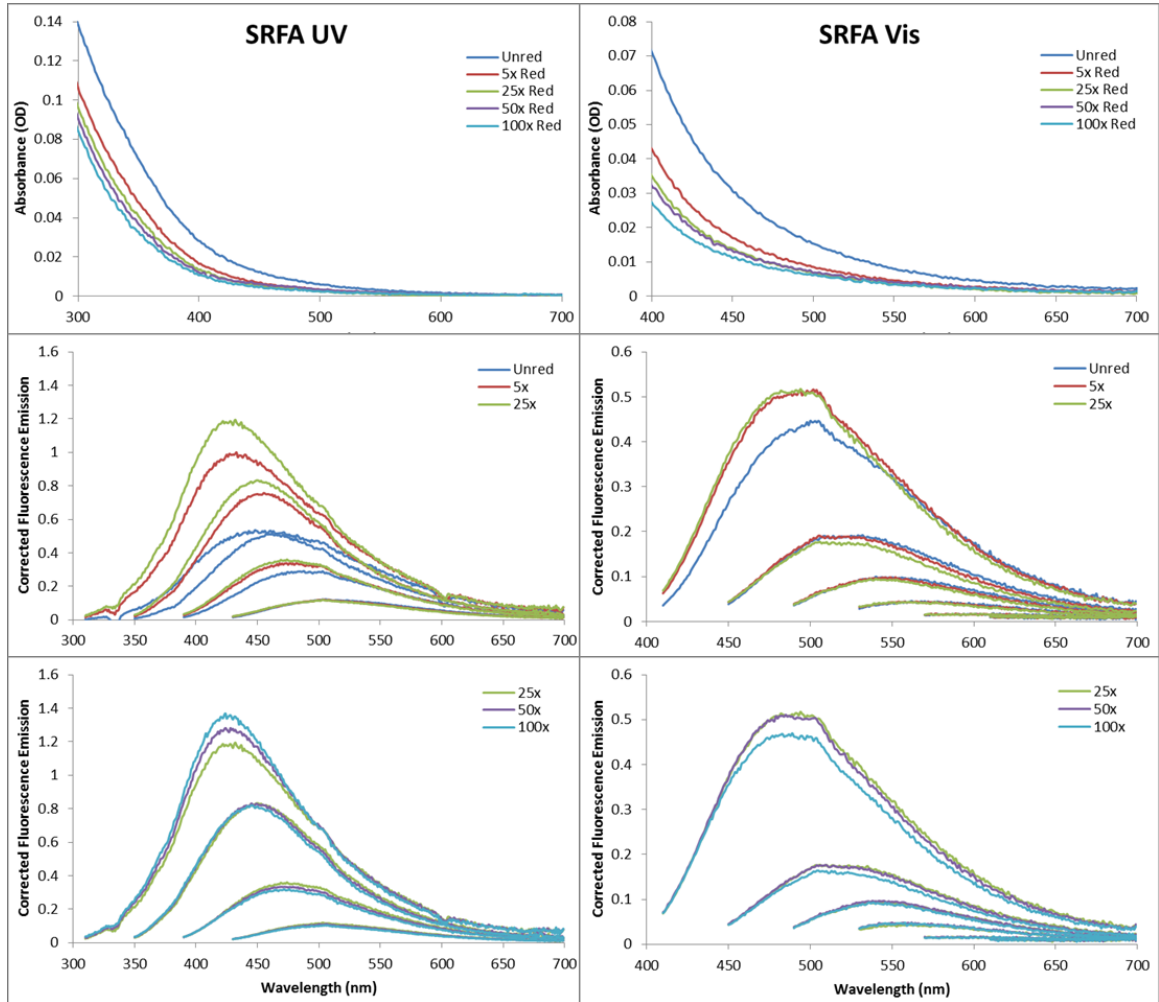


Figure A12-1. Optical changes upon reduction for SRFA prior to and post reduction, pH 7. Left panel SRFA (25 mg/L), the top shows the corresponding absorbance, and the middle and bottom show the fluorescence emission spectra for excitation 300-440 nm, exciting every 40 nm. Right panel SRFA (10 mg/L), the top shows the corresponding absorbance, the middle and bottom show fluorescence emission spectra for excitation 400-600 nm exciting every 40 nm.

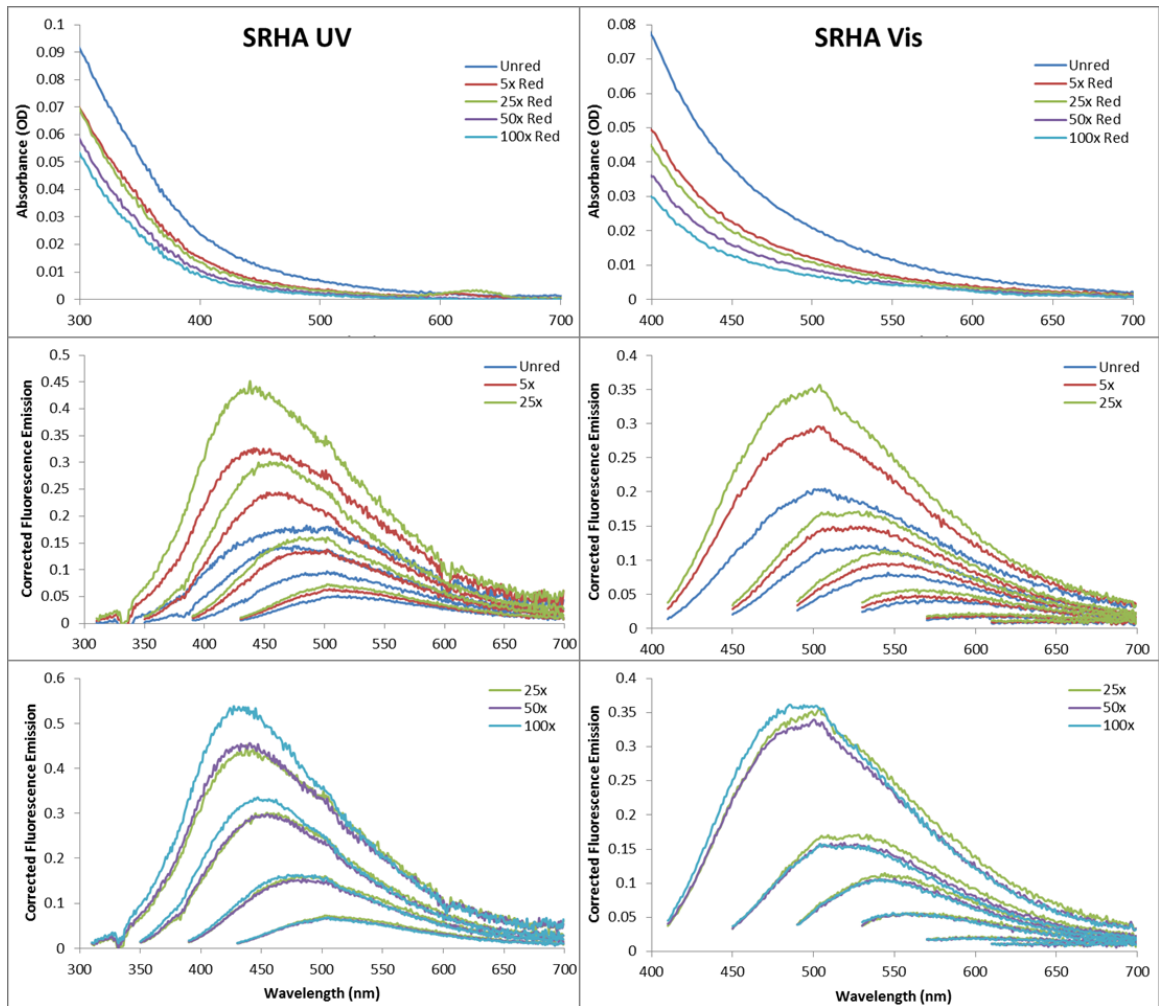


Figure A12-2. Optical changes upon reduction for SRHA prior to and post reduction, pH 7. Left panel SRHA (16 mg/L), the top shows the corresponding absorbance, and the middle and bottom show the fluorescence emission spectra for excitation 300-440 nm, exciting every 40 nm. Right panel SRHA (5 mg/L), the top shows the corresponding absorbance, the middle and bottom show fluorescence emission spectra for excitation 400-600 nm exciting every 40 nm.

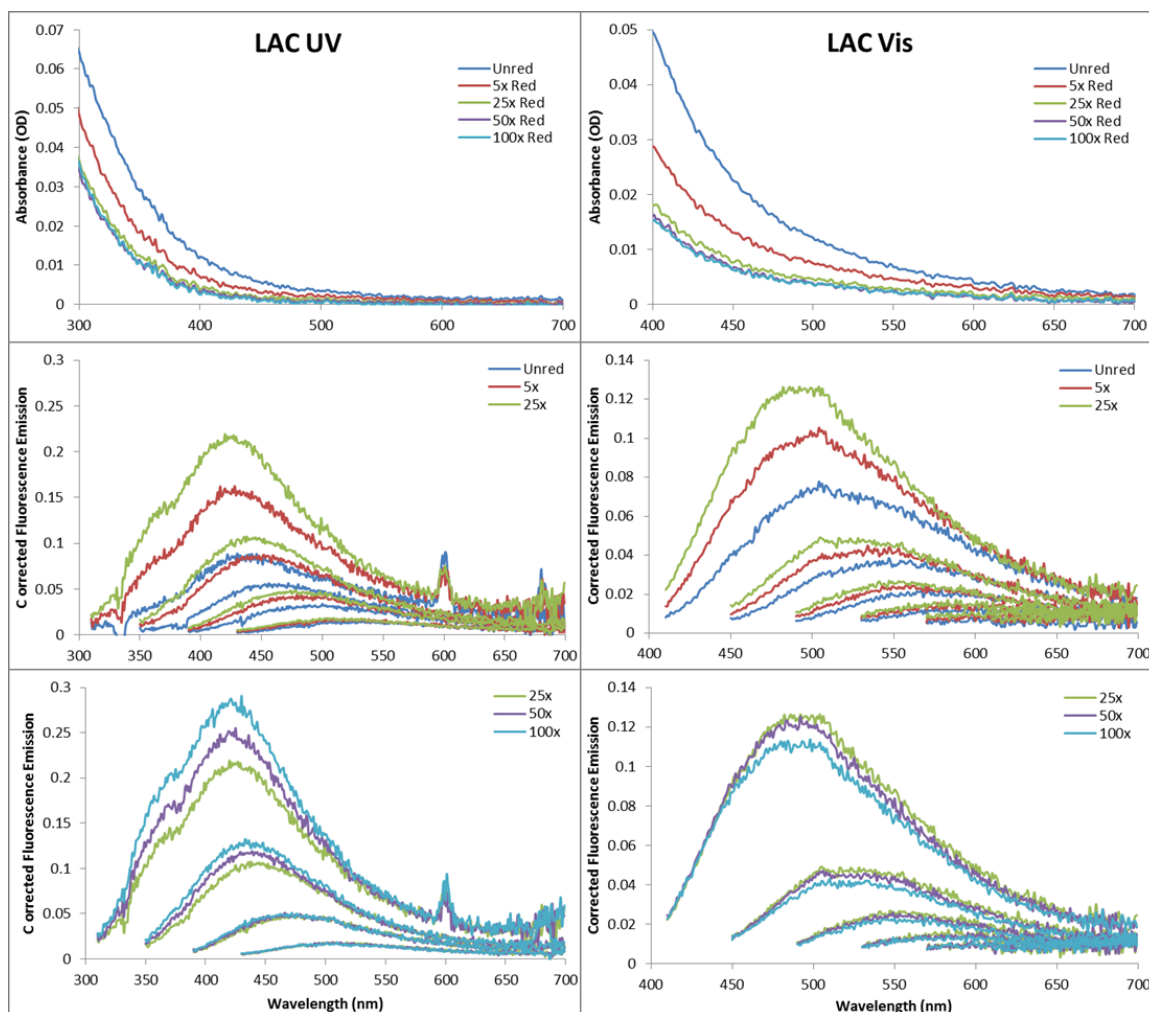


Figure A12-3. Optical changes upon reduction for LAC prior to and post reduction, pH 7. Left panel LAC (40 mg/L), the top shows the corresponding absorbance, and the middle and bottom show the fluorescence emission spectra for excitation 300-440 nm, exciting every 40 nm. Right panel LAC (10 mg/L), the top shows the corresponding absorbance, the middle and bottom show fluorescence emission spectra for excitation 400-600 nm exciting every 40 nm.

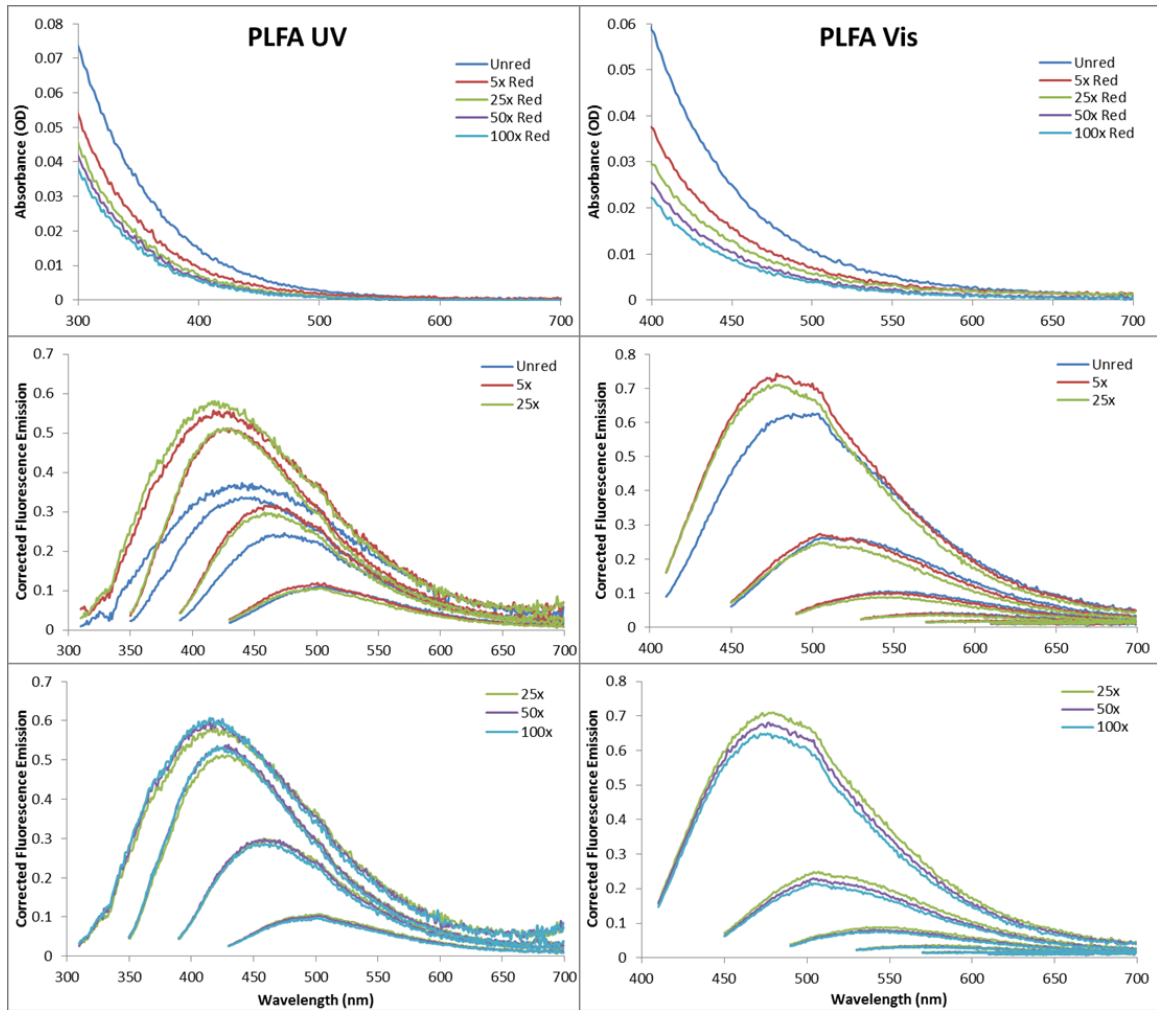


Figure A12-4. Optical changes upon reduction for PLFA prior to and post reduction, pH 7. Left panel PLFA (40 mg/L), the top shows the corresponding absorbance, and the middle and bottom show the fluorescence emission spectra for excitation 300-440 nm, exciting every 40 nm. Right panel PLFA (10 mg/L), the top shows the corresponding absorbance, the middle and bottom show fluorescence emission spectra for excitation 400-600 nm exciting every 40 nm.

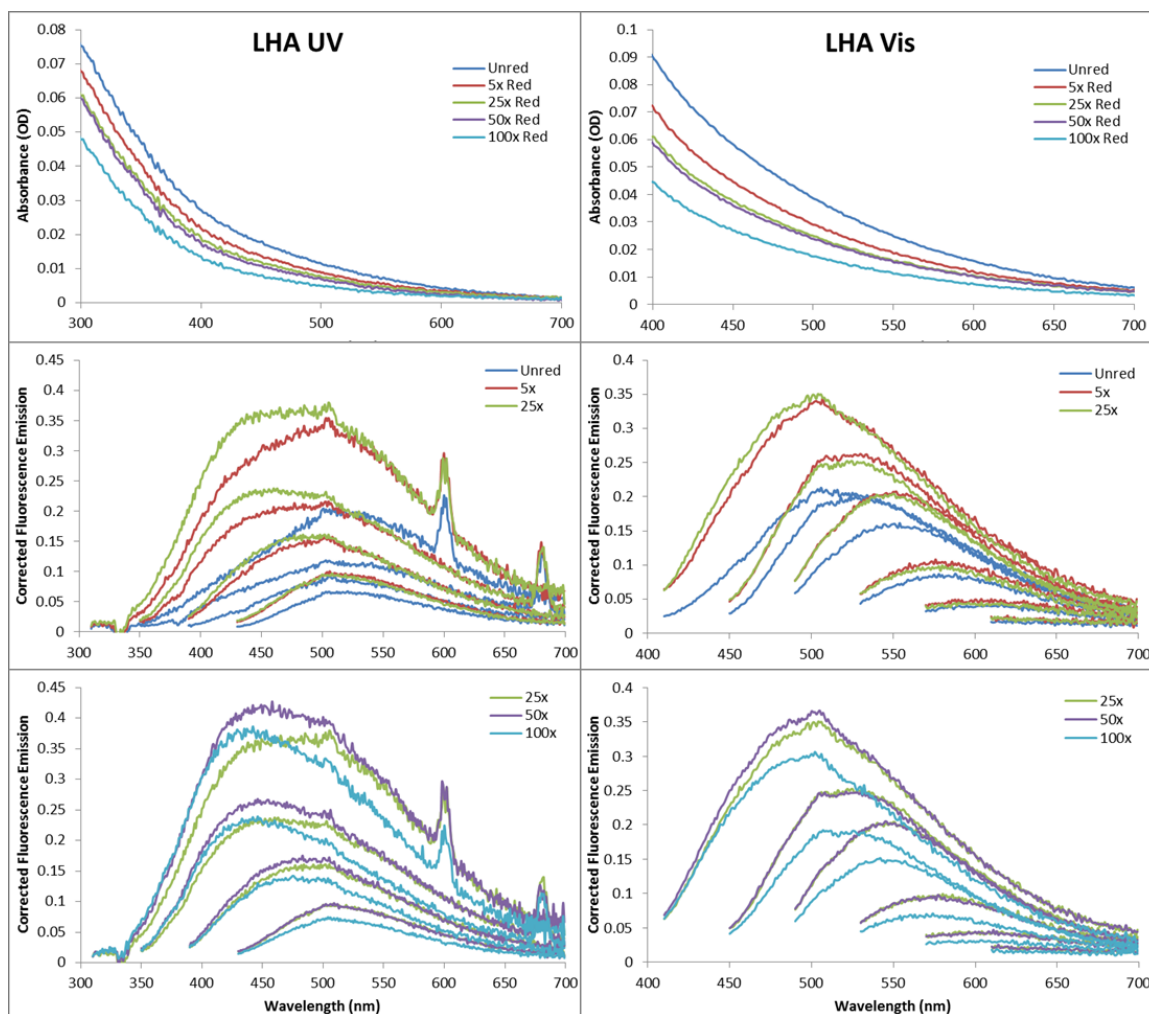


Figure A12-5. Optical changes upon reduction for LHA prior to and post reduction, pH 7. Left panel LHA (10 mg/L), the top shows the corresponding absorbance, and the middle and bottom show the fluorescence emission spectra for excitation 300-440 nm, exciting every 40 nm. Right panel LHA (3 mg/L), the top shows the corresponding absorbance, the middle and bottom show fluorescence emission spectra for excitation 400-600 nm exciting every 40 nm.

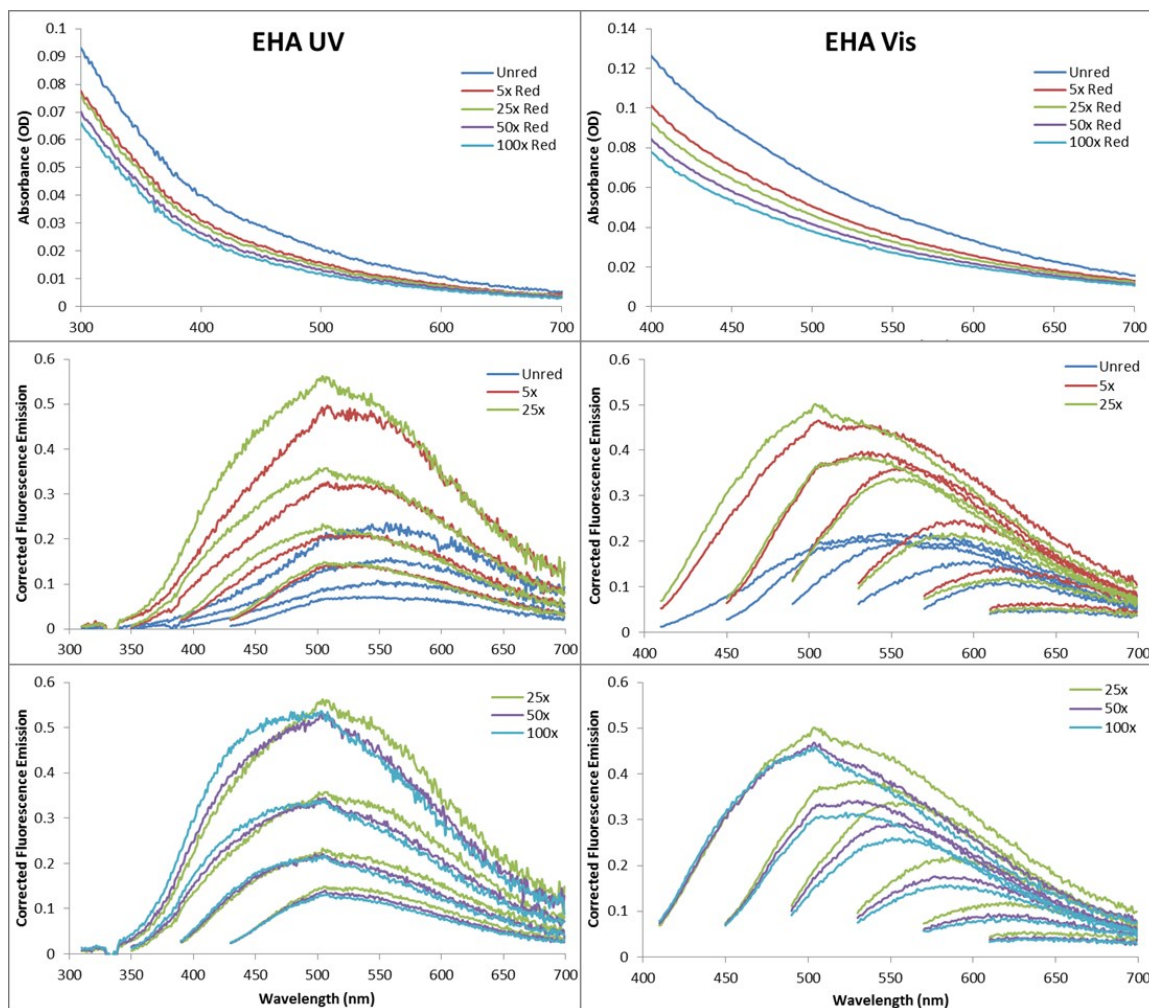


Figure A12-6. Optical changes upon reduction for EHA prior to and post reduction, pH 7. Left panel EHA (10 mg/L), the top shows the corresponding absorbance, and the middle and bottom show the fluorescence emission spectra for excitation 300-440 nm, exciting every 40 nm. Right panel EHA (3 mg/L), the top shows the corresponding absorbance, the middle and bottom show fluorescence emission spectra for excitation 400-600 nm exciting every 40 nm.

Appendix 13.

HS Reduction Fluorescence Emission: Unreduced versus 25-fold Mass Excess Reduction

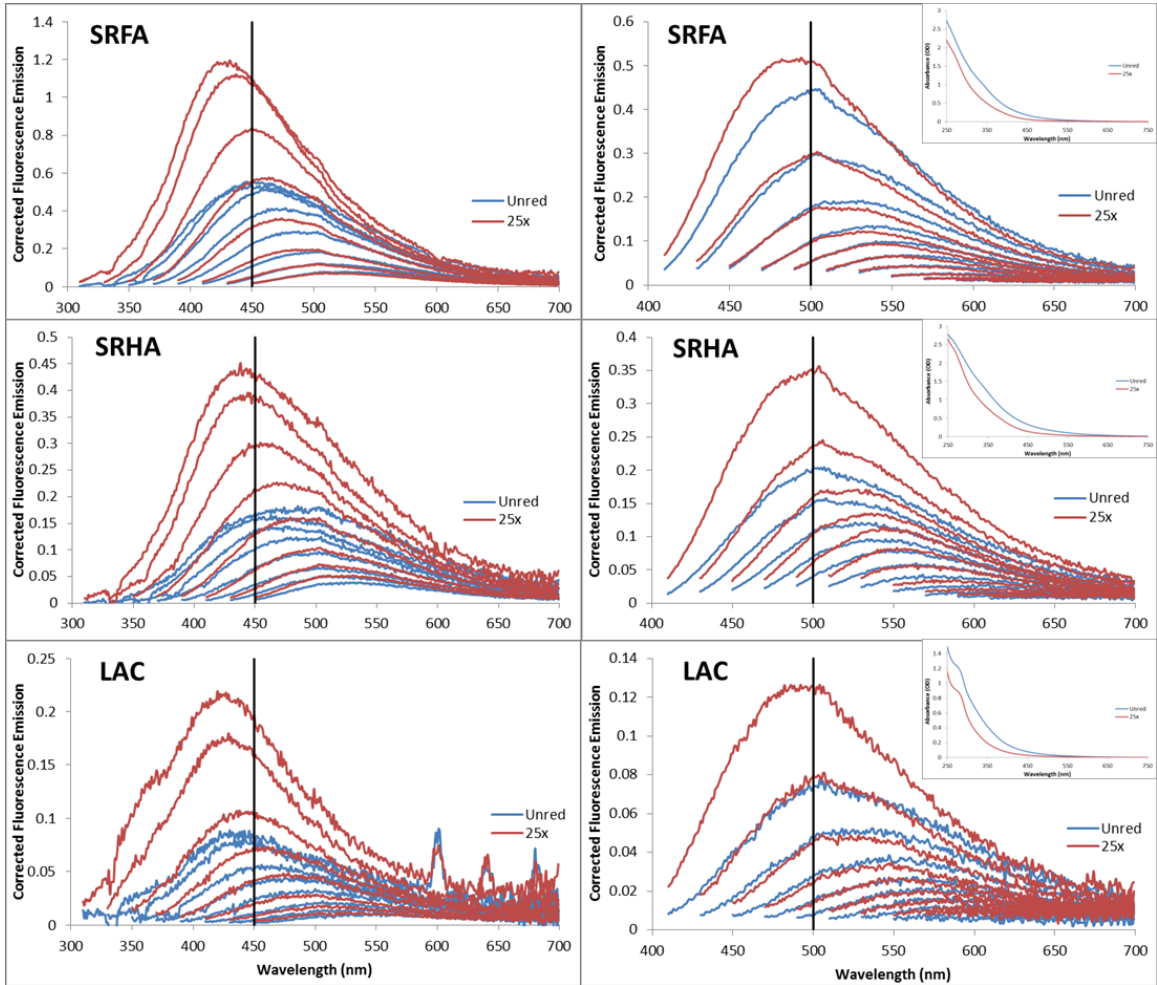


Figure A13-1. Fluorescence emission spectra at pH 7 for unreduced (blue) and 25-fold mass excess reduced (red) HS at the concentrations reported below and the corresponding absorbance at 100 mg/L pH 7 insets. The left panel is excitation 300–440 nm and the right panel is excitation 400–600 nm, exciting every 20 nm for both. SRFA was 25 mg/L, SRHA was 16 mg/L, and LAC was 40 mg/L for the visible region. SRFA and LAC were 10 mg/L and SRHA was 5 mg/L for the UV region.

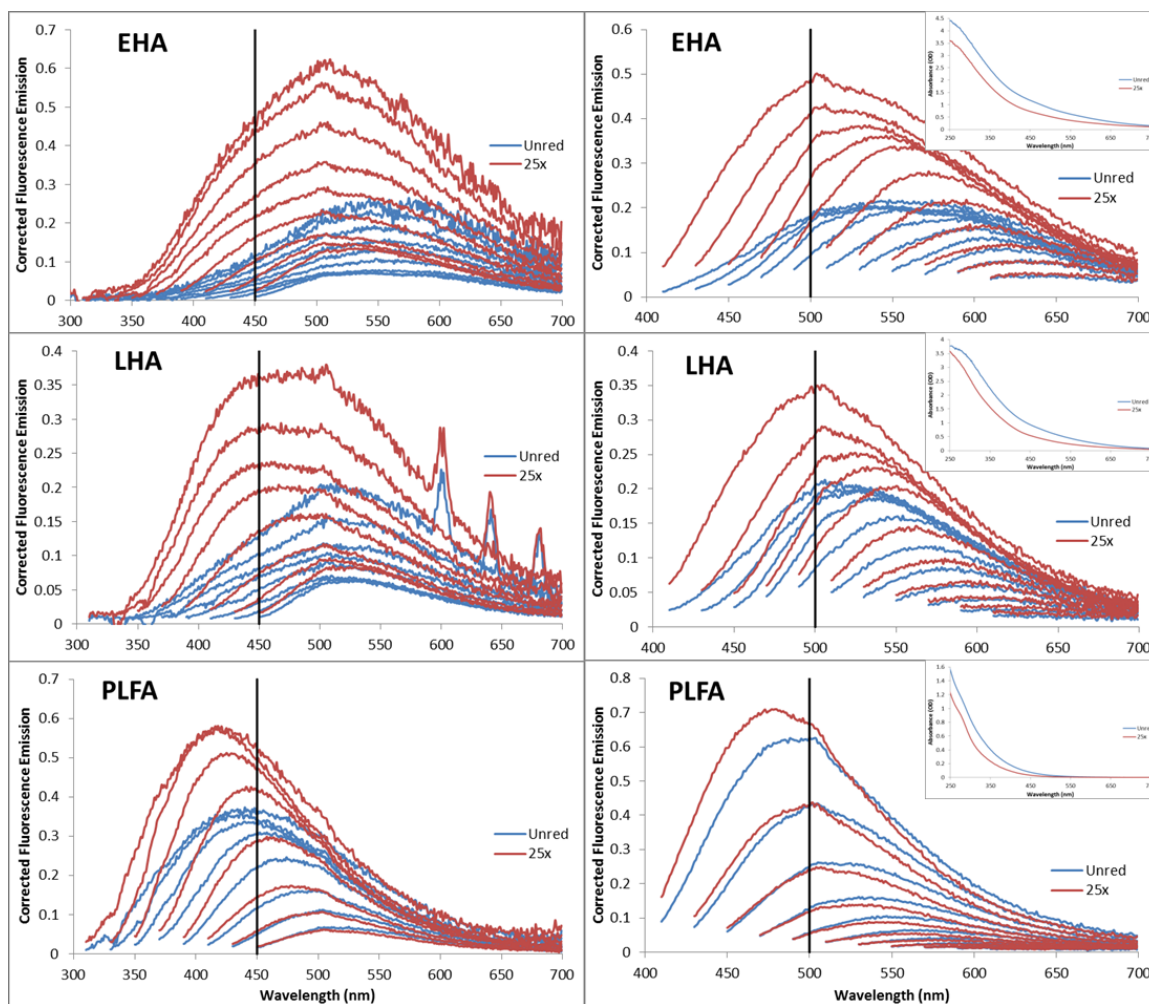


Figure A13-2. Fluorescence emission spectra at pH 7 for unreduced (blue) and 25-fold mass excess reduced (red) HS at the concentrations reported below and the corresponding absorbance at 100 mg/L pH 7 insets. The left panel is excitation 300-440 nm and the right panel is excitation 400-600 nm, exciting every 20 nm for both. PLFA was 40 mg/L and EHA and LHA were 10 mg/L for the visible region. PLFA was 10 mg/L and EHA and LHA were 3 mg/L for the UV region.

Appendix 14.
HS pH Titration: Unreduced versus 25-fold Mass Excess Reduction

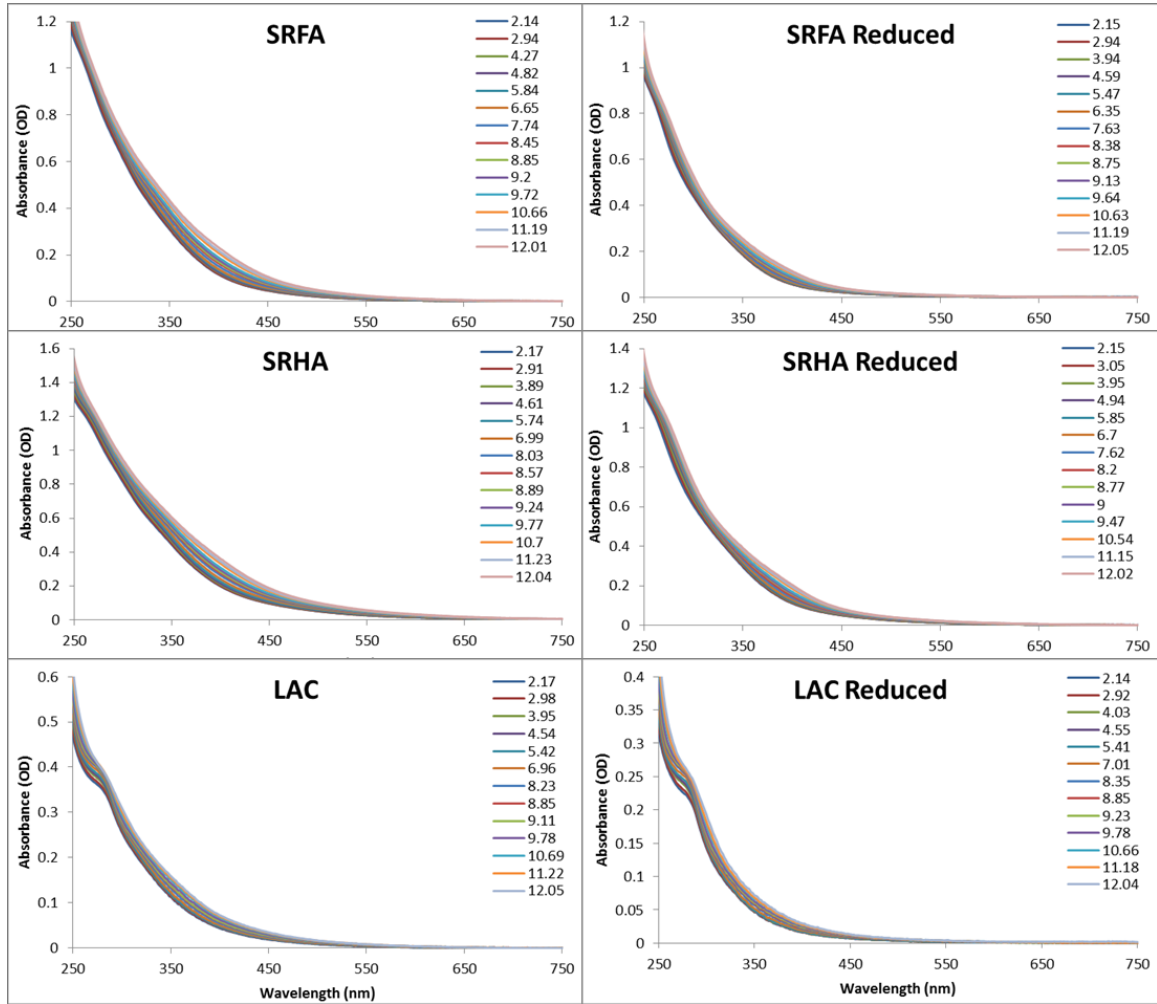


Figure A14-1. Dependence of the absorption spectra on pH following corrections for dilution. Left panel shows the unreduced samples while the right panel shows the corresponding 25-fold mass excess reduced samples. SRFA and SRHA were 50 mg/L and LAC was 43 mg/L for both unreduced and reduced samples.

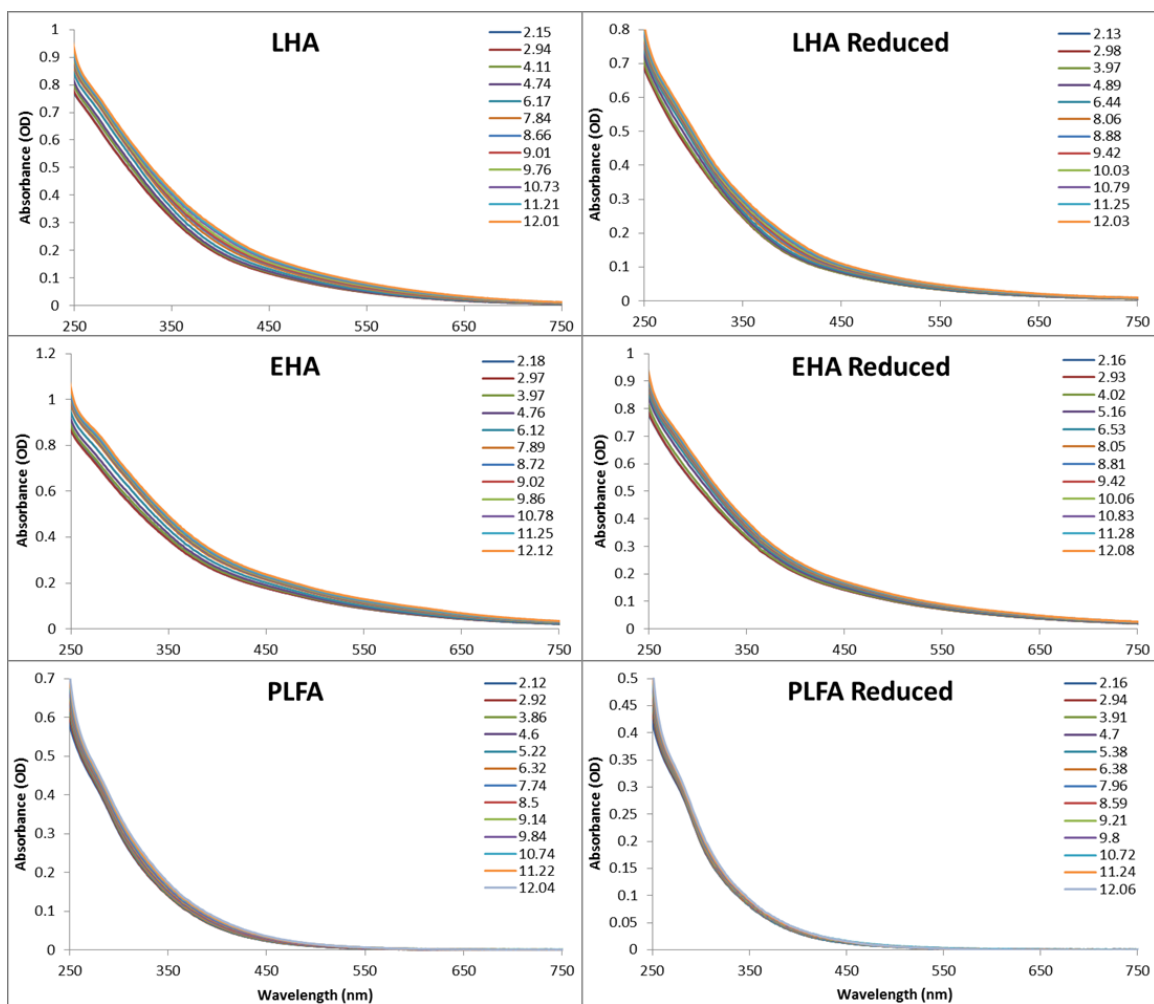


Figure A14-2. Dependence of the absorption spectra on pH following corrections for dilution. Left panel shows the un-reduced samples while the right panel shows the corresponding 25-fold mass excess reduced samples. EHA and LHA were 25 mg/L and PLFA was 44 mg/L for both un-reduced and reduced samples.

Appendix 15.
25-fold Mass Excess Reduction: Fractional Loss due to pH

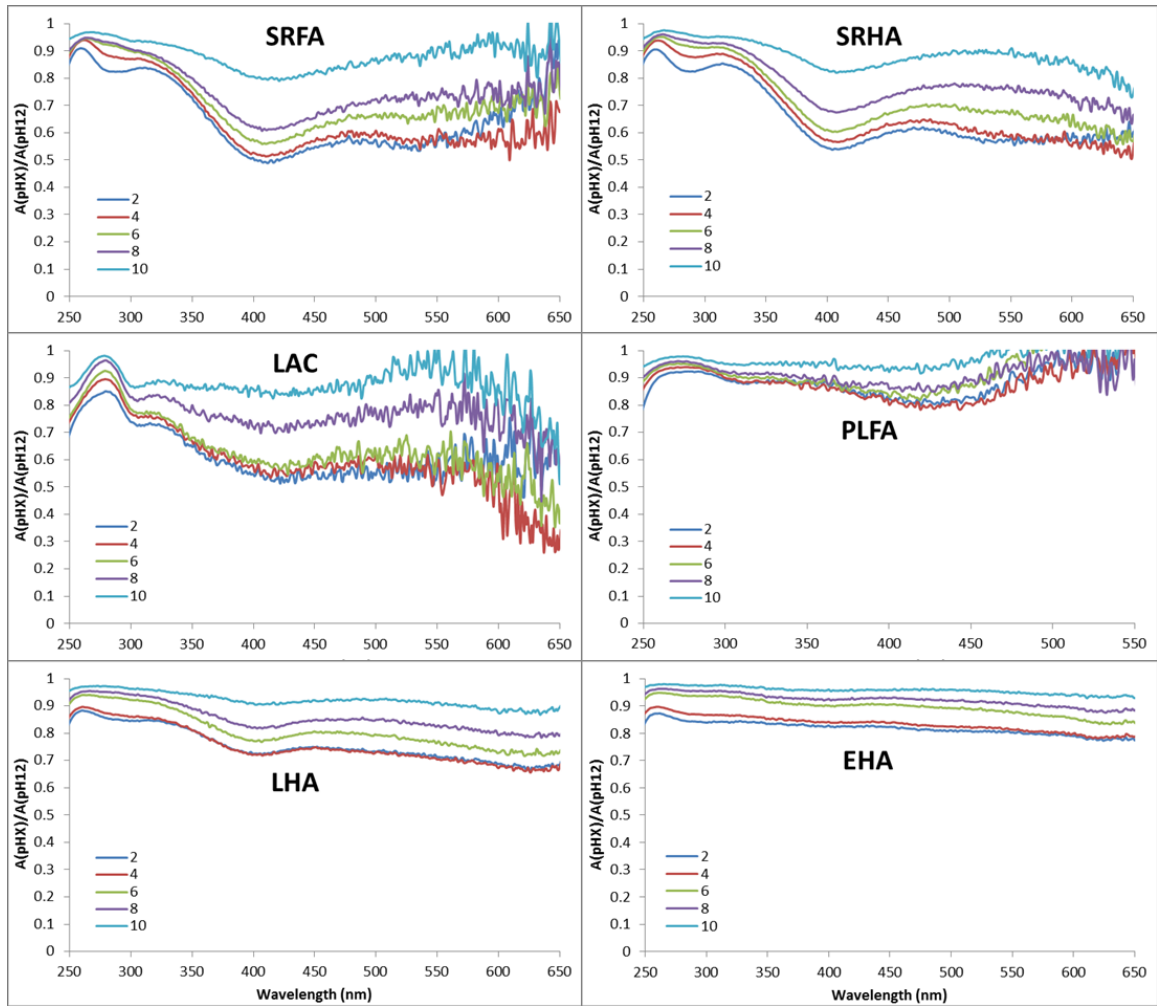


Figure A15-1. Fractional loss of absorbance due to a change in pH, relative to pH 12.

Appendix 16. Analysis of Difference Spectra for HS

The total difference spectra for the HS exhibited contributions from both carboxylic acids and phenolic groups.¹³ Similar to results from previous studies, the difference spectra of SRFA show a peak at approximately 280 nm and a broad peak at approximately 300-400 nm.²³ Similar to SRFA, SRHA and LAC also showed a short-wavelength peak at approximately 280 nm that slightly red-shifted with increasing pH from 2 to 6 (attributed to the deprotonation of aromatic carboxylic acids) which became less apparent at the higher pH values for LAC. SRHA and LAC also exhibited increases in longer wavelength absorption (300-400 nm range) that extended well into the visible over the pH 6 to 12; the maximum of this absorption gain was 400 nm for SRHA and 350 nm for LAC (Appendix 18; Figs. A18-1-3). The carboxylic acid groups clearly exhibited a peak maximum at 280 nm that monotonically decreased with increasing wavelength for SRFA and LAC, while extending farther into the visible for SRHA over the pH 2 to 6 range. The difference spectra over the phenolic groups pK_a range showed a peak at approximately 400 nm for SRFA and SRHA that was blue-shifted for LAC (~350 nm) with a shoulder at shorter wavelengths (~300 nm) evident for SRFA and LAC, but not for SRHA.

PLFA exhibited the least dependence on pH of any of the HS tested in this study. The dual contribution to the optical properties from carboxylic acids and phenolic groups was less obvious: there was a small peak at approximately 300 nm that is largest at higher pHs and decreased with increasing wavelengths (Appendix 18; Fig. A18-4). The carboxylic acids contribution was minimal; and the phenolic groups contribution was blue-shifted (closer to 330 nm) relative to SRFA, SRHA and LAC.

Unlike aquatic and microbial HS (SRFA, SRHA, LAC and PLFA), terrestrial HS (LHA and EHA) exhibited a total difference spectra with monotonically decreasing absorption differences with increasing wavelength. LHA showed a distinct shoulder at approximately 400 nm that was even further red-shifted to ~ 650 nm for EHA (Appendix 18; Figs. A18-5 and A18-6). These features were only present at pH values > 7. The carboxylic acids contribution was similar for both LHA and EHA with a peak at approximately 280 nm. However the phenolic groups contribution was quite different; LHA phenolic groups difference spectral shape had maxima at ~ 400 nm, thus similar to those of SRHA and SRFA but extending further into the visible; EHA still had a slight peak at 350 nm, but not as distinct as that noted in SRHA, SRFA, and LHA and showed the distinct shoulder at 650 nm.

Appendix 17.
Analysis of Difference Spectra for Borohydride Reduced HS

The difference spectra acquired for the reduced SRFA, SRHA and LAC followed closely with those of the untreated HS discussed earlier (Appendix 18; Figs. A18-1-3). The carboxylic acid groups still showed a distinct peak at approximately 280 nm that exhibited only a slight red-shifted absorbance with increasing pH, and the absorbance was no longer extended into longer wavelengths, thus implying that the groups responsible for these shifts were coupled with the carbonyl groups eliminated by reduction. However, the absorption changes over the phenolic groups pK_a range of the reduced HS were blue-shifted (to ~ 380 nm for SRFA and SRHA and to 350 nm for LAC) and had a much smaller intensity thus indicating that reduction eliminates visible-absorbing species that is produced at high pH. This result is consistent with the loss of charge-transfer interactions due to the removal of one possible class of acceptor groups (aromatic ketones/aldehydes). The remaining difference spectra probably represent distinct chromophores more closely.

The difference absorbance spectra for PLFA were even further impacted by reduction (Appendix 18; Fig. A18-4). The carboxylic acid group at approximately 300 nm in the untreated sample disappeared almost completely in the reduced sample while the absorbance over the phenolic groups pK_a range shifted closer to 340 nm.

Terrestrial HS (LHA and EHA) showed similar changes upon reduction as the aquatic HS (Appendix 18; Figs. A18-5 and A18-6). The carboxylic acids difference spectra displayed a peak at approximately 280 nm with rapidly decreasing absorbance at longer wavelengths. A phenolic groups difference spectrum similar in appearance to SRHA and SRFA was also noted, except that the reduced LHA did not show a second

peak at 280 nm and most of the long wavelength absorbance was eliminated with reduction for both LHA and EHA. Further, EHA exhibited a very distinct shoulder at 650 nm in the untreated sample that was significantly decreased in the reduced samples.

Appendix 18.

HS pH Titration: Difference Absorbance of Untreated vs. 25-fold Mass Excess Reduced Samples

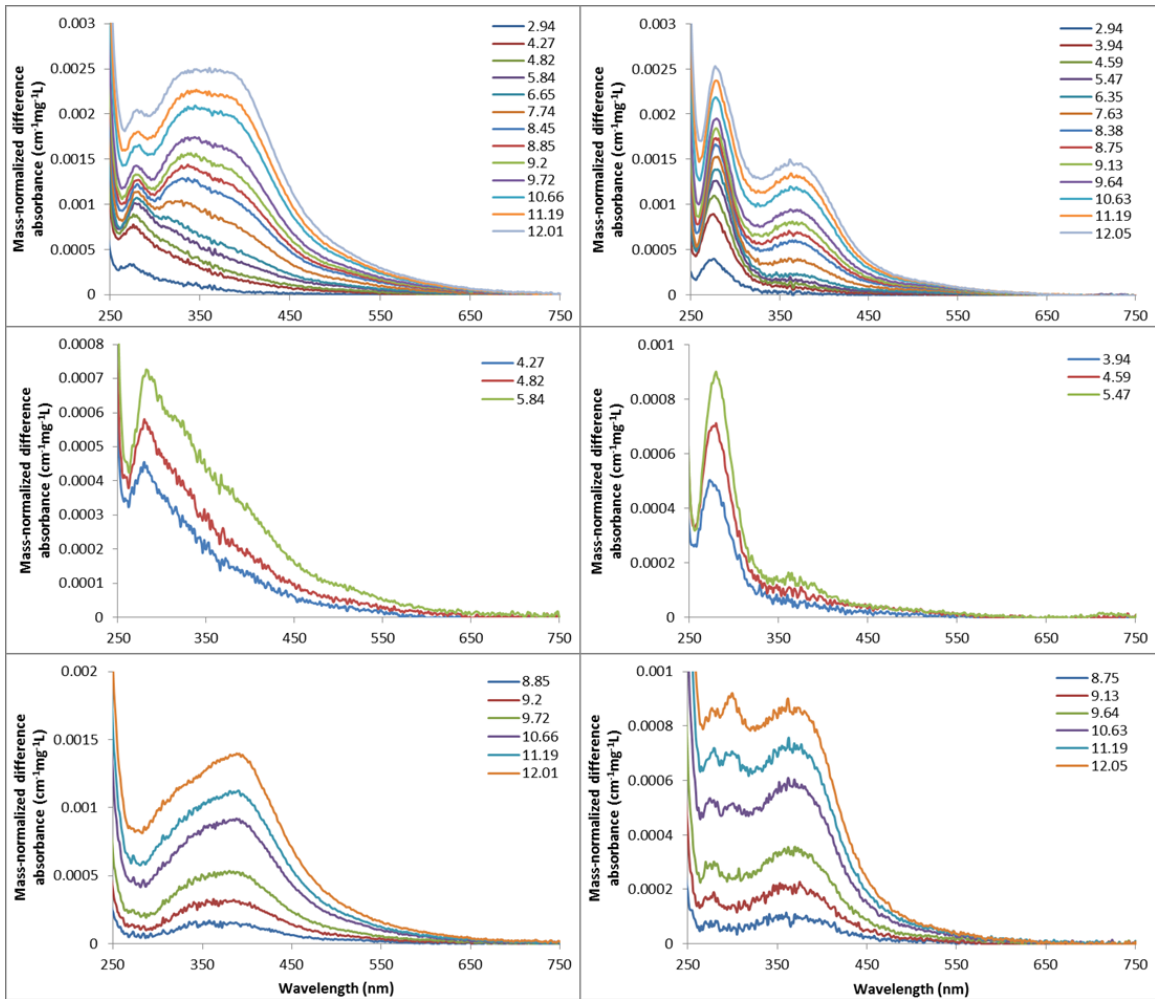


Figure A18-1. Mass normalized difference spectra for SRFA 50 mg/L. The left panel is the unreduced spectra while the right panel is the reduced spectra. The top is the total difference spectra with pH 2 as the reference sample. The middle is the carboxylic difference spectra with pH 3 as the reference sample. The bottom is the phenolic groups difference spectra with pH 7 as the reference sample.

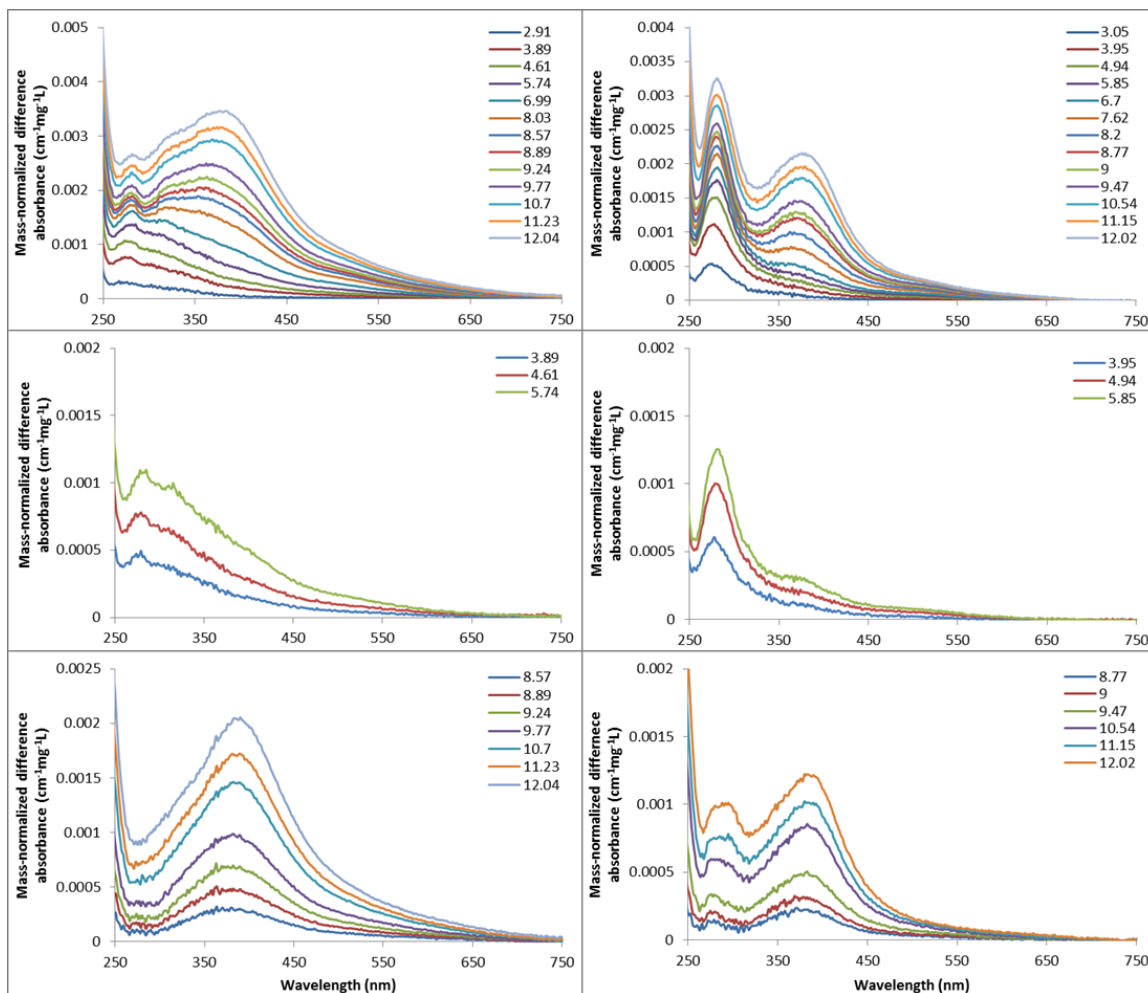


Figure A18-2. Mass normalized difference spectra for SRHA 50 mg/L. The left panel is the unreduced spectra while the right panel is the reduced spectra. The top is the total difference spectra with pH 2 as the reference sample. The middle is the carboxylic difference spectra with pH 3 as the reference sample. The bottom is the phenolic groups difference spectra with pH 7 as the reference sample.

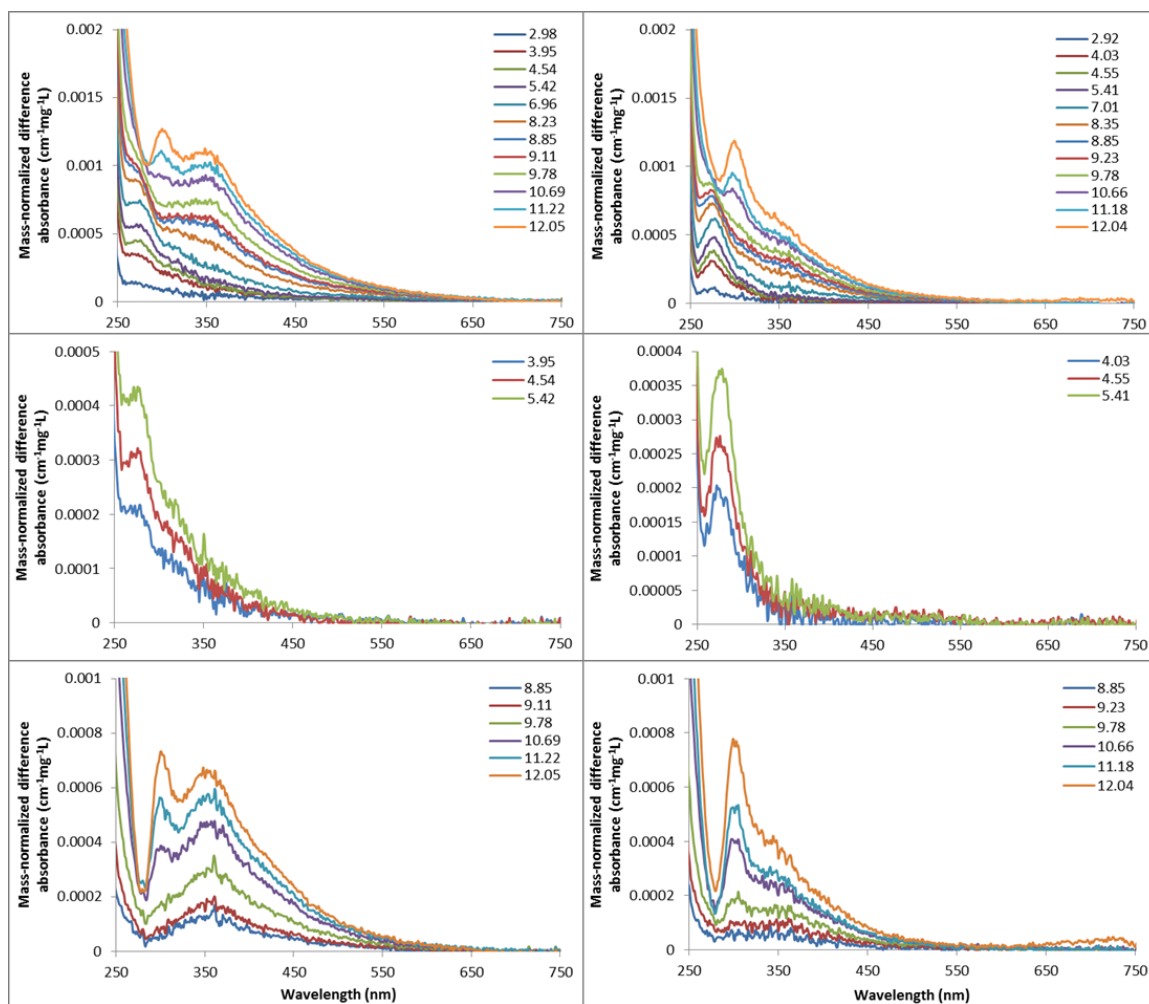


Figure A18-3. Mass normalized difference spectra for LAC 43 mg/L. The left panel is the unreduced spectra while the right panel is the reduced spectra. The top is the total difference spectra with pH 2 as the reference sample. The middle is the carboxylic difference spectra with pH 3 as the reference sample. The bottom is the phenolic groups difference spectra with pH 7 as the reference sample.

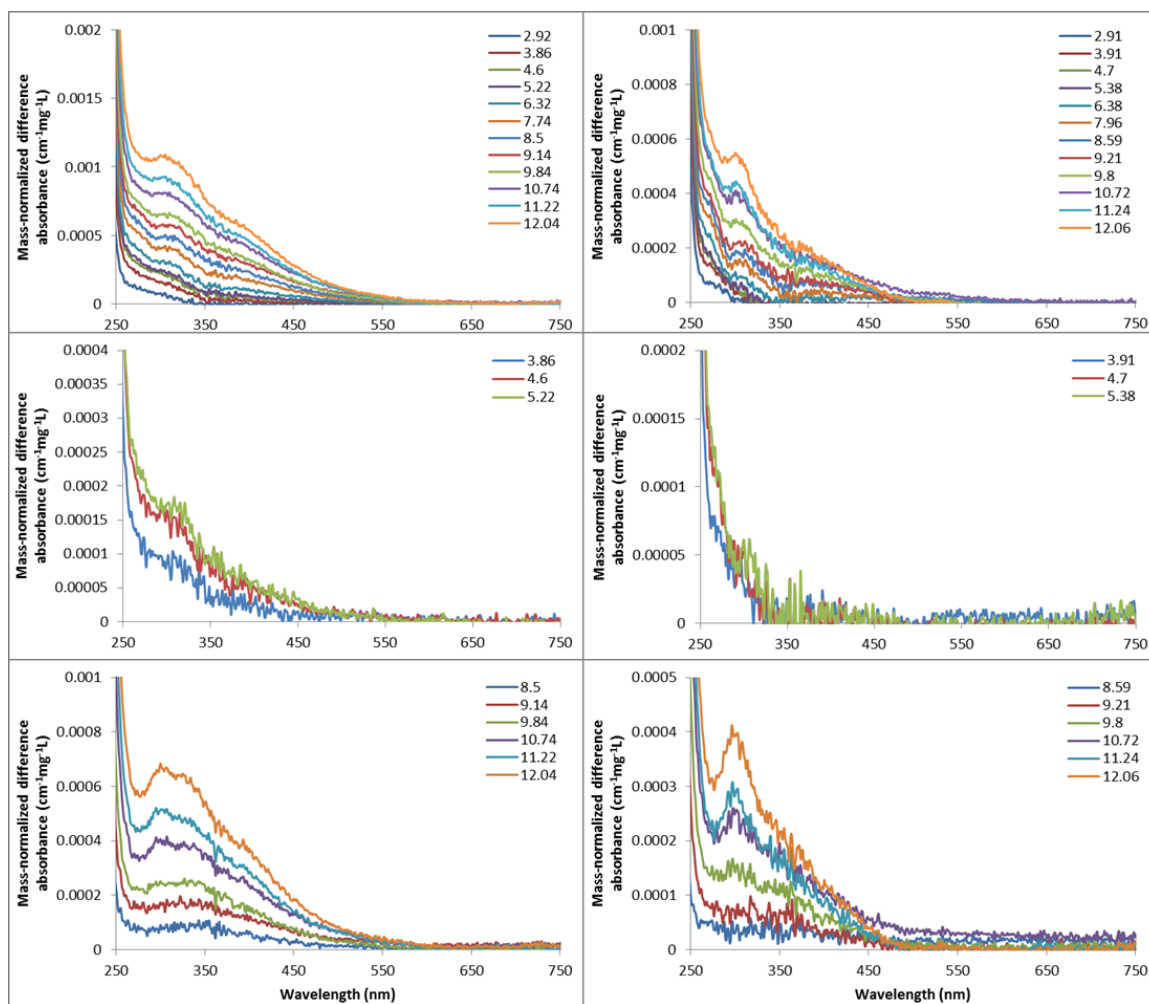


Figure A18-4. Mass normalized difference spectra for PLFA 44 mg/L. The left panel is the unreduced spectra while the right panel is the reduced spectra. The top is the total difference spectra with pH 2 as the reference sample. The middle is the carboxylic difference spectra with pH 3 as the reference sample. The bottom is the phenolic groups difference spectra with pH 7 as the reference sample.

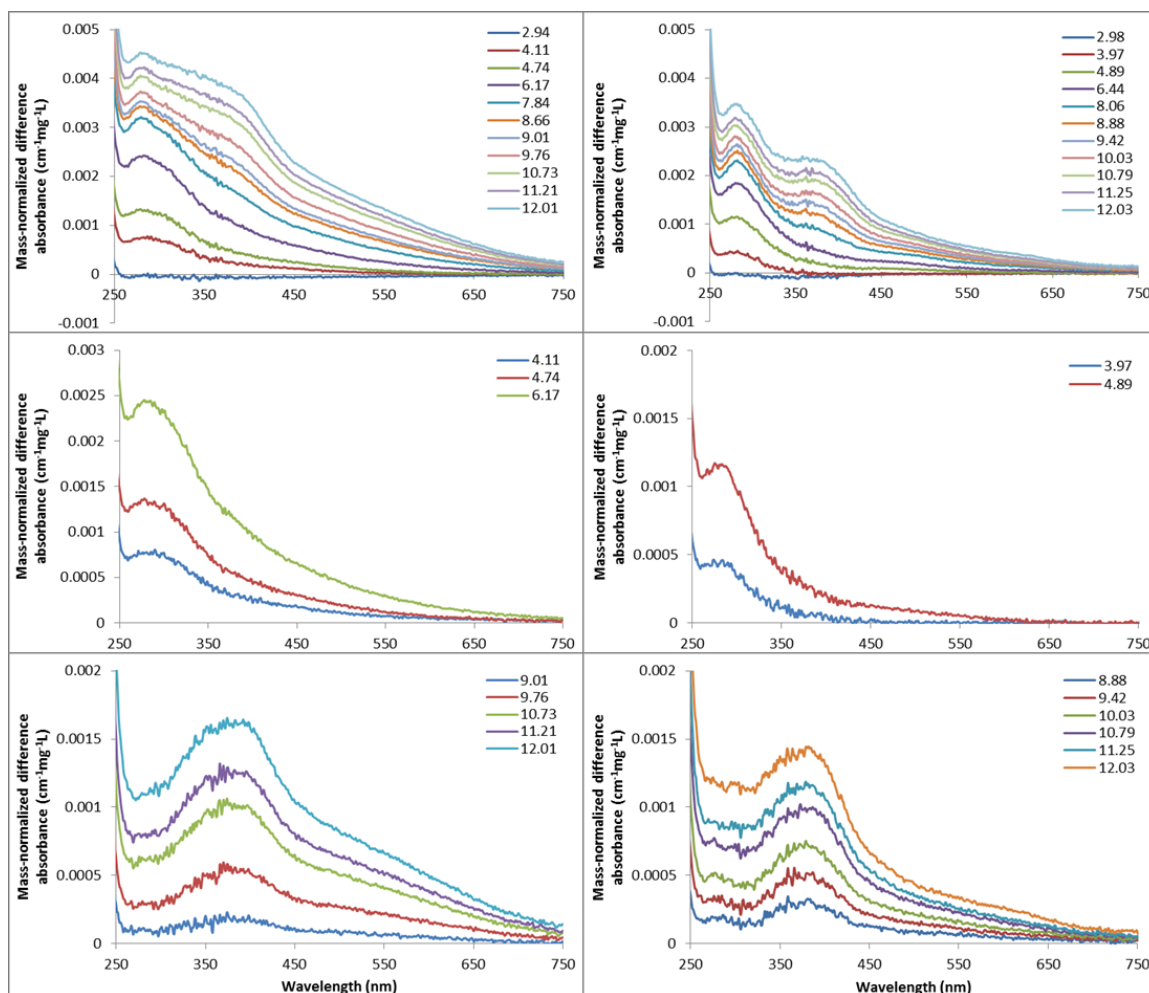


Figure A18-5. Mass normalized difference spectra for LHA 25 mg/L. The left panel is the unreduced spectra while the right panel is the reduced spectra. The top is the total difference spectra with pH 2 as the reference sample. The middle is the carboxylic difference spectra with pH 3 as the reference sample. The bottom is the phenolic groups difference spectra with pH 7 as the reference sample.

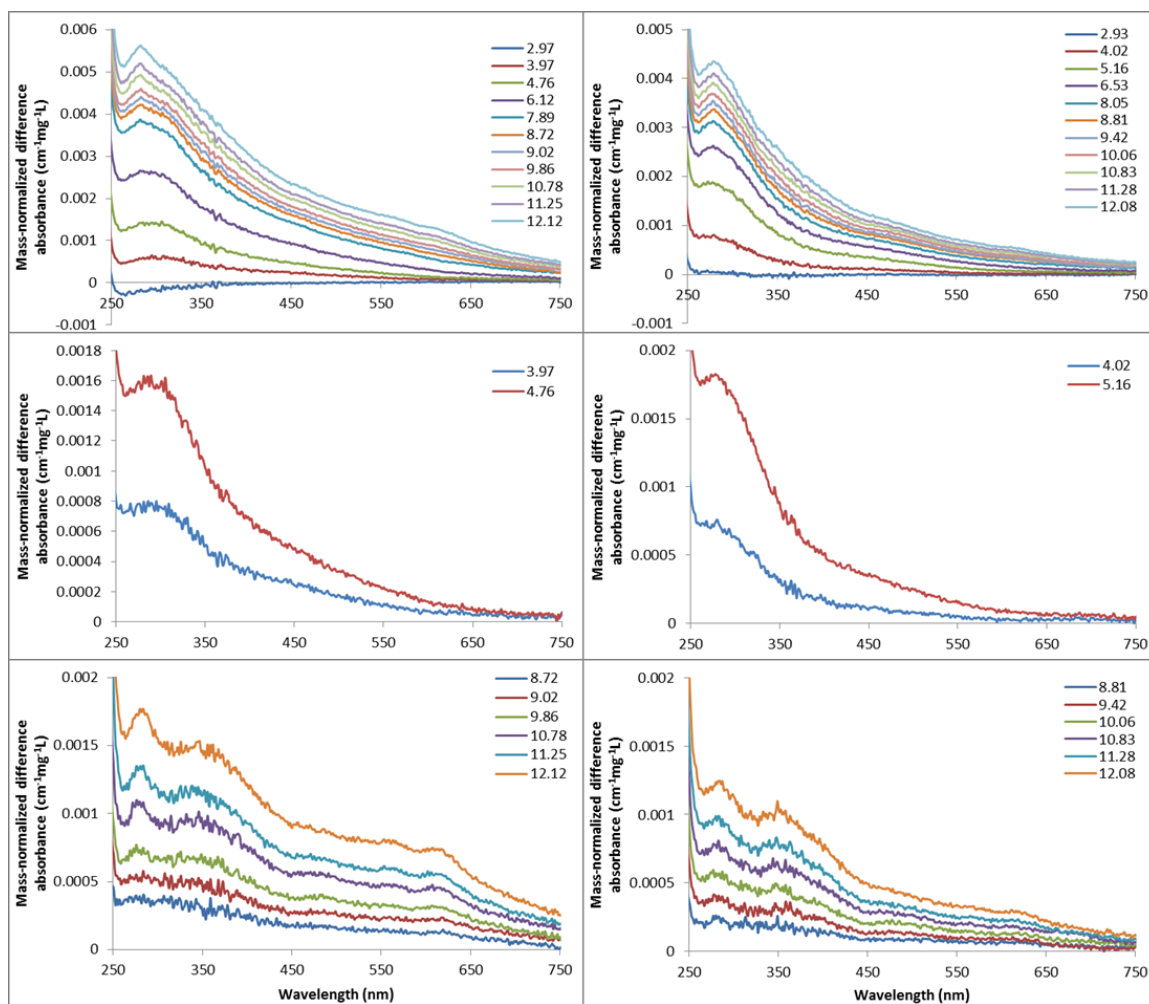


Figure A18-6. Mass normalized difference spectra for EHA 25 mg/L. The left panel is the unreduced spectra while the right panel is the reduced spectra. The top is the total difference spectra with pH 2 as the reference sample. The middle is the carboxylic difference spectra with pH 3 as the reference sample. The bottom is the phenolic groups difference spectra with pH 7 as the reference sample.

Appendix 19.

HS pH Titration: Circumneutral Difference Absorbance of Unreduced versus 25-fold Mass Excess Reduced Samples

Following the procedure set forth by Dryer et. al., the circumneutral spectra was developed for each HS. The purpose of the circumneutral spectrum was to verify that there were no other species present in the HS spectra. To develop this spectrum, the carboxylic acids and phenolic groups spectra were normalized to 400 nm (370 nm for SRFA) for the untreated and reduced samples. 400 nm was chosen because the normalization at that point led to the three groups matching at long wavelengths (>450 nm). Consistent with the observations of Dryer et. al. for SRFA, the spectra for all of the HS showed that the difference absorbance of the normalized pH 7 scan is a linear combination of the carboxylic acids and phenolic moieties scans (Figs. A19-1 and A19-2).

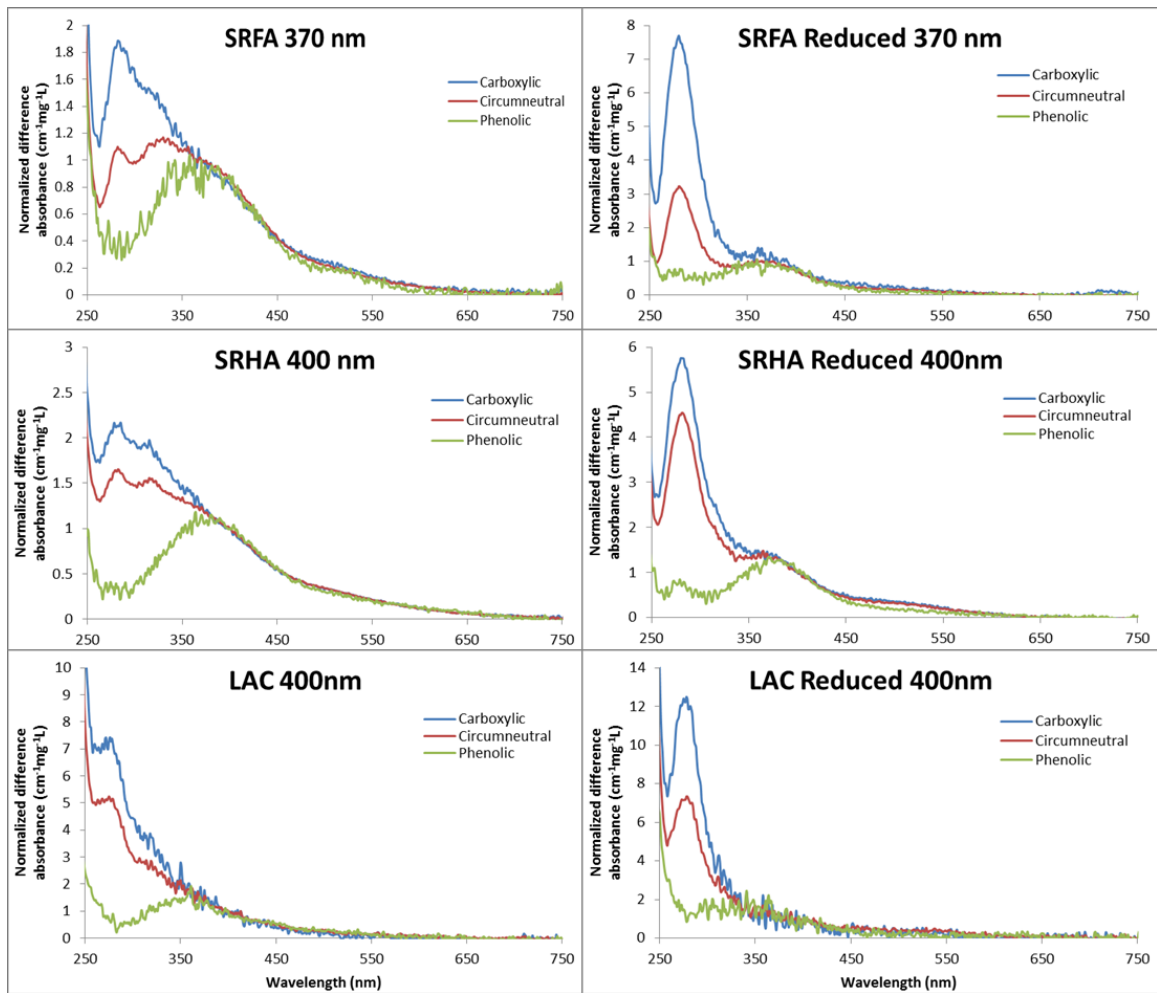


Figure A19-1. Normalized difference spectra for carboxylic (pH 3-5), circumneutral (pH 7), and phenolic (pH > 8) groups.

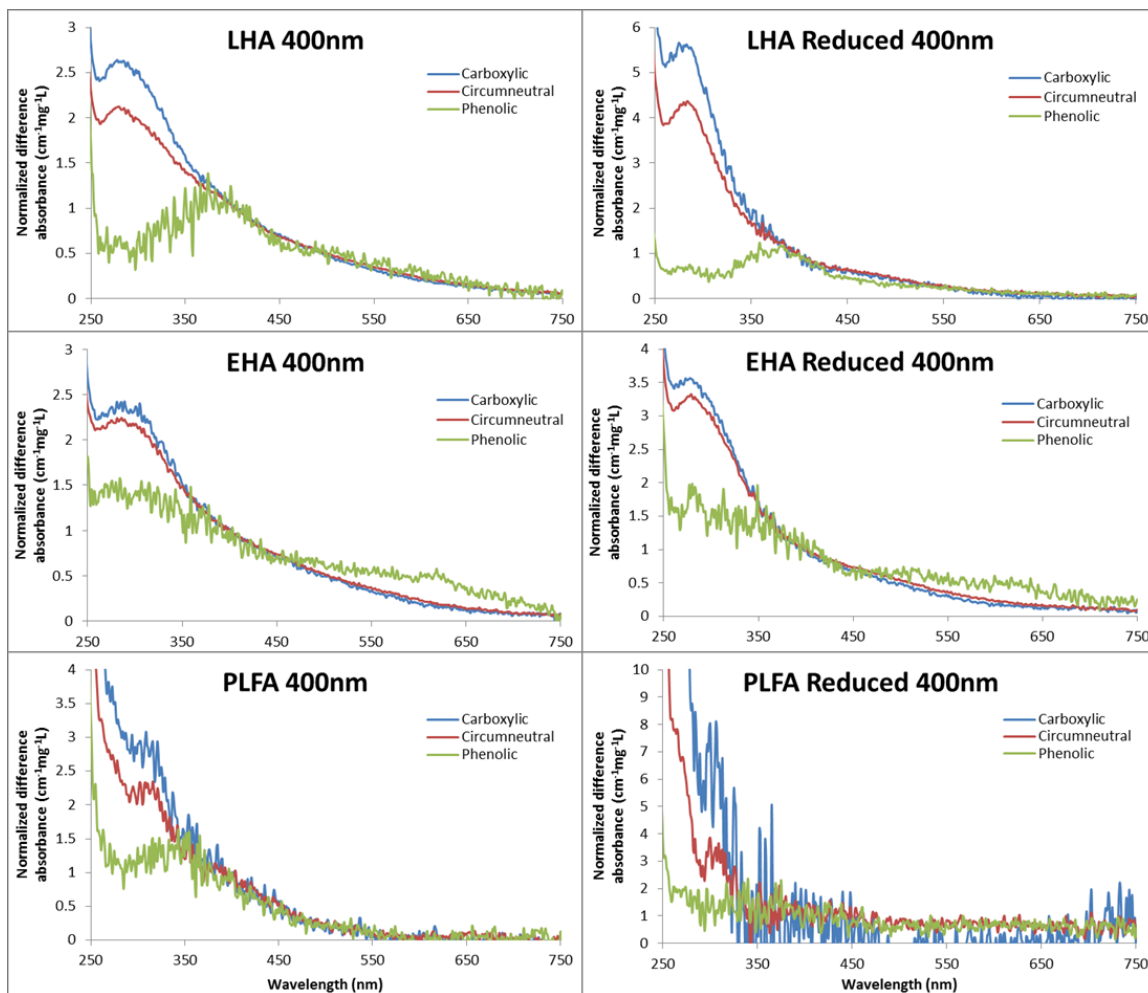


Figure A19-2. Normalized difference spectra for carboxylic (pH 3-5), circumneutral (pH 7), and phenolic (pH > 8) groups.

Appendix 20.
HS Reduction: Difference Absorbance versus pH

The difference absorbance at specific wavelengths was investigated relative to the pH for the unreduced and reduced HS. While the 300 nm scan shows both carboxylic acids ($\text{pH} < 5$) and phenolic ($\text{pH} > 8$) groups, the 400 nm scan only shows phenolic group contributions (Figs. A20-1-6). In addition, the 300 nm scan shows only a slight decrease in the difference absorbance between untreated and reduced samples, meaning that the functional groups at 300 nm are largely unaffected by reduction. At 400 nm, however, a significant decrease in difference absorbance can be noted for all HS. As noted previously, this could be due to the loss in absorbance at long wavelength with reduction stemming from the loss of the charge-transfer interactions.

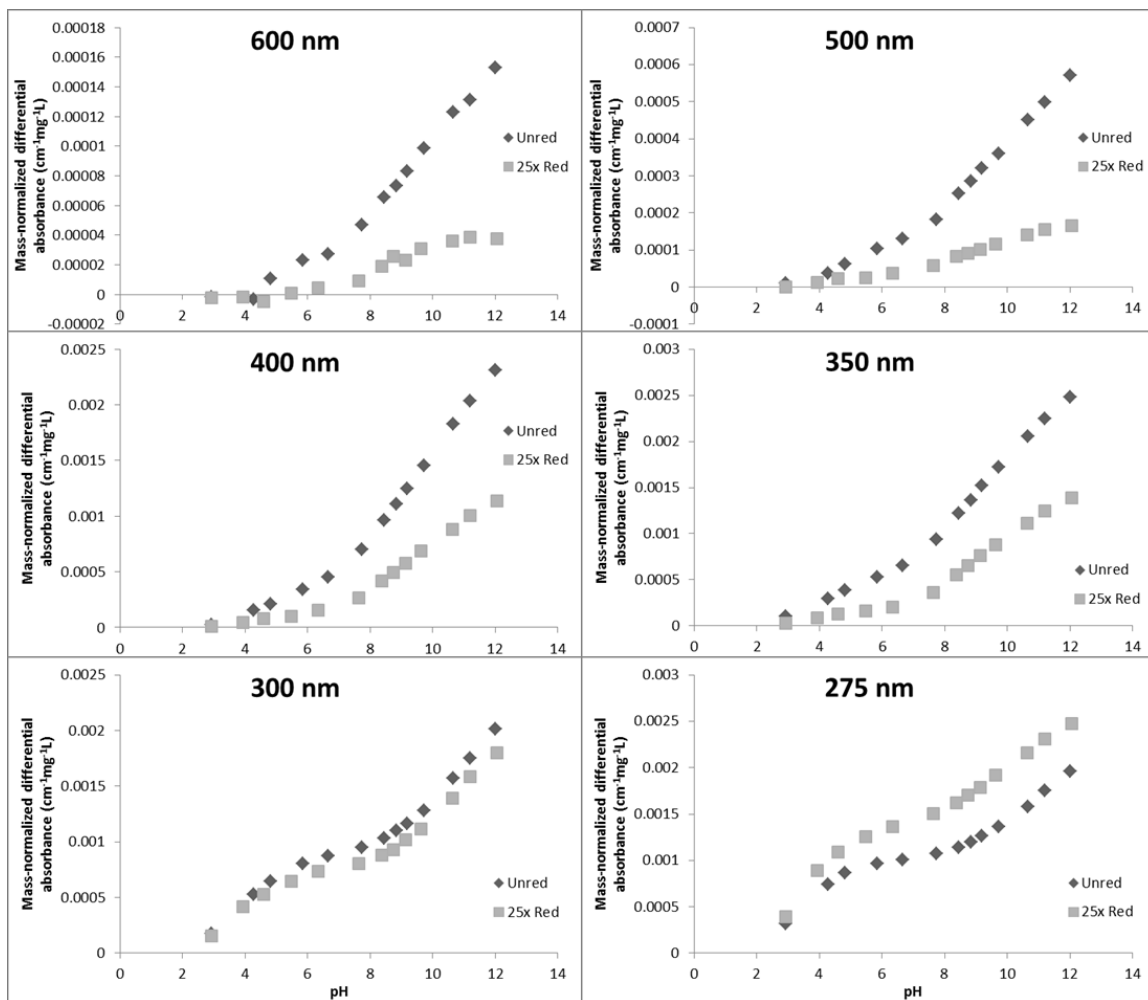


Figure A20-1. Comparison of the mass normalized difference spectra versus pH for SRFA unreduced and 25-fold mass excess reduced samples.

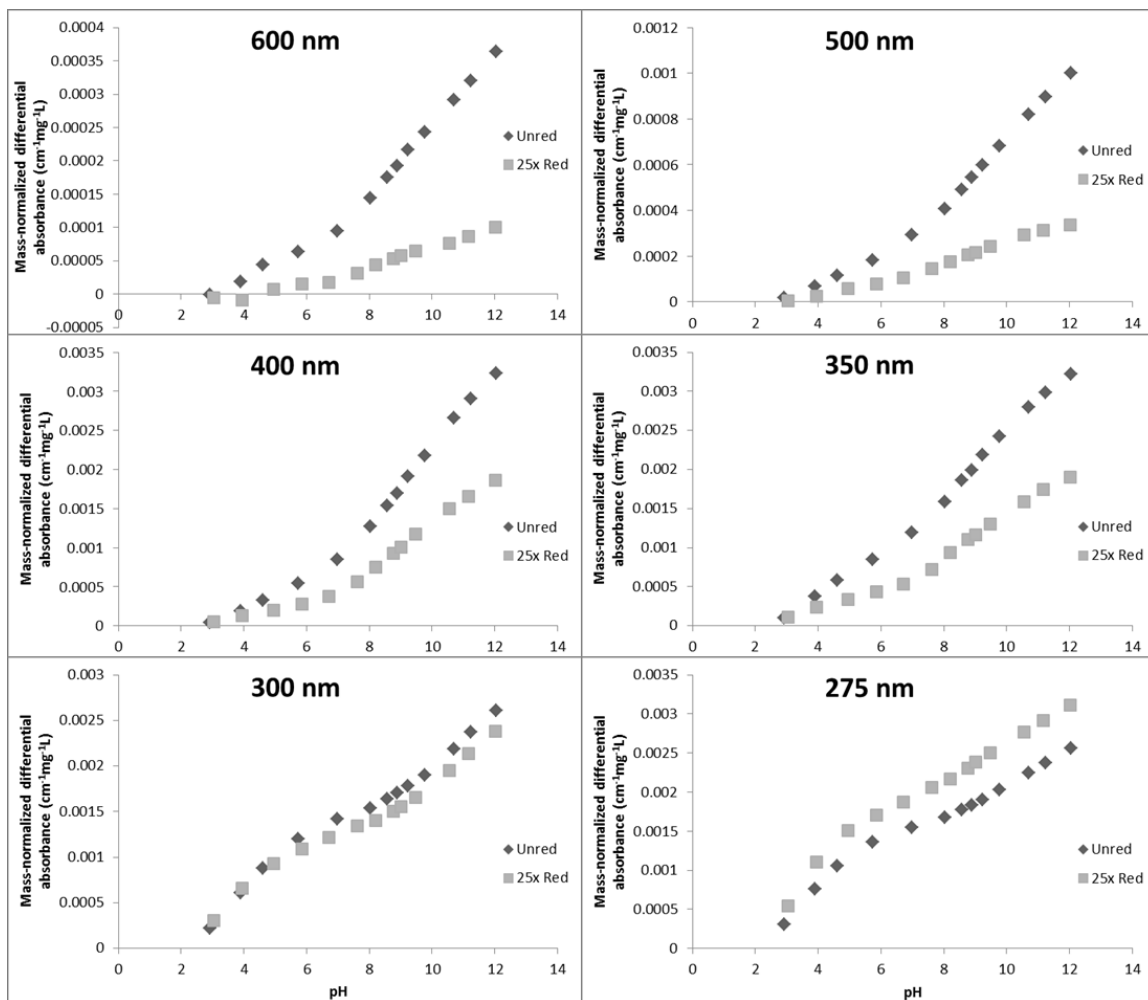


Figure A20-2. Comparison of the mass normalized difference spectra versus pH for SRHA unred and 25-fold mass excess reduced samples.

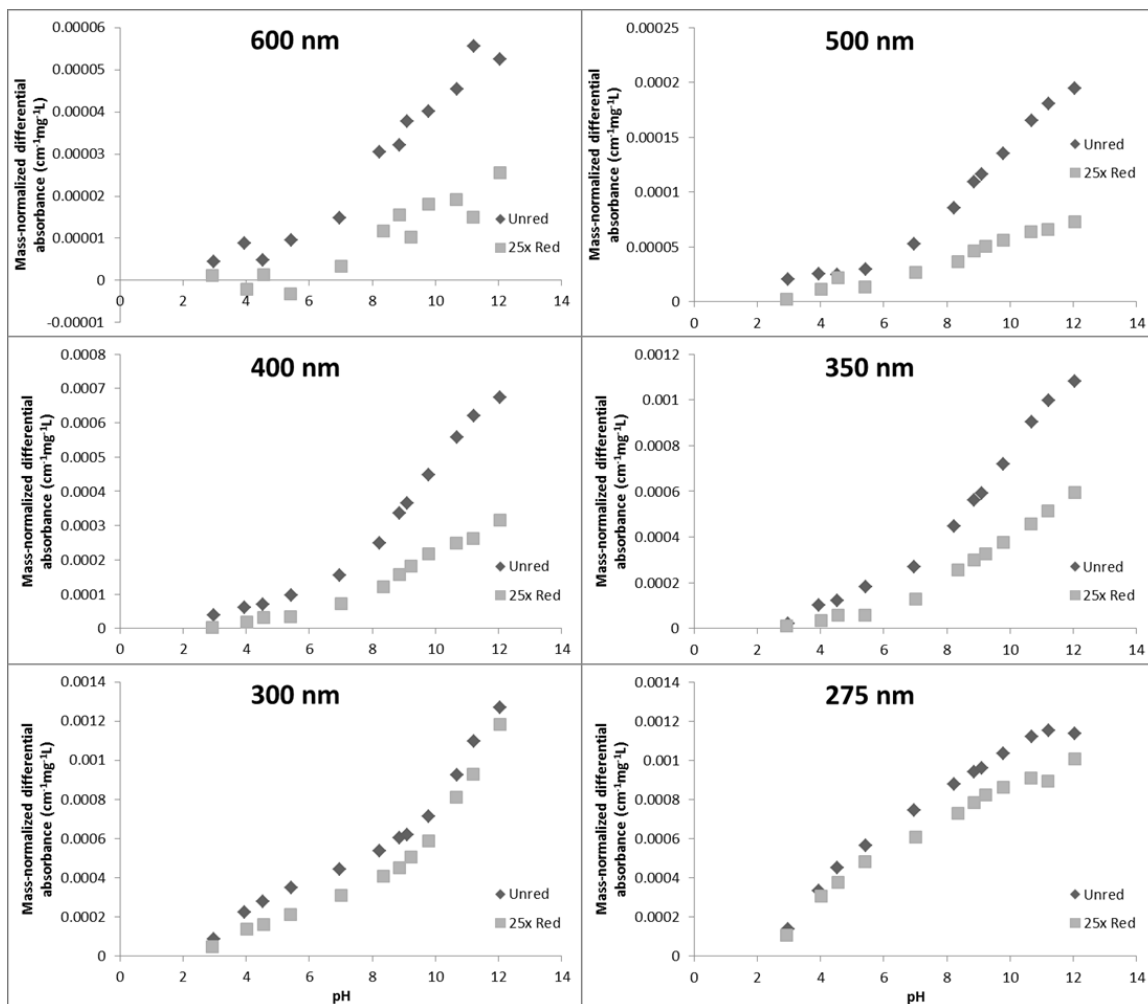


Figure A20-3. Comparison of the mass normalized difference spectra versus pH for LAC unred and 25-fold mass excess reduced samples.

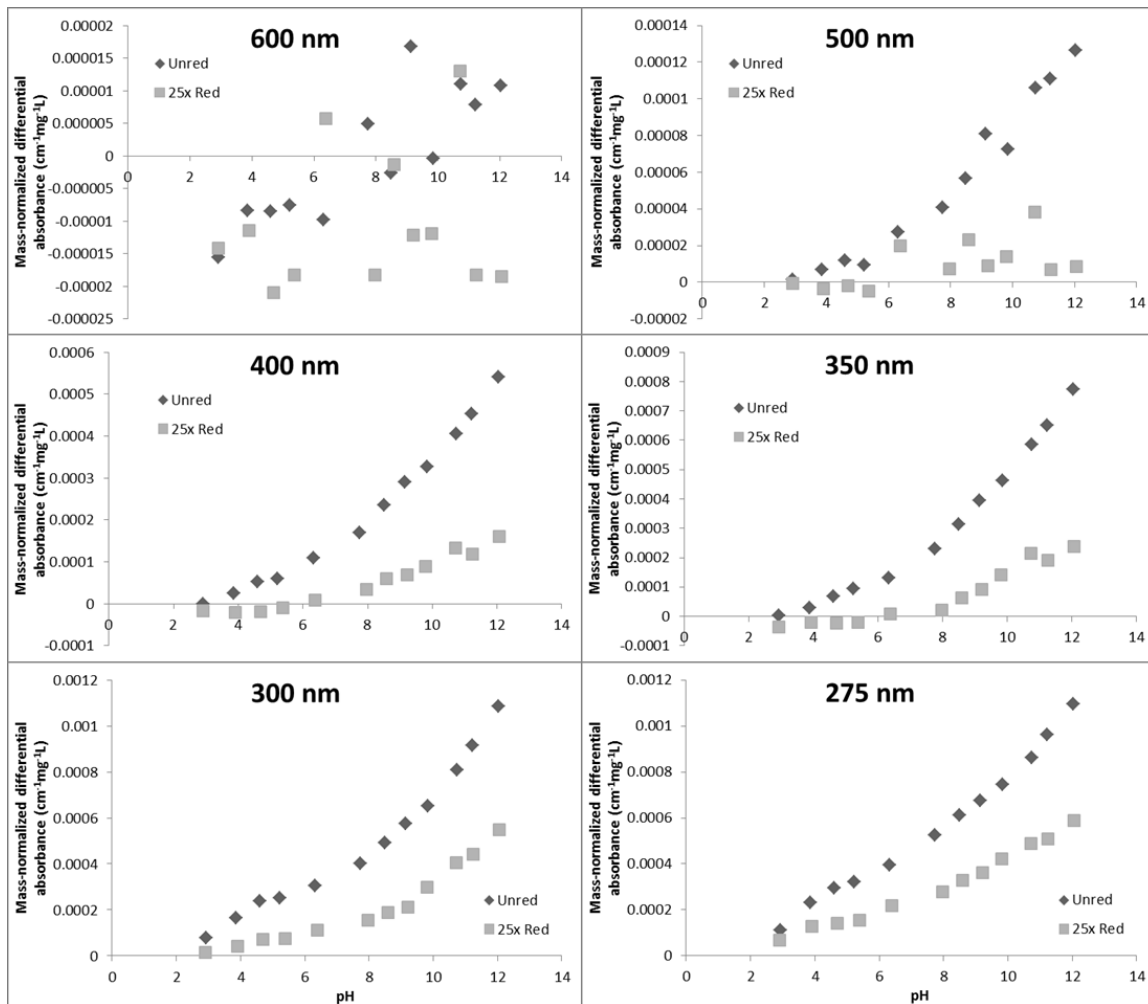


Figure A20-4. Comparison of the mass normalized difference spectra versus pH for PLFA unreduced and 25-fold mass excess reduced samples.

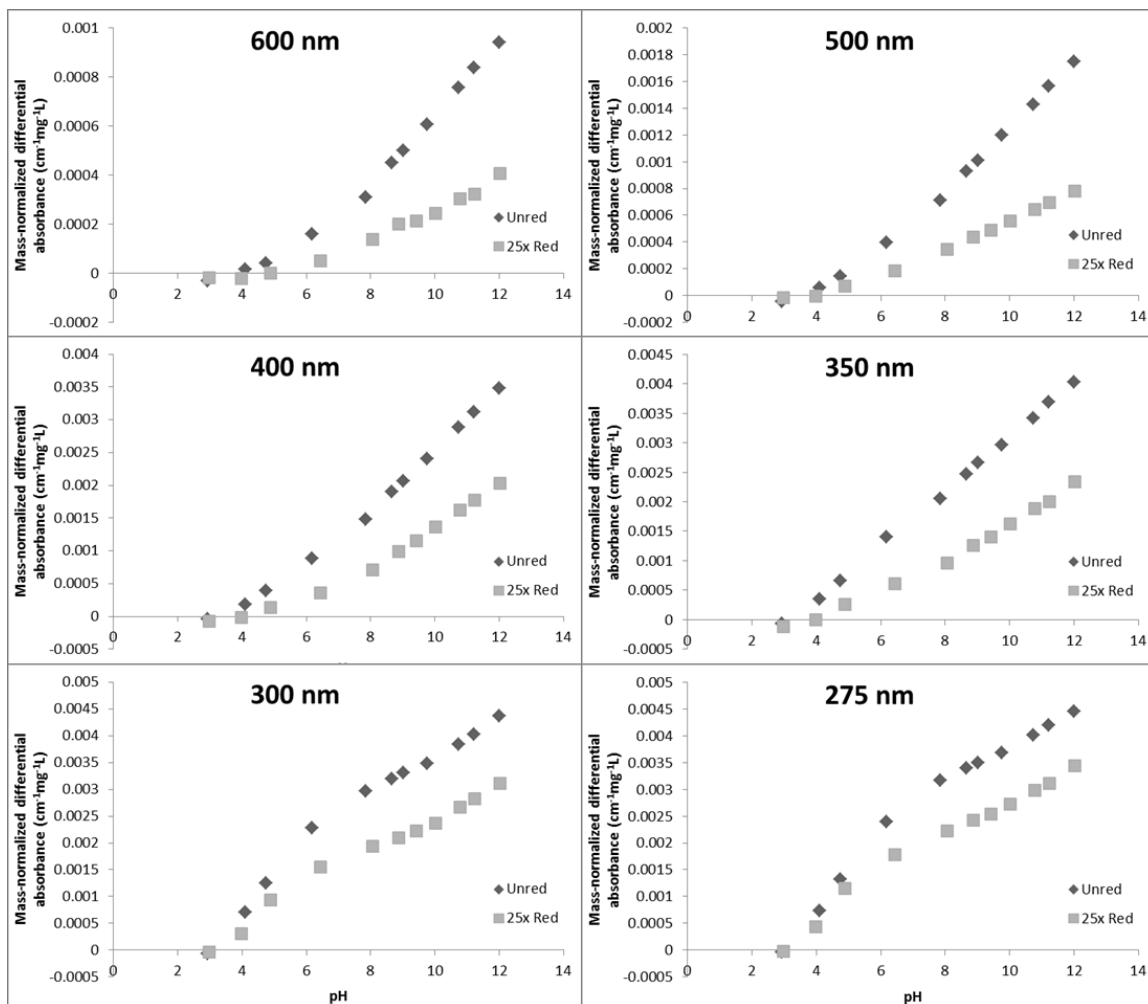


Figure A20-5. Comparison of the mass normalized difference spectra versus pH for LHA unred and 25-fold mass excess reduced samples.

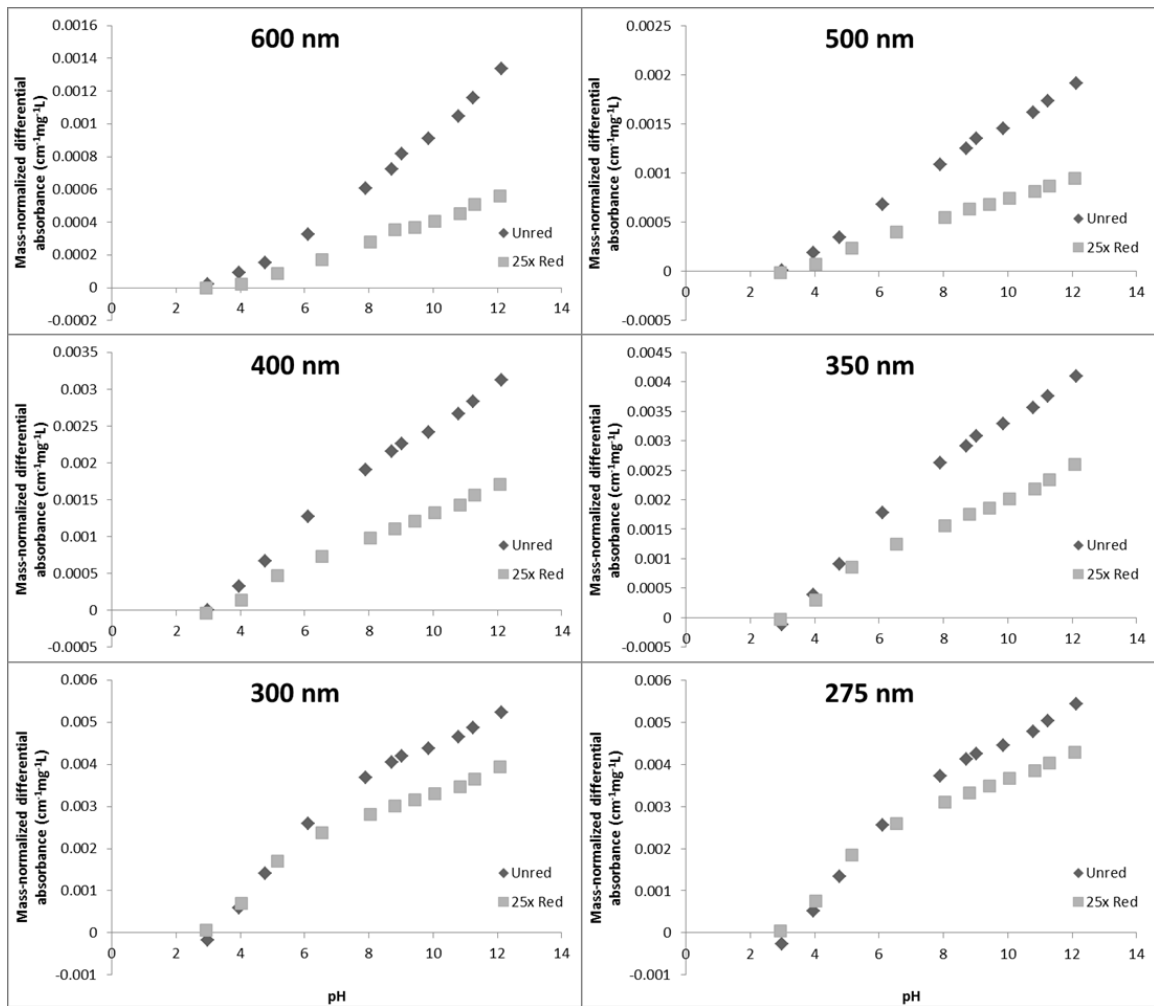


Figure A20-6. Comparison of the mass normalized difference spectra versus pH for EHA unred and 25-fold mass excess reduced samples.

Appendix 21.
Effects of Extent of NaBH₄ Reduction on pH Titration

To test whether the extent of NaBH₄ reduction has an impact on the pH dependence of the optical properties, SRFA was reduced with incremental amounts of NaBH₄ (5-fold, 25-fold, and 50-fold mass excess of NaBH₄ relative to that of the HS) and the optical properties monitored as a function of pH. Consistent with the data for the untreated and 25-fold mass excess reduced samples reported above, the absorption spectra of the reduced SRFA were broad and featureless and decreased with increasing wavelengths and with decreasing pH (Fig. A21-1).

In an effort to gain more insight through the absorbance of the samples, the total difference absorbance spectra were also analyzed relative to the pH 2 spectra. Overall, due to the loss of absorption with reduction, the optical changes decreased with increasing reduction without altering the spectral shape of the absorption spectra (Fig. A21-1). In particular, the 280 nm peak has a difference absorbance of 0.12 independent of treatment and regardless of the reduction amount. The 350 nm peak, on the other hand, decreases in difference absorbance with increasing reduction amount.

This data argues for a constant contribution of carboxylic acid groups that is unaffected by NaBH₄ reduction. In addition, it shows a variable contribution to the absorbance over the phenolic groups pK_a range that decreases with increasing NaBH₄ reduction. In other words, the carboxylic acid groups are decoupled from carbonyl species that are eliminated by reduction (but still coupled with the long-wavelength absorption), while the phenolic groups are somehow coupled with the carbonyl species.

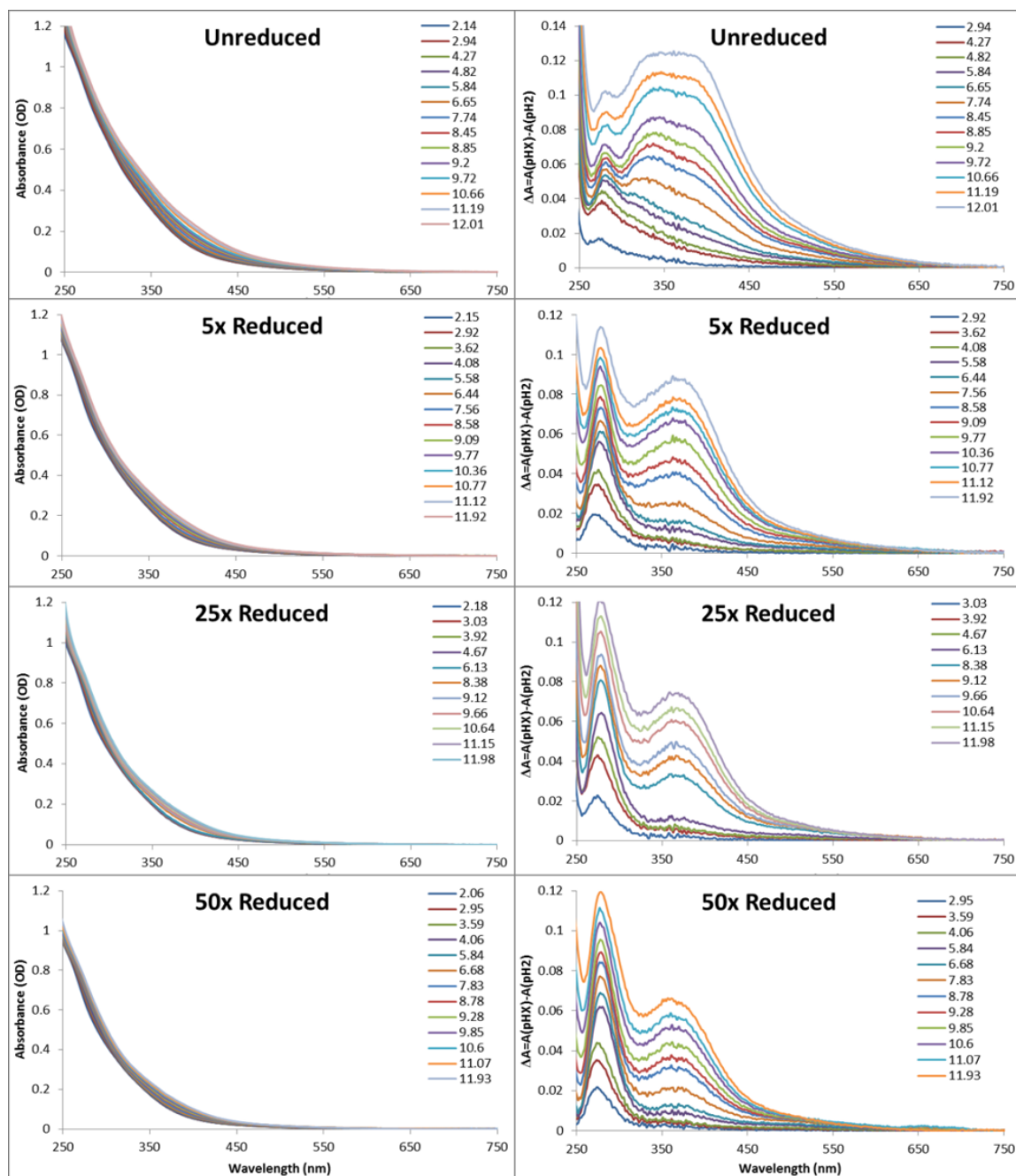


Figure A21-1. The left panel shows the effect of pH on unreduced and various reduced samples of SRFA. The right panel shows the associated difference absorbance spectra with pH 2 acting as the base absorbance. The concentration of SRFA was 50 mg/L for the original and reduced samples.

Observing the difference absorbance at 300 and 400 nm relative to pH shows a trend similar to the trends noted previously. At 300 nm, both the carboxylic acids (pH < 5) and phenolic groups (pH > 8) contributions can be noted, while for 400 nm, only the phenolic groups are noted. In addition, at 300 nm, the difference absorbance versus pH

for each reduction point is overlaid, showing the limited effect of reduction amount at 300 nm, similar to the observations noted previously. At 400 nm, however, there is a slight decrease in absorbance with increased reduction amount, but no change in the overall shape of the slope (Fig. A21-2).

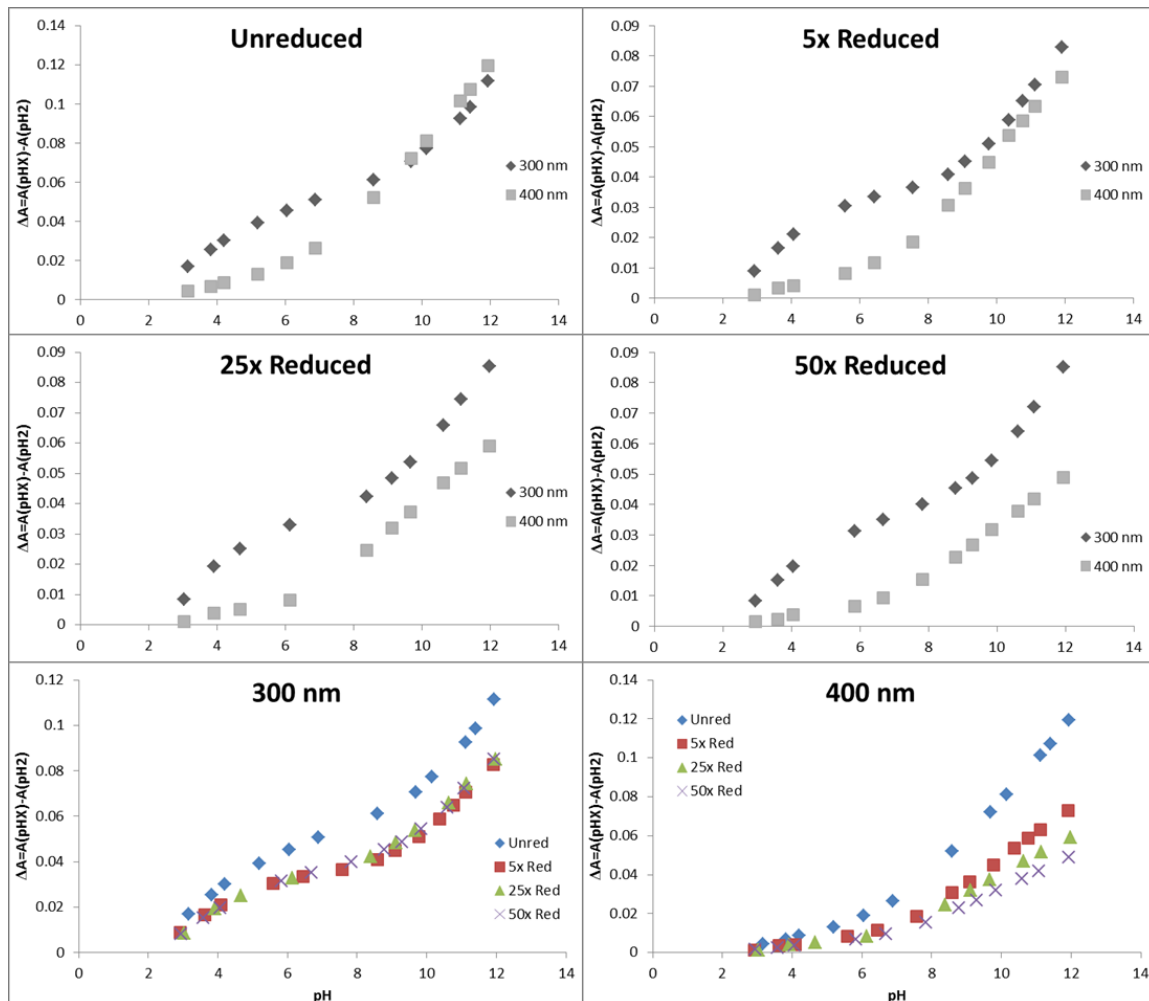


Figure A21-2. Difference absorbance spectra at 300 and 400 nm versus pH for SRFA unreduced and 5-fold, 25-fold, and 50-fold mass reduced samples. The top and middle panel shows each individual reduction amount differences between 300 and 400 nm, while the bottom panel shows differences between the unreduced and reduced samples at specific wavelengths.

These results showed that the extent of reduction had little to no impact on the pH dependence of the HS optical properties. There was an amplification of the results with an increase in reduction, but the spectral shape did not change. The borate in the sample

did not change the results of the pH titration; however, more acid was needed to titrate the excess borate prior to being able to run the titration, thus possibly altering the ionic strength of the solution (Table A21-1). Knowing that the 25-fold reduced sample removes all the borate through the column (see chapter 2) and there were no significant optical changes observed as function of reduction extent, the 25-fold mass excess sample was selected as the best condition for the pH titration study.

Table A21-1. Amount of HClO₄ (0.25 M) Added to Adjust pH to 7

	SRFA	SRHA	LAC	PLFA	LHA	EHA
Unreduced	0.5 µL	1 µL	--	0.5 µL	0.5 µL	0.5 µL
5x	1.5 µL	4 µL	1.5 µL	0.5 µL	1 µL	1 µL
10x	4 µL	3 µL	4 µL	1 µL	5 µL	5 µL
25x	6 µL	8 µL	10 µL	11 µL	7 µL	8 µL
50x	13 µL	21 µL	10 µL	18 µL	13 µL	22 µL
75x	30 µL	30 µL	15 µL	36 µL	1 µL	3 µL
100x	--	45 µL	12 µL	40 µL	15 µL	15 µL

Bibliography

1. Mopper, K.; Stubbins, A.; Ritchie, J. D.; Bialk, H. M.; Hatcher, P. G., Advanced Instrumental Approaches for Characterization of Marine Dissolved Organic Matter: Extraction Techniques, Mass Spectrometry, and Nuclear Magnetic Resonance Spectroscopy. *Chem. Rev. (Washington, DC, U. S.)* **2007**, *107* (2), 419-442.
2. Blough, N. V.; Del Vecchio, R., Chromophoric DOM in the coastal environment. *Biogeochem. Mar. Dissolved Org. Matter* **2002**, 509-546.
3. Wurl, O.; Editor, *Practical Guidelines for the Analysis of Seawater*. 2009; p 401 pp.
4. Coble, P. G., Marine Optical Biogeochemistry: The Chemistry of Ocean Color. *Chem. Rev. (Washington, DC, U. S.)* **2007**, *107* (2), 402-418.
5. Sharpless, C. M.; Blough, N. V., The importance of charge-transfer interactions in determining chromophoric dissolved organic matter (CDOM) optical and photochemical properties. *Environ. Sci. Processes Impacts* **2014**, *16* (4), 654-671.
6. Cory, R. M.; McKnight, D. M., Fluorescence Spectroscopy Reveals Ubiquitous Presence of Oxidized and Reduced Quinones in Dissolved Organic Matter. *Environ. Sci. Technol.* **2005**, *39* (21), 8142-8149.
7. Del Vecchio, R.; Blough, N. V., On the Origin of the Optical Properties of Humic Substances. *Environ. Sci. Technol.* **2004**, *38* (14), 3885-3891.
8. International Humic Substances Society.
<http://www.humicsubstances.org/whatarehs.html> (accessed September).
9. Andrew, A. A.; Del Vecchio, R.; Subramaniam, A.; Blough, N. V., Chromophoric dissolved organic matter (CDOM) in the Equatorial Atlantic Ocean: Optical properties and their relation to CDOM structure and source. *Mar. Chem.* **2013**, *148*, 33-43.
10. Boyle, E. S.; Guerriero, N.; Thiallet, A.; Del Vecchio, R.; Blough, N. V., Optical Properties of Humic Substances and CDOM [chromophoric dissolved organic matter]: Relation to Structure. *Environ. Sci. Technol.* **2009**, *43* (7), 2262-2268.
11. Ma, J.; Del Vecchio, R.; Golanoski, K. S.; Boyle, E. S.; Blough, N. V., Optical properties of humic substances and CDOM: effects of borohydride reduction. *Environ Sci Technol* **2010**, *44* (14), 5395-402.
12. Ritchie, J. D.; Perdue, E. M., Proton-binding study of standard and reference fulvic acids, humic acids, and natural organic matter. *Geochim. Cosmochim. Acta* **2003**, *67* (1), 85-96.
13. Dryer, D. J.; Korshin, G. V.; Fabbicino, M., In Situ Examination of the Protonation Behavior of Fulvic Acids Using Differential Absorbance Spectroscopy. *Environ. Sci. Technol.* **2008**, *42* (17), 6644-6649.
14. Elemental analyses by Huffman Laboratories; Isotopic analyses by Soil Biochemistry Laboratory.

15. Thorn, K. A.; Folan, D. W.; MacCarthy, P., Characterization of the International Humic Substances Society Standard and Reference Fulvic and Humic Acids by Solution State Carbon-13 (^{13}C) and Hydrogen-1 (^1H) Nuclear Magnetic Resonance Spectrometry. U.S. Geological Survey: Water-Resources Investigations Report, 1989; pp 4089-4196.
16. Leenheer, J. A.; Wilson, M. A.; Malcolm, R. L., Presence and potential significance of aromatic-ketone groups in aquatic humic substances. *Org. Geochem.* **1987**, *11* (4), 273-80.
17. Gel Filtration Principles and Methods 2010, p. 123.
18. Sodium Borohydride Digest.
http://www.dow.com/assets/attachments/industry/pharma_medical/chemical_reagents/reducing_agents/sodium_borohydride_digest.pdf (accessed 2/9/14).
19. Tinnacher, R. M.; Honeyman, B. D., A New Method to Radiolabel Natural Organic Matter by Chemical Reduction with Tritiated Sodium Borohydride. *Environ. Sci. Technol.* **2007**, *41* (19), 6776-6782.
20. Aeschbacher, M.; Sander, M.; Schwarzenbach, R. P., Novel Electrochemical Approach to Assess the Redox Properties of Humic Substances. *Environ. Sci. Technol.* **2010**, *44* (1), 87-93.
21. Aeschbacher, M.; Vergari, D.; Schwarzenbach, R. P.; Sander, M., Electrochemical Analysis of Proton and Electron Transfer Equilibria of the Reducible Moieties in Humic Acids. *Environ. Sci. Technol.* **2011**, *45* (19), 8385-8394.
22. Maurer, F.; Christl, I.; Kretzschmar, R., Reduction and Reoxidation of Humic Acid: Influence on Spectroscopic Properties and Proton Binding. *Environ. Sci. Technol.* **2010**, *44* (15), 5787-5792.
23. Korshin, G. V.; Benjamin, M. M.; Li, C.-W., Use of differential spectroscopy to evaluate the structure and reactivity of humics. *Water Sci. Technol.* **1999**, *40* (9), 9-16.